

ACTIVE PROTECTION OF REINFORCED CONCRETE STRUCTURES BY FRP SHEETS

A thesis report submitted in partial fulfilment
of the requirements for the award of degree of

**MASTER OF CIVIL ENGINEERING
(STRUCTURES)**

Submitted by

SUNIL KUMAR

Registration No. 801022019



Under the guidance of

Dr. SHWETA GOYAL

Assistant Professor

DEPARTMENT OF CIVIL ENGINEERING

THAPAR UNIVERSITY

PATIALA-147001

2012

CERTIFICATE

This is to certify that the thesis report on “**Active Protection of Reinforced Concrete Structures by FRP sheets**” submitted by **SUNIL KUMAR, Roll No. 801022019** in partial fulfilment of the requirements for the award of degree of **MASTERS OF ENGINEERING IN CIVIL (STRUCTURES) at Thapar University, Patiala**, is an authentic record of student’s own work carried out under our supervision and guidance.



(Dr. Shweta Goyal)

Assistant Professor
Department of Civil Engineering
Thapar University
Patiala-147001(Punjab)

Countersigned by:



(Dr. Maneek Kumar)

Professor and Head
Department of Civil Engineering
Thapar University, Patiala



(Dr. S.K. Mohapatra)

Dean of Academic Affairs
Thapar University, Patiala

ACKNOWLEDGEMENT

I express my deep gratitude and respects to **Dr. Shweta Goyal, Assistant Professor in CED** for their keen interest and valuable guidance, strong motivation and constant encouragement during the course of the work. I am indebted to her for sparing her valuable time in giving me valuable suggestions and increasing my knowledge through fruitful discussions.

I owe my sincere thanks to **Dr. Maneek Kumar, H.O.D. in CED** and all the staff members of **Civil Engineering Department** for their support and encouragement.

I would like to convey my sincere gratitude to my friends and colleagues for their support, co-operation and their timely help and valuable discussions.

And above all, I pay my regards to the **Almighty** for his love and blessings.

Place: *Patiala*

Dated :


(SUNIL KUMAR)

ABSTRACT

Reinforced concrete is one of the most commonly used construction materials in civil engineering but its durability problems have been obsessing people. The worst of these problems is caused by corrosion of steel in concrete, inducing the early deterioration of concrete infrastructures. Structural deterioration of reinforced concrete structures affected by corrosion is a gradual process consisting of a few different phases during service life, including corrosion initiation, concrete cracking, excessive deflection and final collapse due to loss of structural strength.

A large number of reinforced concrete structures that have been damaged due to corrosion of steel reinforcements are rehabilitated with fiber reinforced polymer (FRP) composites. FRP offers superior performance such as resistance to corrosion, high stiffness-to-weight ratio, high tensile strength, light weight, high durability and easy installation etc. The present work investigates the progression of corrosion of steel in concrete after it has been treated with surface bonded FRP. Study is carried out with accelerated corrosion through impressed current to get quick results.

The present work also investigates active protection of the steel embedded in concrete that is treated with surface bonded carbon FRP. The electrically conductive carbon fiber is used as anode while the reinforcing bar is used as cathode in the present active protection. Anodic current was passed through the reinforcement in specimens to initiate cracking in concrete. Carbon FRP sheets have been adhesively bonded to the specimens. Specimens were exposed to highly corrosive environment for specified times. The active protection technique is very effective in retarding the corrosion of steel. However, Active (cathodic) protection is one of the efficient technologies that have proven to stop corrosion in existing reinforced concrete structures, regardless of the amount of chloride content in the concrete. This thesis investigates carbon FRP (CFRP) composites for active protection of RC structures by using non destructive monitoring techniques.

CONTENTS

| | |
|---|-----------|
| CERTIFICATE | i |
| ACKNOWLEDGEMENT | ii |
| ABSTRACT | iii |
| CONTENTS | iv |
| LIST OF FIGURES | vii |
| LIST OF TABLES | x |
| | |
| 1 INTRODUCTION | 1 |
| 1.1 Reinforced Concrete | 1 |
| 1.2 Corrosion Process | 2 |
| 1.2.1 Causes of corrosion | 3 |
| 1.2.1.1 Carbonation | 3 |
| 1.2.1.2 Chloride | 3 |
| 1.2.1.3 Water-Cement Ratio | 4 |
| 1.2.1.4 Low Concrete Tensile Strength | 4 |
| 1.2.1.5 Moisture | 4 |
| 1.2.2 Mechanism of Corrosion | 4 |
| 1.2.3 Effects of Rebar Corrosion | 9 |
| 2 CATHODIC PROTECTION OF RC STRUCTURES | 10 |
| 2.1 Introduction | 10 |
| 2.2 Theory of Cathodic Protection | 10 |
| 2.2.1 Cathodic Protection | 10 |
| 2.2.2 Types of Cathodic Protection | 11 |
| 2.2.3 Merits and Demerits of Cathodic Protection | 12 |
| 2.3 Principle of Cathodic Protection | 12 |
| 2.4 Operating a Cathodic Protection System | 13 |
| 2.5 Impressed Current Cathodic Protection | 15 |
| 2.5.1 Anode selection for Impressed Current Cathodic Protection | 16 |

| | | |
|----------|--|----|
| 3 | LITERATURE REVIEW | 20 |
| 4 | EXPERIMENTAL PROGRAMME | 58 |
| | 4.1 General | 58 |
| | 4.2 Test programme | 58 |
| | 4.3 Materials used | 60 |
| | 4.3.1 Cement | 60 |
| | 4.3.2 Fine Aggregates | 60 |
| | 4.3.3 Coarse Aggregates | 61 |
| | 4.3.4 Water | 62 |
| | 4.3.5 Steel Reinforcement | 62 |
| | 4.3.6 CFRP material | 63 |
| | 4.3.7 Adhesives | 63 |
| | 4.4 Design of Concrete Mix | 64 |
| | 4.5 Test Procedure | 64 |
| | 4.5.1 General | 64 |
| | 4.5.2 Preparation and Preconditioning of Steel Bars | 65 |
| | 4.5.3 Preparation of Slab Specimen | 65 |
| | 4.6 Inducing corrosion in steel rebar | 65 |
| | 4.7 Wrapping the pre-corroded specimens | 66 |
| | 4.8 Active Protection | 67 |
| | 4.9 Corroding the wrapped specimens | 67 |
| | 4.10 Corrosion monitoring techniques | 68 |
| | 4.10.1 Electrochemical Techniques | 68 |
| | 4.10.1.1 Half cell potential measurements | 69 |
| | 4.10.1.2 Linear polarization resistance (LPR) measurements | 70 |

| | | |
|----------|---------------------------------------|----|
| 5 | RESULTS AND DISCUSSIONS | 73 |
| | 5.1 General | 73 |
| | 5.2 Electrochemical measurements | 73 |
| | 5.2.1 Half-cell measurements | 73 |
| | 5.2.1.1 Observation | 76 |
| | 5.2.2 Corrosion Rate by LPR Technique | 77 |
| | 5.2.2.1 Observation | 77 |
| 6 | CONCLUSIONS | 82 |
| 7 | REFERENCES | 83 |

LIST OF FIGURES

| Fig.No. | Description | Page No. |
|----------|---|----------|
| Fig. 1.1 | Corrosion in Reinforced Concrete Structures | 1 |
| Fig. 1.2 | Local-cell Corrosion | 5 |
| Fig. 1.3 | Microcell Corrosion | 6 |
| Fig. 1.4 | Macro cell Corrosion | 7 |
| Fig.1.5 | Cracking and spalling of concrete due to penetration of chloride ions | 8 |
| Fig.2.1 | The principle of Cathodic Corrosion Protection | 13 |
| Fig.2.2 | Impressed current cathodic protection installation process using discrete anodes | 15 |
| Fig.2.3 | System design activated titanium anode mesh | 17 |
| Fig.3.1 | The schematic of the anodic polarization test setup | 22 |
| Fig.3.2 | Testing apparatus configuration for cathodic protection test | 26 |
| Fig.3.3 | Protection current distribution with different impressed current density | 27 |
| Fig.3.4 | Protection current distribution with different impressed current density | 27 |
| Fig.3.5 | The relationship between impressed current density and standard deviation of protection current distribution values | 28 |
| Fig.3.6 | Schematic illustration of the anodic behaviour of steel in the presence of chlorides | 29 |
| Fig.3.7 | Schematic illustration of steel behaviour in concrete as a function of the chloride content | 30 |
| Fig.3.8 | Steel behaviour in concrete for different potentials and chloride contents | 31 |
| Fig.3.9 | Schematic representation of slab and position of the cores | 33 |
| Fig.3.10 | Bond strength development for specimens with w/c = 0.48 | 34 |
| Fig.3.11 | Bond strength development for specimens with w/c = 0.58 | 35 |
| Fig.3.12 | Bond strength development for specimens with w/c = 0.66 | 35 |
| Fig.3.13 | Bond strengths versus total concentration of potassium and sodium ions | 36 |
| Fig.3.14 | Effect of the corrosion rate on current and potential distribution | 38 |
| Fig.3.15 | Effect of the concrete resistivity on current and potential distribution | 38 |

| | | |
|----------|---|----|
| Fig.3.16 | Effect of the applied current on current and potential distribution | 39 |
| Fig.3.17 | Effect of concrete resistivity, bar spacing and cover depth on current distribution | 39 |
| Fig.3.18 | Relationship between maximum tensile strength and applied cathodic potential in as-welded and post-weld heat treated specimen | 41 |
| Fig.3.19 | Relationship between elongation and applied cathodic potential in as-welded and post-weld heat treated specimen | 42 |
| Fig.3.20 | Relationship between time-to-fracture and applied cathodic potential in as-welded and post-weld heat treated specimen | 43 |
| Fig.3.21 | Relationship between strain to failure ratio and applied cathodic potential in as-welded and post-weld heat treated specimen | 43 |
| Fig.3.22 | Bond Strength as a function of time | 45 |
| Fig.3.23 | Hydrogen Ion versus Bond Strength | 46 |
| Fig.3.24 | The average bond strength versus the polarization time | 49 |
| Fig.3.25 | Bond strength reduction versus current density | 50 |
| Fig.3.26 | The average bond strength versus ψ | 51 |
| Fig.3.27 | Schematic representation of the device for accelerated corrosion | 52 |
| Fig.3.28 | Variation of half cell potential with time | 54 |
| Fig.3.29 | Variation of pullout strength with% mass loss | 54 |
| Fig.4.1 | Specimens and the Power Supplies Used to Accelerate Corrosion | 59 |
| Fig.4.2 | CFRP sheet used in the experiment | 63 |
| Fig.4.3 | View of Stainless Steel Mesh | 66 |
| Fig.4.4 | Dripping With 5% NaCl Solution | 66 |
| Fig.4.5 | Top View of Beam Showing Terminals for Active Protection | 68 |
| Fig.4.6 | ACM Setup Used for Electrochemical Monitoring | 69 |
| Fig.4.7 | Half Cell Arrangement | 70 |
| Fig.4.8 | Guard Ring Arrangement | 71 |

| | | |
|---------|---|----|
| Fig.5.1 | Variation of half-cell potential with time for slab C-1 | 73 |
| Fig.5.2 | Variation of half-cell potential with time for slab C-2 | 74 |
| Fig.5.3 | Variation of half-cell potential with time for slab C-3 | 75 |
| Fig.5.4 | Longitudinal crack along the length of rebar | 76 |
| Fig.5.5 | Variation of LPR with time for slab C-1 | 78 |
| Fig.5.6 | Variation of LPR with time for slab C-2 | 79 |
| Fig.5.7 | Variation of LPR with time for slab C-3 | 80 |

LIST OF TABLES

| Sr. No. | Description | Page No |
|---------|---|---------|
| 1 | Testing conditions of concrete specimens | 22 |
| 2 | Typical set of model input parameters | 38 |
| 3 | Nomenclature of specimens tested for a period of 2-6 months | 45 |
| 4 | Test specimens | 59 |
| 5 | Test samples | 53 |
| 6 | Physical properties of Cement | 60 |
| 7 | Physical Properties of Fine Aggregates | 61 |
| 8 | Sieve Analysis of Fine Aggregate | 61 |
| 9 | Physical Properties of Coarse Aggregates | 62 |
| 10 | Sieve Analysis of Coarse Aggregates | 62 |
| 11 | Properties of Reinforcing Bars Used for Casting of RC Beam | 62 |
| 12 | Properties of CFRP Sheets | 63 |
| 13 | Properties of Saturant | 64 |
| 14 | The ASTM Interpretation of Half-Cell Potential Readings | 70 |

CHAPTER 1 INTRODUCTION

1.1 REINFORCED CONCRETE

Reinforced concrete (RC) is an extremely popular construction material. It has proven to be successful in terms of both structural performance and durability. Because of the nature and role of concrete in the creation, rehabilitation and regeneration of the infrastructure system of any country, Reinforced concrete plays a very important part in a nation's economic development. Lack of durability of Reinforced concrete structures has thus not only massive economic implications to a nation's well-being, but it is also one of the greatest threats to sustainable growth of concrete and construction industries.

Whatever the source of deterioration and the mechanism of its development, corrosion of embedded reinforcement is recognized as the major problem affecting the durability of concrete structures. It has been found that 40% failure of structures is on account of corrosion of embedded steel in concrete (Sethy, 2005). Therefore, corrosion control of steel reinforcement is a subject of paramount importance. Reinforcing steel in good quality concrete does not corrode even if sufficient moisture and oxygen are available. This is due to the spontaneous formation of a thin protective oxide film (passive film) on the steel surface in the highly alkaline pore solution of the concrete. When sufficient chloride ions (from deicing salts or from sea water) have penetrated to the reinforcement or when the p_H of the pore solution drops to low values due to carbonation, the protective film is destroyed and the reinforcing steel is depassivated.

Corrosion is a form of damage which is often insidious and hidden until striking at the worst moment of a system operation. The reason of these phenomena is explainable with the mechanism of corrosion. When reinforcement corrodes, the corrosion products generally occupy considerably more volume than the steel. The magnitude of this increase in volume varies approximately 2 or 3 times the volume of the original material. As a result, the corrosion products produce an internal stress that destroys the neighbouring concrete under tensile stress.

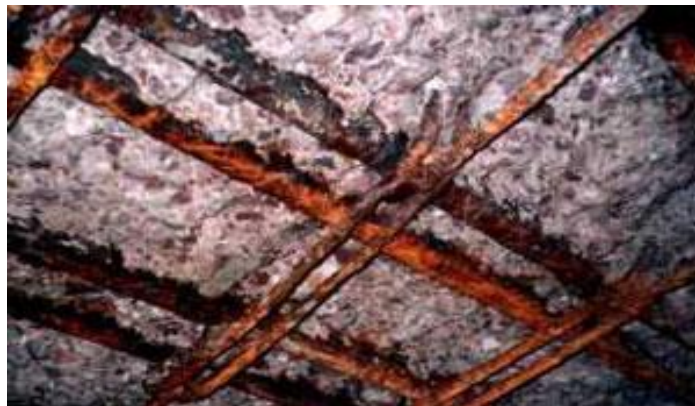


Fig.1.1 Corrosion in Reinforced concrete structures

Although corrosion of steel may not immediately affect the integrity and the ultimate load carrying capacity of a Reinforced concrete structural member, it is the most complex, insidious and destructive form of damage. Once it starts, it is almost impossible to stop the process until eventually the safety, stability and design service life are all drastically reduced with time.

1.2 CORROSION PROCESS

Steel in concrete is normally protected from corrosion by a passive film of iron oxides on the steel surface resulting from the natural alkaline environment of the concrete. The passive film is chemically stable in the absence of carbonation and chloride ions. The ingress of chloride ions (Cl^-) to the level of the steel reinforcing bars destroys the passive film and initiates corrosion. This makes reinforced concrete structures in coastal areas and/or marine environments vulnerable to damage by corrosion of steel reinforcement. Reinforced concrete infrastructures located in cold environments are also susceptible to corrosion damage due to the use of deicing salts. Carbonation penetrates concrete cover and destroys the passive film by neutralizing alkalinity of concrete. Once corrosion is initiated, electrochemical reactions occur, leading to the formation of expansive corrosion products that create tensile stresses in the concrete surrounding the corroding steel reinforcing bar. This results in concrete cracking and spalling, which aggravates the progressive damage, thus affecting the durability of the structure.

It is well known that if bright steel is left unprotected in the atmosphere a brown oxide rust quickly forms and will continue to grow until a scale flakes from the surface. In the concrete structures, reinforcing steel-bars (rebars) normally do not corrode because of a passive film formed on the surface of rebar in concrete of high pH. When chloride concentration at the level of rebar in concrete, however, exceeds the threshold value for corrosion, the passive film is destroyed and corrosion is initiated in rebar. The electro-chemical reaction continues with supplying oxygen and water. Then, due to expansion of corrosion products, corrosion-induced cracks are generated in concrete.

Sound concrete is an ideal environment for steel but the increased use of deicing salts and the increased concentration of carbon dioxide in modern environments principally due to industrial pollution, has resulted in corrosion of the rebar becoming the primary cause of failure of this material. The scale of this problem has reached alarming proportions in various parts of the world.

Carbonation of concrete or penetration of chlorides into the concrete, are the major causes of reinforcement corrosion. Chlorides in concrete either penetrate from the surrounding chloride-bearing environment (such as moisture, oxygen, humidity, temperature, bacterial attack, stray currents, etc.) or contribute from the concrete ingredients (such as concrete quality, w/c ratio, cement content, impurities in the concrete ingredients, presence of surface cracks, etc).

1.2.1 CAUSES OF CORROSION

Following are the two most common contributing factors leading to reinforcement corrosion:

- (i) Localized breakdown of the passive film on the steel by chloride ions called chloride attack.
- (ii) General breakdown of passivity by neutralization of the concrete, predominantly by reaction with atmospheric carbon dioxide called carbonation.

These major factors along with various other factors that lead to rebar corrosion are explained in detail in the following sections.

1.2.1.1 CARBONATION

Carbon dioxide, which is present in the air at around 0.3 per cent by volume, dissolves in water to form a mildly acidic solution. This forms within the pores of the concrete, here it reacts with the alkaline calcium hydroxide forming insoluble calcium carbonate. The pH value then drops from more than 12 to about 8.5.

In the case of carbonation, atmospheric carbon dioxide (CO₂) reacts with pore water alkali according to the generalized reaction,



It consumes alkalinity and reduces pore water pH to the 8–9 range, where steel is no longer passive.

The carbonation process moves as a front through the concrete, on reaching the reinforcing steel, the passive layer decays when the pH value drops below 10.5. If the carbonated front penetrates sufficiently deeply into the concrete to intersect with the concrete reinforcement interface, protection is lost and, since both oxygen and moisture are available, the steel is likely to corrode. The extent of the advance of the carbonation front depends, to a considerable extent, on the porosity and permeability of the concrete and on the conditions of the exposure.

1.2.1.2 CHLORIDE

The passivity provided by the alkaline conditions can also be destroyed by the presence of chloride ions, even though a high level of alkalinity remains in the concrete. The chloride ion can locally de-passivate the metal and promote active metal dissolution. Chlorides react with the calcium aluminate and calcium aluminoferrite in the concrete to form insoluble calcium

chloroaluminates and calcium chloroferrites in which the chloride is bound in non-active form. However, the reaction is never complete and some active soluble chloride always remains in equilibrium in the aqueous phase in the concrete. It is this chloride in solution that is free to promote corrosion of the steel. At low levels of chloride in the aqueous phase, the rate of corrosion is very small, but higher concentration increases the risks of corrosion.

1.2.1.3 WATER-CEMENT RATIO

The porosity and the rate of penetration of deleterious species are directly related to the water-cement ratio (w/c) ratio. For high-performance concretes, the ratio is generally less than 0.40 and can be as low as 0.30 with the use of suitable water-reducing admixtures. In general, a reduced w/cm results in improved corrosion resistance.

1.2.1.4 LOW CONCRETE TENSILE STRENGTH

Concrete with low tensile strength facilitates corrosion damage in two ways. First, the concrete develops tension or shrinkage cracks more easily, admitting moisture and oxygen, and in some cases chlorides to the level of the reinforcement. Second, the concrete is more susceptible to developing cracks at the point when the reinforcement begins to corrode.

1.2.1.5 MOISTURE

If the surface of the concrete is subjected to long-term wetting, the water will eventually reach the level of the reinforcement, either through diffusion through the porous structure of the concrete, or by traveling along cracks in the concrete. This moisture reacts with Carbon dioxide and form a mildly acidic solution. This mildly acidic solution is responsible for initiating the corrosion in reinforced concrete.

1.2.2 MECHANISM OF CORROSION

The corrosion process that takes place in concrete is electrochemical in nature. Corrosion will result in the flow of electrons between anodic and cathodic sites on the rebar. For corrosion to occur, four basic elements are required:

- Anode – site where corrosion occurs and current flows from.
- Cathode – site where no corrosion occurs and current flows to.
- Electrolyte – a medium capable of conducting electric current by ionic current flow (i.e. soil, water or concrete).
- Metallic Path – connection between the anode and cathode, which allows current return and completes the circuit.

The anode is the location on a steel reinforcing bar where corrosion is taking place and metal is being lost. At the anode, iron atoms lose electrons to become iron ions (Fe^{+2}). This oxidation reaction is referred to as the anodic reaction. The cathode is the location on a steel reinforcing bar where metal is not consumed. At the cathode, oxygen in the presence of water, accepts electrons to form hydroxyl ions (OH^-). This reduction reaction is referred to as the cathodic reaction. The electrolyte is the medium that facilitates the flow of electrons (electric current) between the anode and the cathode. Concrete, when exposed to wet and dry cycles, has sufficient conductivity to serve as an electrolyte. Fig.1.2 illustrates the corrosion cell for a steel reinforcing bar embedded in concrete where the anode and the cathode are on the same steel reinforcing bar.

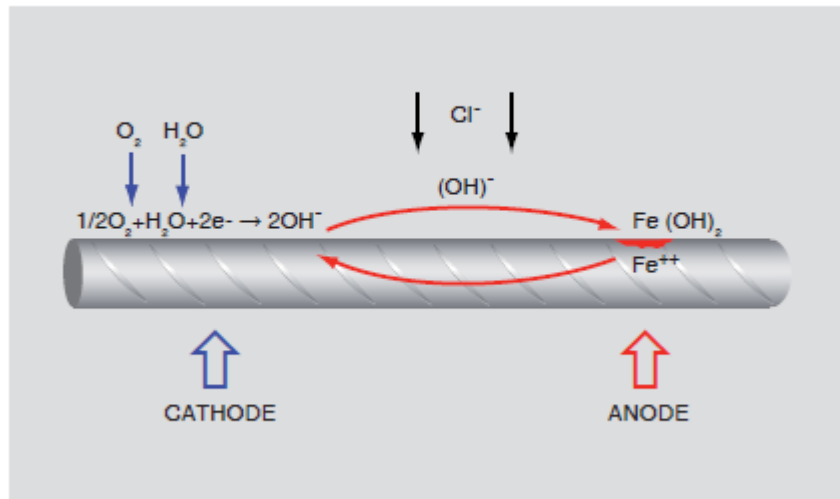


Fig.1.2 Local-cell corrosion [Source: www.vc-austria.com]

The corrosion of steel in concrete in the presence of oxygen but without chlorides takes place in several steps:

At the anode, iron is oxidized to the ferrous state and releases electrons



These electrons migrate to the cathode where they combine with water and oxygen to form hydroxyl ions



The hydroxyl ions combine with the ferrous ions to form ferrous hydroxide



In the presence of water and oxygen, the ferrous hydroxide is further oxidized to form Fe_2O_3



The anodic and cathodic reactions described above take place at the anode and the cathode, respectively. Currents flow through concrete from the cathode to anode by ion flow and through the reinforcing steel from the anode to the cathode by electron flow.

Two types of corrosion cells develop within concrete: microcells and macrocells. When a microcell develops within concrete, the anode is very close to the cathode on the same reinforcing bar as shown in figure 1.3. Carbonation-induced corrosion usually occurs on a microcell. When a macrocell develops, the anode and cathode are often well separated as shown in figure 1.4. Chloride-induced corrosion is prone to development of macrocells.

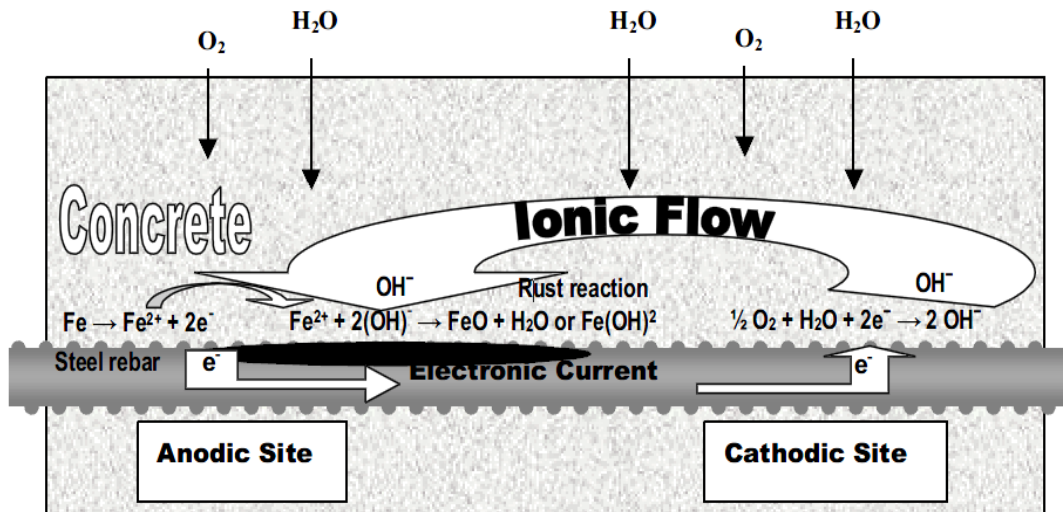


Fig.1.3 Microcell corrosion [Source: Bennett et al. 1993]

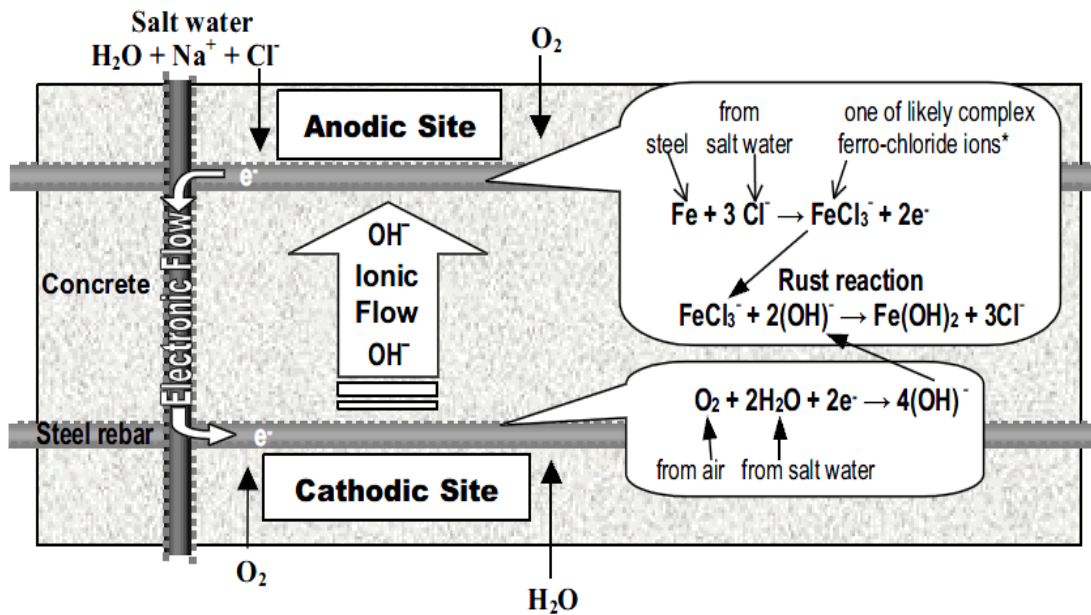


Fig.1.4 Macro cell Corrosion [Source: Bennett et al. 1993]

Corrosion of steel reinforcing bars embedded in concrete may be due to a combination of macro cells and micro cells.

When carbon dioxide (CO₂) from the atmosphere penetrates concrete and dissolves in the pore solution, carbonic acid is formed. This acid reacts with the alkali in the cement to form carbonates and to lower the pH of the concrete. When the alkalinity reaches a low enough level, the steel reinforcing bar becomes depassivated and in the presence of sufficient water and oxygen, corrosion is initiated and propagated. However carbonation advances very slowly in sound concrete and is generally not a big factor in corrosion initiation.

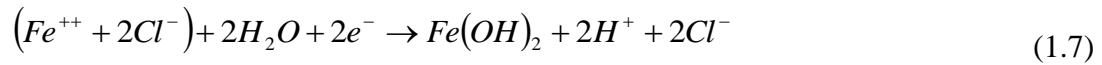
The concentration of chlorides in concrete is not uniform due to the heterogeneity of the concrete. The chlorides enter the concrete from the exposed surface. These differences in chloride concentrations establish anodes and cathodes on individual steel bars and result in the formation of micro cells.

The corrosion of steel in concrete in the presence of chlorides, but with no oxygen (at the anode), takes place in several steps:

At the anode, iron reacts with chloride ions to form an intermediate soluble iron-chloride complex



When the iron–chloride complex diffuses away from the bar to an area with higher pH and concentration of oxygen, it reacts with hydroxyl ions to form $Fe(OH)_2$. This complex reacts with water to form ferrous hydroxide.



The hydrogen ions then combine with electrons to form hydrogen gas



As in the case of corrosion of steel without chlorides, the ferrous hydroxide, in the presence of water and oxygen, is further oxidized to form Fe_2O_3



The corrosion products resulting from the corrosion of steel reinforcing bars occupy a volume five to ten times that of the original steel. This increase in volume induces stresses in the concrete that result in cracks, delamination and spalls. If left untreated, the process continues which further accelerates the corrosion process by providing an easy pathway for water and chlorides to reach the steel until the concrete becomes structurally unsound as shown in Fig.1.5.

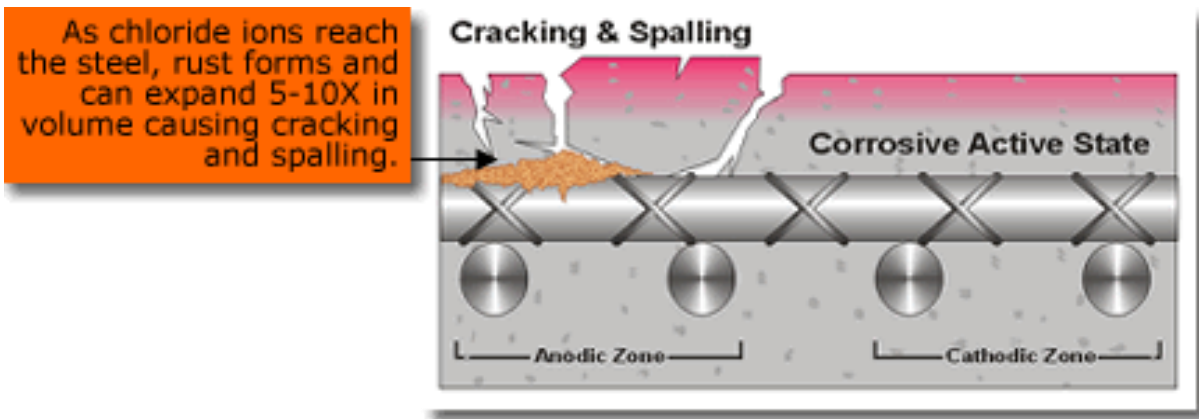


Fig.1.5 Cracking and spalling of concrete due to penetration of chloride ions

The minimum chloride ion concentration needed to initiate corrosion of steel reinforcing bars is also called the chloride threshold. Although the concept of chloride threshold is generally accepted, there is agreement on what the threshold value is. Several factors influence the chloride

threshold value: the composition of the concrete (resistivity), the amount of moisture present, and the atmospheric conditions (temperature and humidity). The threshold concentration depends on the pH level and the concentration of oxygen. When chlorides are uniformly distributed, higher concentrations are needed to initiate corrosion. The amount of tricalcium silicate (C_3S) present in the cement influences the threshold level. Regardless of what concentration of chloride ions is needed to initiate corrosion, an increase in the chloride ion concentration increases the probability that corrosion of steel reinforcing bars will occur.

1.2.3 EFFECTS OF REBAR CORROSION

There are several factors that affect the corrosion process. The corrosion process leads to several coupled effects such as:

1. Longitudinal cracking of concrete cover due to expansive corrosion products.
2. Steel cross section reduction.
3. The degradation of steel–concrete bond.

As a result of these effects, the service life and the load-bearing capacity of reinforced concrete elements are considerably reduced. The corrosion rate is a key element in determining the time from corrosion initiation to corrosion cracking, which is usually used to predict the functional service life of a corroded RC structure. After corrosion initiation, the corrosion rate depends mainly on the availability of oxygen and moisture at the cathode and on the concrete resistivity, which is mainly affected by the internal moisture content and concrete porosity. The initiation and continuation of the corrosion process are controlled by the environment in the concrete that is surrounding the steel reinforcing bars.

CHAPTER 2 CATHODIC PROTECTION OF REINFORCED CONCRETE STRUCTURES

2.1 INTRODUCTION

Cathodic protection (CP) has been used since the early 1800s to protect ship hulls from corrosion. During the early 1920's, the use of cathodic protection spread to oil and gas pipelines and underground steel storage tanks. Today, federal regulations in the USA require that all underground steel pipelines and underground storage tanks containing and/or transporting hazardous liquids or gases must be cathodically protected to prevent corrosion. It has been more than 30 years since the first cathodic protection system was installed on a reinforced concrete bridge deck in 1973 near Sly Park, California. Today it is estimated that over 2 million m² of concrete structures are cathodically protected worldwide (www.corrpro.com).

2.2 THEORY OF CATHODIC PROTECTION

Cathodic corrosion protection method attacks-in contrast to other systems-the problem at its roots. The success of the method rests on the connection between the potential of steel and the corrosion rate. The potential of the reinforcement is brought to a stable passive state through installation of a negative protective current. Through the formation of hydroxide ions on the reinforcement the protective passive layer is restored.

2.2.1 CATHODIC PROTECTION

Cathodic protection is a method based on the knowledge that the corrosion of a metal is a result of an electrical current flowing from one part of the metal to the other. Corrosion occurs where current leaves the steel. In the corrosion circuit, those locations where the current leaves the rebar are called the anodes or anodic areas, as opposed to other nearby areas on the rebar which receive current are called the cathodes or cathodic areas. Cathodic protection works on the principle of reversing the natural corrosion current flow and thereby protecting the anode. The reversing of corrosion current flow is achieved by giving a negative potential to the rebar either by introducing a direct current or by introduction of sacrificial anode in the system. Cathodic protection is a well-proven method of preventing corrosion of buried, partially buried, and submerged metallic structures. A properly designed and installed system will be able to prevent the corrosion of the structure as a whole. This technique is considered to be the most preferred technique for chloride corrosion of reinforcing steel.

Cathodic protection of reinforced concrete will result in the following conditions.

- A shift of the reinforcing steel potential in the negative direction.

- Production of hydroxyl ions at the reinforcing steel (cathode) which in turn increases alkalinity and helps build up passive layer.
- Flow of chloride ions from the cathode toward anode, resulting in a reduction of chloride content at the reinforcing steel surface.

The benefit of cathodic protection for a new reinforced concrete structure can be shown in its ability to reduce chloride ion migration toward the reinforcing steel. The chloride ion itself is negative and will be repelled by the negatively charged cathode. The generation of hydroxyl ions will help maintain a high degree of alkalinity and a passive layer at the reinforcing steel surface. By properly designing and executing cathodic protection, corrosion of the reinforcing steel will be eliminated and structural deterioration as a result of corrosion will not commence.

2.2.2 TYPES OF CATHODIC PROTECTION

There are two types of cathodic protection: sacrificial cathodic protection, which works on a "passive" method of protection, and impressed current cathodic protection, which is an "active method of protection."

Sacrificial cathodic protection which is also known as: Galvanic cathodic protection is based on the principle of dissimilar material corrosion and the relative position of specific metals in the galvanic series. Commonly used sacrificial anodes for reinforced concrete are cast zinc and aluminium anodes and thermally sprayed zinc-aluminium-indium alloys. Cast anodes are used for protecting buried or immersed concrete structures and thermally sprayed anodes are used for cathodic protection of atmospherically exposed concrete structures. Sacrificial cathodic protection has the advantage of no auxiliary power supply but has the disadvantage of the anode being dissolved and consumed. This system is commonly used for rehabilitation of salt contaminated existing concrete structures. This method has a shorter life expectancy.

Cathodic protection by the impressed current method uses a power supply or rectifier and an anode such as catalyzed titanium, to protect the metal or structure by making it a cathode. A low voltage direct current is driven from the anode through the concrete to the surface of the steel. This method of Cathodic protection is used both for the rehabilitation of existing structures, as well for the protection of new structures. For new structures, the cathodic protection system will be incorporated in the member at the time of construction. This method has a longer life expectancy and is known to be the best method for the protection of concrete structures. Cathodic protection is based on the knowledge that corrosion of any metal is a result of an electrochemical current flowing from one part of metal to the other. The cathodic protection process uses the application of direct current to the rebar using an introduced anode material in sufficient quantity to reverse or counteract the natural corrosion current.

2.2.3 MERITS AND DEMERITS OF CATHODIC PROTECTION

The expected advantages and limitations with the implementation of cathodic protection include the following.

Advantages

- The installation work takes a short time compared to most other repair techniques and often the structure can be used for its intended purpose during the renovation works.
- The extensive costs of traditional concrete renovation are reduced as sound concrete does not have to be removed, even if it is chloride contaminated.
- There is a lesser requirement for structural stabilization or support as large volumes of concrete do not normally have to be removed.
- Steel reinforcement can be protected from further corrosion to a depth considerably greater than the first layer of reinforcement.

Limitations

Cathodic protection of the reinforcement has only one purpose. This is to arrest the corrosion of the reinforcement steel in the concrete. This means it has the following limitations.

- The residual load bearing capacity of the reinforcement must still be sufficient after the corrosion has been halted; otherwise additional strengthening must be included in the repair.
- Cathodic protection does not solve any other problems with the structure such as crumbling concrete, construction defects, or changes in statutory requirements.
- In order to apply cathodic protection, the structure must have substantial electrical continuity of the reinforcement. Normally this does not lead to any significant problems in applying cathodic protection.
- Cathodic protection cannot be used to protect on pre or post tensioned tendons in ducts, as the protection current cannot pass through the dielectric shield that the duct forms. The outside of a steel duct can be protected if there are concerns about the ducts perforating.

2.3 PRINCIPLE OF CATHODIC CORROSION PROTECTION

The principle of cathodic protection is in connecting an external anode to the metal to be protected and the passing of an electrical dc current so that all areas of the metal surface become cathodic and therefore do not corrode. The external anode may be a galvanic anode, where the current is a result of the potential difference between the two metals, or it may be an impressed current anode, where the current is impressed from an external dc power source. In electro-chemical terms, the electrical potential between the metal and the electrolyte solution with which

it is in contact is made more negative, by the supply of negative charged electrons, to a value at which the corroding (anodic) reactions are stifled and only cathodic reactions can take place. The cathodic protection of reinforcing carbon steel in reinforced concrete structures can be applied in a similar manner. Cathodic protection can be achieved in two ways:

- by the use of galvanic (sacrificial) anodes
- by impressed current

Galvanic anode systems employ reactive metals as auxiliary anodes that are directly electrically connected to the steel to be protected. The difference in natural potentials between the anode and the steel, as indicated by their relative positions in the electro-chemical series, causes a positive current to flow in the electrolyte, from the anode to the steel. Thus, the whole surface of the steel becomes more negatively charged and becomes the cathode. The metals commonly used, as sacrificial anodes are aluminum, zinc and magnesium. These metals are alloyed to improve the long-term performance and dissolution characteristics. Impressed-current systems employ inert (zero or low dissolution) anodes and use an external source of dc power (rectified ac) to impress a current from an external anode onto the cathode surface. The connections are similar for the application of cathodic protection to metallic storage tanks, jetties, offshore structures and reinforced concrete structures (Berkley and Pathmanaban 1990).

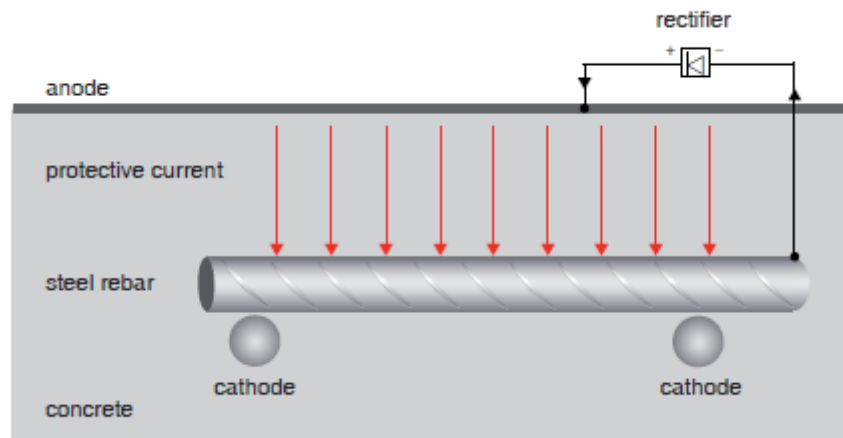


Fig.2.1 The principle of cathodic corrosion protection [Source: www.vc-austria.com]

2.4 OPERATING A CATHODIC PROTECTION SYSTEM

Cathodic protection involves the establishment of a small DC current from an external anode, through the concrete to the rebar. The current charges the steel negatively and it becomes cathodic, i.e. not corroding. By passing this very small current from a supplemental anode to embedded reinforcement, corrosion can be halted for an indefinite period. The supplemental anode transmits electrons which are consumed at the reinforcing steel. Other benefits of this

process include the production of hydroxyl ions at the steel surface (thus reverting the pore water in the concrete to an alkaline state) and the gradual migration of the negatively charged chloride ions towards the new anode and away from the steel.

When a cathodic system is energized, the rebars are polarised to the 'protection potential', which is the electrochemical potential at which the corrosion rate becomes negligible. This requires a negative potential shift, from the natural (as found) potential, of the order of 100-300 mV and it is generally defined as that which will give a potential decay of at least 100 mV in the 4 to 24 hours following complete disruption of the DC current.

Before designing a cathodic protection system for a reinforced concrete structure, various parameters need to be established, mainly by non-destructive testing. The electrical continuity of the reinforcement must be established, to ensure that all bars will be protected. The electrical resistivity of the concrete is measured in order to determine operating voltages. The location and extent of the corrosion damage (anodic areas) are determined by means of a half-cell potential survey. The applied current densities are calculated on the basis of steel surface area and extent of corrosion damage. Typical initial cathodic protection current densities in chloride contaminated structures are in the range of 1 to 20 mA/m² of steel surface. During the operation of the cathodic protection system, the initial current density can be reduced as chloride migration away from the rebar proceeds and the pH level increases. Reactions at the anode surface in a cathodic protection system generate acidity and the anode current density must therefore be kept within certain limits in order to prevent excessive production of acidity. A maximum anodic current density of 110 mA/m² is recommended by National Association of Corrosion Engineers (NACE). It is also necessary to ensure that no steel is polarized to a more negative potential than -1150 mV versus a copper/copper sulphate reference electrode (CSE) to avoid the possibility of hydrogen embrittlement of the steel surface.

Cathodic protection systems are generally powered by mains electricity converted to DC at the required voltage by a transformer/rectifier. The positive terminal is connected to the anode and the negative to the reinforcing steel. Solar power can be used at remote sites. Various criteria have been proposed to establish the effectiveness of a cathodic protection system once it has been energized. These included parameters such as:

Potential shift;

Potential decay;

Operating potential; and Current-potential relationship.

The criterion generally accepted today is that the system is performing effectively if the 100mV potential decay has been achieved. After commissioning, this performance is monitored by means of reference cells embedded in the concrete close to the reinforcement. The half cells may be composed of silver/silver chloride, activated titanium, zinc or other materials, the primary requirements being stability, accuracy and longevity. The operating voltage and current are also

monitored and adjusted as necessary; this can be done manually at the control cabinet, through a local computer or by modem connection to a remote computer. It is normal for a cathodic protection system to be tuned over the first two years or so of operation as potentials stabilize and current demands reduce. Monitoring of protection levels and trends is therefore required at intervals of three or six months in the initial stages and annually thereafter until the system has balanced and needs only regular checking of its operational status.

2.5 IMPRESSED CURRENT CATHODIC PROTECTION

Impressed current cathodic protection (ICCP) systems are another type of electrochemical corrosion mitigation system. Impressed current cathodic protection systems start with the installation of permanent anodes. Some of favorable Conditions for Impressed Current Cathodic Protection are given below.

- Remaining structure service life is relatively long (> 30 years).
- AC power is available.
- High level of cathodic protection current density is required due to high chloride concentration (> 1500 ppm) and/or high rebars density.
- Owner's ability to monitor and maintain rectifiers or willingness to contract the maintenance responsibility to an outside source.
- Concrete structure is exposed to cyclical wet and dry conditions.
- Concrete structure is not subject to occasional wetting.

An external DC power source is applied with the anode being connected to the positive (+) terminal and the embedded reinforcing steel connected to the negative (-) terminal. Sufficient current is delivered to the steel to overcome the natural corrosion activity.

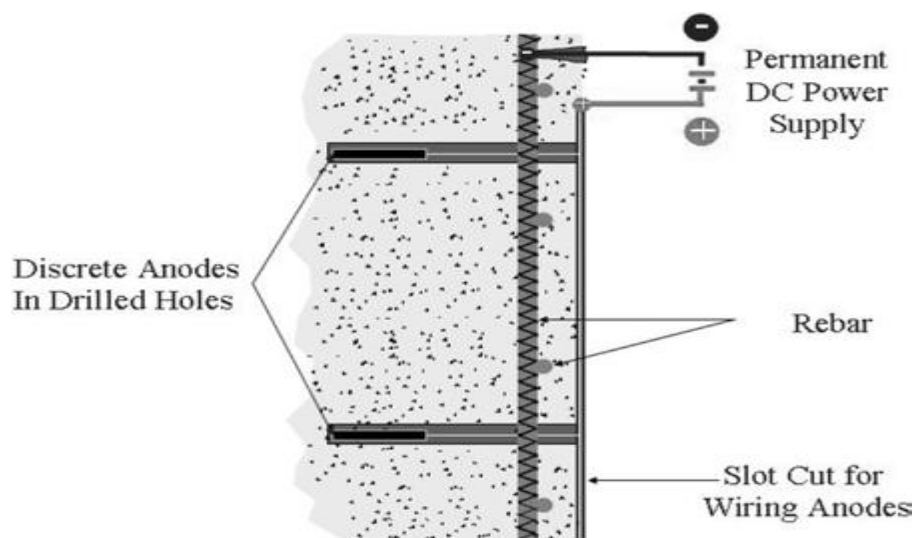


Fig.2.2 Impressed current cathodic protection installation process using discrete anodes
[Source: Ball and Whitmore 2005]

Impressed current system is considered to be providing cathodic protection when the system polarises the reinforcing steel sufficiently to result in a 100 mV depolarization after the system is turned off. Properly designed, installed, and maintained Impressed current cathodic protection systems can provide long term protection to the reinforcing steel. Impressed current cathodic protection systems can be a cost effective option when used to protect large areas and the initial costs are spread over time. Installed Impressed current cathodic protection systems are monitored and adjusted over time if the system is not continuing to provide corrosion protection to embedded steel. Because the system requires an external power source, periodic inspection and maintenance of the system is required. If the implementation of a long-term system monitoring and maintenance program is unlikely, other corrosion mitigation strategies should be considered.

2.5.1 ANODE SELECTION FOR IMPRESSED CURRENT CATHODIC PROTECTION

The anode is one of the most critical components of the cathodic protection system. It is usually the most expensive component and several options may exist. In theory, given that all other parameters are defined, the anode is the primary electrode that is used to discharge current into the electrolyte and achieve cathodic protection of the reinforcing steel. In reality, however, different anode systems are more suitable for certain applications. Installation methods may also play a major role in anode selection. Where a large amount of concrete repair is required, an anode directly attached to the exposed reinforcing steel and installed in the repair or overlay area may be preferable. Where access to the lower surface of a structural component is limited, such as the soffit of a beam or pile cap in a marine jetty, a discrete anode system installed in drilled holes may be more appropriate. The selection of the anode system must also be considered when a particular maintenance requirement exists. For example, in industrial plants where frequent shutdowns occur, access to the work area is critical and therefore the anode system must be robust enough to withstand periodic maintenance activities that may occur. The selection of the anode type is also dependent on the remaining life of the structure. Requirements for excessive life of the cathodic protection system components may sometimes be required for no reason other than a longer life is perceived to be more desirable. Design life should therefore reflect the remaining service life of the structure.

Conductive Coating One of the first anode systems used on concrete structures is the conductive coating or carbon loaded paint. One of the advantages of the conductive coating is its ability to be applied easily to irregular surfaces, such as deck soffits and bridge piers. The paint is sprayed, rolled or brush applied over a platinum niobium wire, at a thickness of approximately 300 microns DFT. The wires are typically spaced at 3-6 m intervals. The conductive coating is black, so a decorative paint is required as an overcoat. Conductive paint systems are particularly subject to short circuits from exposed steel such as rebar chairs that exist on the underside of structural elements. Furthermore long term durability in marine environments is suspect, especially in areas subject to surface wetting.

Arc Sprayed Zinc The technique of zinc metalizing as used in cathodic protection of reinforced concrete was first developed by the California Department of Transportation in 1983. The Oregon Department of Transportation now use arc sprayed zinc Impressed current cathodic protection to control corrosion on historic arch bridges along the Pacific coastal highway. The process of metalizing involves the melting of a metal or alloy in the form of wire, typically by a high amperage arc, and spraying the molten metal onto the concrete with compressed air. The zinc coating is typically applied to a dry film thickness of 300-400 microns. The system works similar to a conductive coating, except the platinized niobium wire is replaced with a metal pad. Testing arc sprayed zinc systems through electrochemical aging has shown that bond strengths actually increase with time due to secondary mineralization of the zinc reaction products. As with conductive coatings, arc sprayed zinc Impressed current cathodic protection systems are also subject to short circuits from exposed steel at the concrete surface.

Titanium Anode Mesh Encapsulation Catalyzed titanium mesh anodes consist of expanded titanium mesh with a mixed metal oxide catalyst applied to the surface. The mesh is typically fastened to the patched and prepared concrete surface using nonmetallic fasteners and then overlaid or otherwise encased in portland cement concrete. These systems are normally designed and installed such that the average anode current density does not exceed 110 mA/m^2 . As reported above, the life expectancy of these anodes can readily exceed 75 years. Power is delivered to the mesh via lead wires and titanium current distributor bars. Such systems perform well because the precious metal oxide coating is the active anode, which slowly oxidizes with time. Under normal anodic conditions, the titanium substrate will passivate and is not consumed. The anode is therefore considered dimensionally stable.

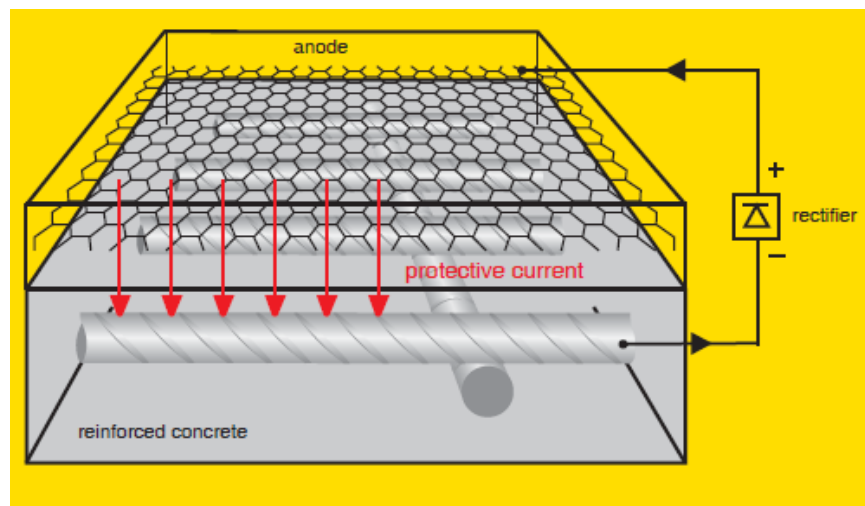


Fig.2.3 System design activated titanium anode mesh

[Source: www.vc-austria.com]

Titanium Anode Mesh Integral Pile Jacket System Another system known as the integral pile jacket cathodic protection system has been used on over 800 concrete bridge pilings in Florida. This system uses a prefabricated fiberglass jacket, which is supplied with the mesh anode attached to the inside of the jacket using special offsets. The jacket system is mounted to the piles using compression bands and the void between the jacket and concrete surface is filled with a cementitious grout. The systems installed with pile jackets have been successful in controlling corrosion on bridge piles in the splash and tidal zones. The jackets have the additional benefit of acting as electrical insulators, thus preventing the flow of current through seawater to submerged steel. Since the catalyzed titanium anodes have extremely low consumption rates and long life expectancy (i.e. > 75 years), life cycle costs are generally favorable regarding their use.

Titanium Ribbon Mesh Slotted System This system involves the use of a catalyzed titanium ribbon and a no shrink cementitious grout as the slot backfill. Ribbon mesh sizes are typically 13-mm and 19-mm wide. Slot spacing is dependent on steel density, but is typically 200-400 mm on center. A typical concrete slot is 10-mm wide by 25-mm deep for the 13-mm wide anode and 32-mm deep for the 19-mm wide anode. In areas of stalled and delaminated concrete, the ribbon can be attached to exposed rebar with plastic clips, and covered with shotcrete. Titanium current distributor bars provide continuity between the strips and are spot-welded to the ribbon mesh in the transverse direction. This system has been especially useful for concrete structures that cannot tolerate the additional dead load of a concrete overlay or where bonding of the overlay for mesh encapsulation is a concern. Sufficient cover over the rebar must be present, or the steel must be located with a pachometer so the slots can be installed between the bars.

Discrete Anode System The discrete anode system is one of the most cost effective systems for beams, piles and columns. The anodes are relatively easy to install and do not require extensive saw cutting or use of concrete overlays. The discrete anodes are typically inserted into drilled holes that are 20-25 mm in diameter and backfilled with a non-shrink cementitious grout. The length and spacing of the anode is dependent on the steel density and protection requirements for cathodic protection. Several systems are available. These include a discrete titanium ribbon mesh system, ceramic anodes and platinized titanium wire with a carbon rich backfill. Current densities at the anode-concrete interface should be limited to 220 mA/m^2 , otherwise degradation of the cement paste at the anode-concrete interface may result.

Thermally Sprayed Titanium Thermally sprayed titanium anodes for cathodic protection of reinforced concrete have been applied to several structures in the field on a trial basis. The first installation was in 1994 on the Depoe Bay Bridge in Oregon. The results of the field trials to date indicate that the systems are operating at relatively low output levels and are achieving criteria for cathodic protection of steel in concrete. Arc sprayed titanium is somewhat more difficult to apply than arc sprayed zinc, due to the hardness of the wire and subsequent wear of the spray tips. Titanium, however, is relatively inert in the environment and there are no known

environmental impacts using this type of system. In theory, the anode has very long life expectancy (i.e., >100 years) and it is possible that the liquid catalyst may be reapplied to the titanium surface in the future, if needed.

Cast iron and MMO titanium anodes Impressed current systems using cast iron and mixed metal oxide (MMO) titanium anodes have been used to cathodically protect the immersed section of concrete structures below mean low water and portions of the tidal zone. Both tubular and rod type anodes have been used. The anodes are installed individually in the mud or in specially constructed sleds to distribute current through the water to the concrete reinforcement. Heavy cables are fed from the anodes, through the mud to the rectifier.

Inert Anodes When the remaining life of a structure is considered long (i.e., > 30 years), an impressed current system using an inert anode is generally recommended, since these anodes do not require replacement during the remaining life of the structure. Activated titanium anode mesh, titanium ribbon mesh and discrete titanium or conductive ceramic anodes are available. Life expectancy may vary between 25 and 100 years depending on the type of anode and catalytic coating that is used.

Carbon Based Anodes Carbon based anodes include conductive polymers, a carbon based paste that is used as a backfill around discrete anodes, surface applied conductive coatings and carbon fibers that are dispersed in a cementitious overlay. Although the initial cost of carbon-based anodes may be less than titanium or ceramic anodes, durability and performance problems may develop over time. These may include:

- When a carbon-based anode (not an inert material) discharges cathodic protection current, the anodic reaction involves oxidation of the carbon. As a result, the conductivity of the anode material may decrease with time, resulting in failure of the anode.
- Carbon-based anodes are generally more subject to chlorine gas evolution at lower levels of current than titanium or ceramic based anodes. Acid may develop in sufficient quantity to dissolve the cementitious paste around the carbon-based anode, resulting in disbondment of the anode.
- Surface applied impressed current anodes, such as carbon-based conductive coatings, are particularly subject to electrical short circuits at the concrete surface. The short circuits are due to exposed or partially embedded rebar chairs and wire ties that come in contact with the anode.
- Carbon-based conductive coatings may disbond from the concrete surface if exposed to excessive moisture (i.e., splashing water or leaking expansion joints) due to high anodic current discharge in the affected area. Also, in dry concrete conditions the anode may “dry-out” with time resulting in increased circuit resistance and high driving voltage at the rectifier.

CHAPTER 3 LITERATURE REVIEW

Bertolini et al. (2004) studied behaviour of a cementitious conductive overlay anode used for cathodic protection (CP) of steel in concrete. The anode is made of nickel-coated carbon fibers in a cementitious mortar. Tests were carried out on concrete specimens with two layers of rebars that simulated reinforced concrete slabs. Concrete was mixed with 350 kg/m³ of Portland cement, water-to-cement ratio of 0.5, 1850 kg/m³ of aggregate with maximum size of 15 mm; it was moist-cured at ambient temperature for 28 days. Each specimen had 22 parallel steel bars, 20 mm in diameter, placed at 20 and 140 mm from the anode, respectively, for the upper and lower bars. External copper wires electrically connected all the bars. An activated titanium pseudo-reference electrode was embedded in each specimen, on the central upper bar. A layer of 8–10 mm of a commercial conductive mortar for Cathodic protection anode was applied on the surface of the specimens.

Concrete specimens were chloride contaminated both by adding CaCl₂ to the mixing water of the concrete or conductive mortar and by ponding with a 5% NaCl solution on the upper surface of the specimens. Testing conditions are given in table 3.1. Cathodic protection was energized about 3 months after casting. Constant currents in the range between 10 and 100 mA/m² referred to the concrete surface covered by the anode were applied for a total of 24 months, divided in two periods as shown in table 3.1. Steel and anode potentials, as well as feeding voltage, were monitored. Four-hour decay and the distribution of current and potential were regularly measured. The maximum anode current output was evaluated. After the damage of the anode that occurred on the specimens energized at high current densities during the first 3 months of testing, the conductive overlay was repaired. The conductive mortar was removed and replaced for about 50 mm around the primary anode. A lower current density was then applied to these specimens.

Table 3.1 Testing conditions [Source: Bertolini et al. 2004]

| Mixed in chlorides (by mass of cement) | Specimen | Chloride ponding | Anodic current density (mA/m ²) | |
|--|----------|------------------|---|-------------|
| | | | 1-3 months | 4-24 months |
| 3% in the overlay | 1 | No | 10 | 10 (50) |
| | 2 | No | 50 | 50 |
| | 3 | No | 100 | 20 |
| None | 4 | Yes | 10 | 10 |
| | 5 | Yes | 50 | 20 |
| | 6 | Yes | 100 | 20 |
| 2% in the concrete | 7 | No | 100 | 20 |
| | 8 | Yes | 100 | 20 |
| | 9 | yes | 50 | 10 |

It was observed that specimen subjected to anode current density of 10 mA/m^2 have feeding voltages only slightly higher than 2 V. Anode current densities of 50 and 100 mA/m^2 led to an increase with time of the feeding voltage to values more than 5 V. This occurred in the first month of application of Cathodic protection in the specimens that were not subjected to chloride ponding. Specimens with chloride ponding initially showed feeding voltage values of 2–3 V. After about 2 months, when the ponding solution was removed, a sharp increase in the feeding voltage was observed and values higher than 5 V were soon reached. When the feeding voltage increased, an increase both in the anode potential and in the ohmic drop at the anode also occurred. The lowering of the steel potential (i.e. the cathodic polarization) increased as the anode current output increased. However, the potential of the polarized steel was rather constant.

The cementitious conductive coating for Cathodic protection studied in this work showed a satisfactory behaviour when a current density up to 20 mA/m^2 was applied for 2 years. Vice versa, when current densities of 50 or 100 mA/m^2 were applied, the cementitious matrix of the anode was destroyed in the vicinity of the primary anode due to the acidity produced by the anodic reaction after only 1–2 months of functioning. Based on these results, a maximum current density of $10\text{--}15 \text{ mA/m}^2$, referred to the surface of concrete covered by the anode, and a distance of 1 m between primary anodes can be suggested for a safe design. Substitution of the primary anode and patch repair of the surrounding conductive mortar could not remedy to the damage of the anode induced by high current supply.

Jing and Wu (2010) studied behavior of a new type of secondary anode material made of carbon fiber reinforced cement used for cathodic protection of steel in concrete was studied. The mechanical, electrical and electrochemical properties of this conductive mortar were investigated. Results indicate that the addition of carbon fiber enhances the strength and ductility of the mortar, as well as the electrical property. The anodic polarization behavior was tested on specimens immersed in aqueous solutions of saturated Ca(OH)_2 in the presence or absence of 3% NaCl.

Two different sizes of specimen were fabricated in the test. One is the cylindrical specimen, 30 mm in diameter and 30 mm in height, used for the study of electrochemical behavior of the conductive mortar. A primary anode, made of a 2 mm wire of titanium, was embedded in the axial position of the specimen. The upper and lower surfaces of the cylinders were then masked with epoxy resin. The surface ratio of the mortar and the primary anode was 15. The other is the rectangular bar specimen of size $40 \text{ mm} \times 40 \text{ mm} \times 160 \text{ mm}$, used for the electrical and mechanical test.

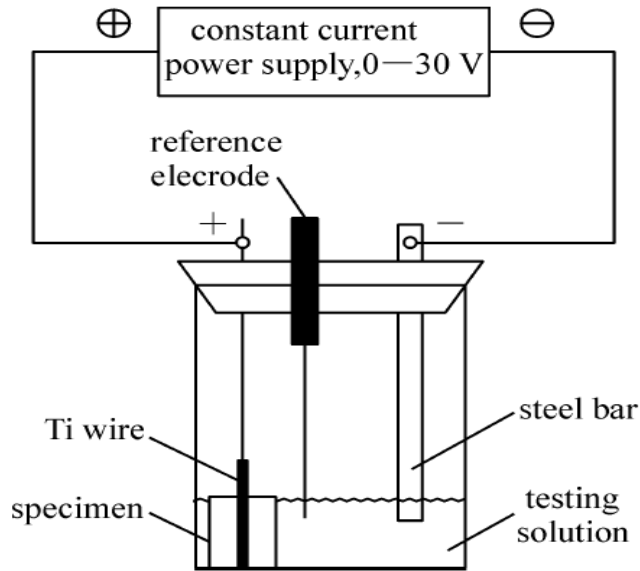


Fig.3.1 The schematic of the anodic polarization test setup
[Source: Jing and Wu 2010]

In order to improve the anodic polarization and shorten the experimental cycle, a designed current density of 200 mA/m^2 referred to the surface of the probe in contact with the testing solution was applied. The anode potential was measured periodically against a saturated calomel electrode (SCE). Fig.3.1 describes the test setup of the anodic polarization testing. Electrochemical Impedance Spectroscopy measurements were performed every 7 days to determine electrochemical parameter changes of conductive mortar. The measuring system was made up of three electrodes. The titanium wire in the axial position of probe was the working electrode. A mild steel bar was the auxiliary electrode, while the saturated calomel electrode served as the reference electrode. Measurements were performed in the galvanostatic mode in the 1 Hz to 100 kHz frequency range. Also, one should take into account the economic factor connected with the use of greater power of the cathodic protection station and a more rapid consumption of anode material, as well as a hazard of local increase of anode temperature.

Not only the fiber content, but also the solution composition influences the electrochemical behavior of conductive mortar. The one containing greater quantities of fiber is characterized by lower resistance and higher potential stability during anodic polarization. However, electrochemical property of mortar with higher fiber content is more inclined to deteriorate when chloride ions exist. The optimum fiber content in the conductive mortar should be in the range of 0.5% vol. to 0.7% vol. The obtained results confirm the possibility of using this new type of conductive overlay as anodes in cathodic protection systems of reinforced concrete structures.

Cramer et al. (1999) studied the stable operation of cobalt catalyzed thermal sprayed titanium anodes for cathodic protection (CP) of bridge reinforcing steel. The Cobalt catalyst dispersed into the concrete near the anode concrete interface with electrochemical aging to produce a more diffuse anode reaction zone. The titanium anode had a porous heterogeneous structure composed of a-titanium containing interstitial oxygen and nitrogen, and a phase thought to be Ti(O,N). Splat cooling rates were 10 to 150 K/s, and microstructures were produced by equilibrium processes at the splat solidification front. Nitrogen gas atomization during thermal spraying produced a coating with more uniform composition, less cracking, and lower resistivity than using air atomization.

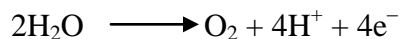
Thermal sprayed titanium anodes were applied using the twin-wire, arc-spray process. The feed wire was 3.2 mm diameter annealed grade 1 titanium wire. Spray parameters were electric arc, 36 to 40 V_{dc} and 300 A; atomizing gas, air or N₂ at 0.62 to 0.76 MPa spray orientation, normal to surface at a distance of 15 to 23 cm (6 to 9 in). The final titanium anode thickness was 50 to 150 mm (2-6 mils). Laboratory application to concrete slabs (5 cm thick), concrete plates (1.5 cm thick), and borosilicate glass plates was performed with the same hand-held spray gun mounted to an Oregon Department of Transportation robotic XY traversing device to achieve a more uniform coating thickness than hand spraying. Prior to spraying, concrete surfaces were lightly sandblasted to expose some aggregate and yield a medium sandpaper surface texture, and then blown free of dust. The borosilicate glass plates were degreased but not etched.

Anodes prepared using N₂ atomization had good conductivity and did not require carbon coating prior to electron beam microanalysis; anodes prepared using air atomization were carbon coated. Electrochemical aging was studied using catalyzed titanium anodes thermal sprayed on concrete slabs containing a steel mesh cathode. The experiments were conducted to determine changes occurring in anode bond strength, resistivity, and mechanical durability as a consequence of passing an electrical charge across the anode-concrete interface. In addition, measurements were made to determine the effect of aging on the chemistry of the anode-concrete interface and on anode operating performance and service life.

The catalyzed titanium anode serves solely as a current carrier to distribute charge to the reinforcing bar and as a support for the cobalt catalyst. In a basic environment, such as unaged concrete, the anode reaction is:



The consequence of this reaction is the loss of hydroxyl ions at the anode-concrete interface and a decrease in the interfacial pH. As this reaction progresses and the interface loses its basic character, the reaction becomes:



Water is a key constituent in both of these reactions, in the first reaction as a source of replenishing hydroxyl ions produced by ionization of water and in the second reaction as the primary reactant. Consequently, delivery of moisture to the anode by humid air, dew, fog, and precipitation is crucial to successful operation of the anode.

Laboratory concrete slabs were prepared to physically and mechanically approximate a section of a reinforced concrete structure in a thermal sprayed titanium anode cathodic protection system. The concrete slabs measured 23 by 33 by 5 cm (9 by 13 by 2 in.) and were cast with 3.2 cm concrete cover over No. 16 expanded steel mesh simulating the rebar. The concrete mix design approximated that used in Oregon's coastal bridges in the 1930s and had a water-cement ratio of 0.48. Sodium chloride was added to the concrete mix at 3 kg NaCl/m³ of concrete to approximate the present salt content of older coastal bridges in Oregon. Slabs were cured for four weeks in a moist room, and then air dried for one week. The top surface of each slab was prepared in the same way as concrete surfaces in the anode characterization part of the study, by sandblasting and then blowing free of dust. Prior to thermal spraying, the area around the wire that leads to the steel mesh was masked off to a distance of 2.5 cm to prevent electrical contact between the lead wires and the titanium anode to be applied. The slab surface was then thermal sprayed with titanium using robotic control and the same application conditions used in the anode characterization part of the study.

The titanium anode was catalyzed using a cobalt-nitrate amine complex, which was converted to cobalt oxide, Co₃O₄, during its application as an aqueous acidic solution (pH 3.47). The solution consisted of divalent and trivalent cobalt, contained a total of 60 g Co/L, with the divalent cobalt present as cobalt nitrate, the trivalent cobalt present as an amine complex, and a Co(III)/Co(II) ratio of 0.25. It was applied to the anode with the Impressed current cathodic protection system operating, that is, with the titanium anode polarized anodically to the rebar. Impressed current cathodic protection operation was continued for a minimum of 72 h after catalyst application. In this way, the cobalt absorbed into pores of the anode and cement paste was converted to the active catalyst, Co₃O₄. The cobalt catalyst was brush applied to the titanium anode at full strength and at an application rate of 0.344 L/m² (0.0087 gal/ft²) approximately two months after the slabs were thermal sprayed. Catalyst application was done with the titanium anode polarized anodically to the steel mesh at a current density of 29 mA/m². Anodic polarization of the titanium anode was continued for a period of one month. Anodes on four concrete slabs were catalyzed in this way. A fifth slab was used as a control and had no catalyst applied to the anode.

Primary cracks in the anode occurred in the heavily oxidized reaction zones at the interface between adjacent splats. These cracks were the source of secondary cracks that radiated from the interfacial cracks into and across splats to other reaction zones. Comparison with anodes formed

using N₂ atomization showed the latter had a more uniform coating chemistry, and there was less primary and secondary cracking. Applicators of thermal sprayed titanium anodes commonly use anode resistance to determine when the coating is sufficiently conductive to meet design specifications. For service as an electrical conductor, designers of cathodic protection systems need an anode with low, uniform initial resistance and with a resistance that does not change significantly with electrochemical age.

Xu and Yao (2009) studied the current distribution in a designed three-layer reinforced concrete cathodic protection system, with carbon fiber reinforced cement (CFRC) as the conductive mortar overlay anode. The influence of steel bars initial corrosion state, concrete resistivity and magnitude of impressed current density on the current distribution was observed, respectively.

A total of four specimens, 150 mm×150mm×150 mm, were fabricated. Concrete was mixed with 350 kg/m³ of normal Portland cement which corresponds to ASTM Type I, water/cement ratio of 0.5, 1850 kg/m³ aggregate with maximum size of 25 mm. Silica sand was used as fine aggregate (specific gravity of 2.65) and crushed limestone as coarse aggregate. The steel concrete cover used was 10 mm. Each specimen had 9 parallel steel bars, 8 mm in diameter, placed in three layers and with rebar spacing of 60 mm. The zone of steel bars exposed atmospherically was isolated by epoxy resin and external copper wires electrically connected all the bars through soldering. Activated titanium strip was embedded in the conductive mortar as primary anode. Carbon fibers were used in the amount of 1% by mass of cement. From the four specimens, two (specimens 1 and 2) were used without chloride contamination and the other two (specimens 3 and 4) were chloride contaminated by adding NaCl (3% by cement weight) to the mixing water. Afterwards, all specimens were weekly sprayed with saturated NaCl solution for the entire experimental procedure cathodic protection was energised about 2 months after casting. Before the cathodic protection test, electrochemical measurements of the potential and the corrosion rate of rebars were performed.

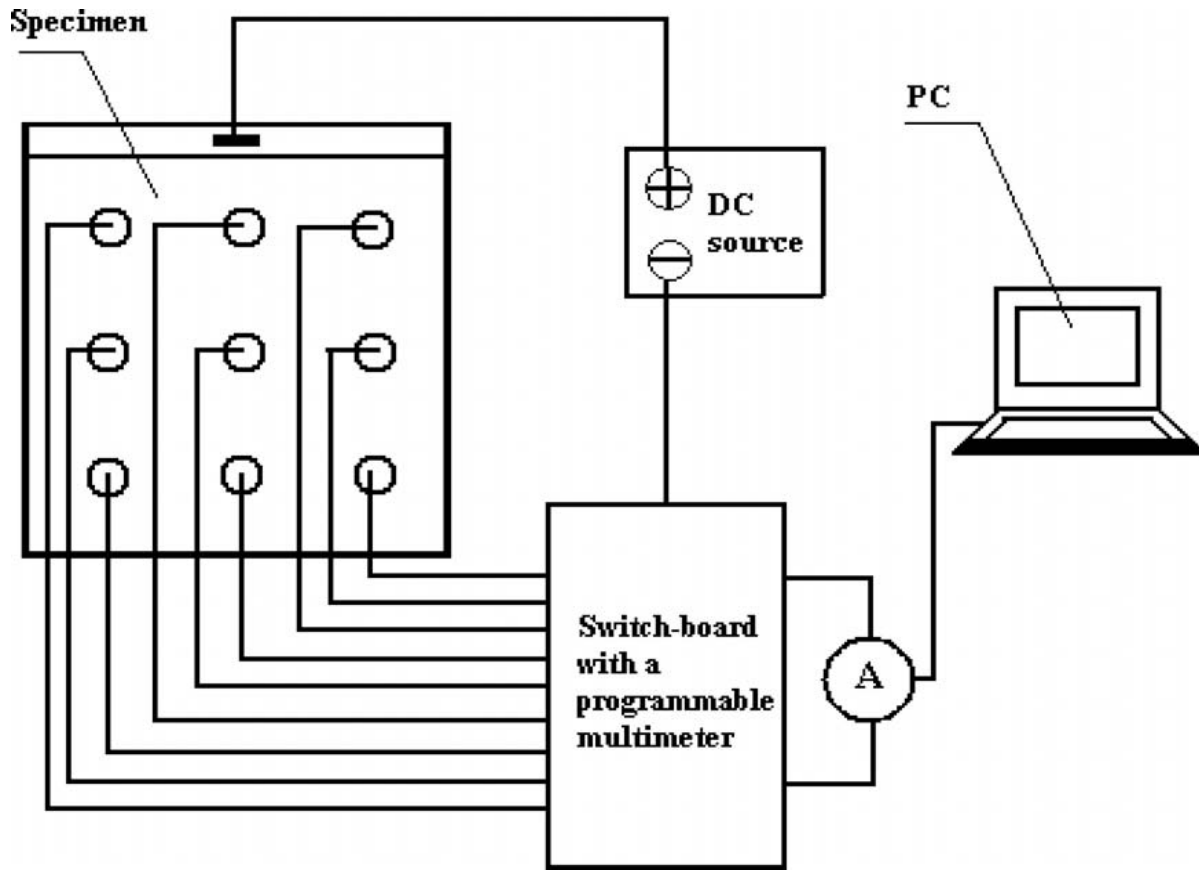


Fig.3.2 Testing apparatus configuration for cathodic protection test
 [Source: Xu and Yao 2009]

Current distribution at different impressed current density, specimens 1 and 3 were tested with applied current density of 40 mA/m^2 , 20 mA/m^2 and 10 mA/m^2 , referred to the surface of steel, respectively. Corrosion current density (i_{corr}) of specimens 3 and 4, which were both chloride contaminated, are around 20 mA/m^2 ; indicating a high corrosion rate due to an accelerating corrosion process induced by chlorides. In contrast, the i_{corr} values of specimens 1 and 2 are 3.3 mA/m^2 and 6.1 mA/m^2 , respectively, indicating that the steel is active ($i_{\text{corr}} > 2 \text{ mA/m}^2$), but the corrosion rate is relatively low. Nonetheless, the potential of all the specimens are below -500 mV (vs. saturated calomel electrode), significantly lower than the critical value -250 mV (vs. saturated calomel electrode) according to ASTM C 876-95. This phenomenon may be attributed to the high moisture content of specimens during the potential measurement, resulting in a low diffusion rate of oxygen through concrete matrix to the interface of steel and concrete. Therefore, free electrons accumulate at the interface, leading to the negative potential shift.

Fig.3.3 and fig.3.4 show the protection current distribution of specimens 1 and 3 with different magnitude of impressed current density.

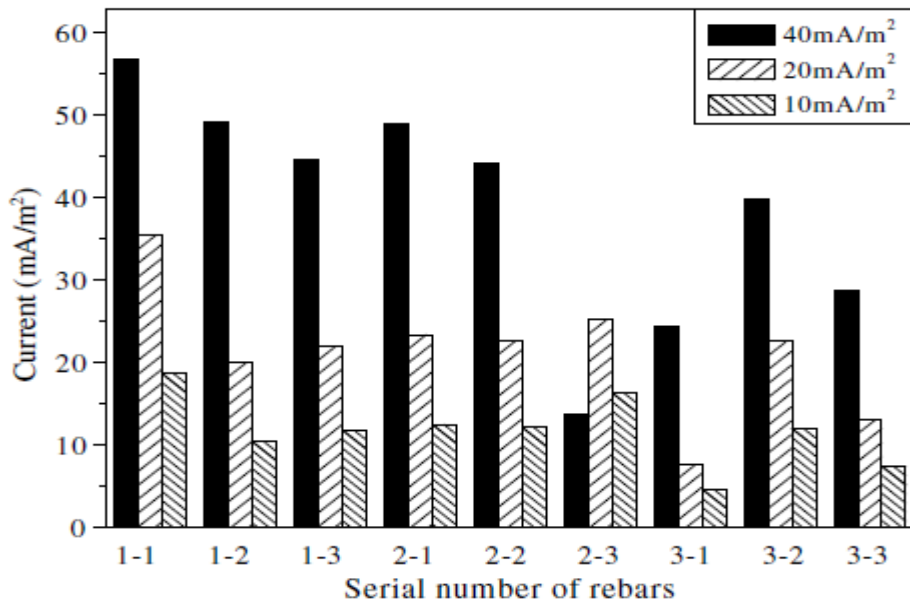


Fig.3.3 Protection current distribution with different impressed current density (Specimen 1) [Source: Xu and Yao 2009]

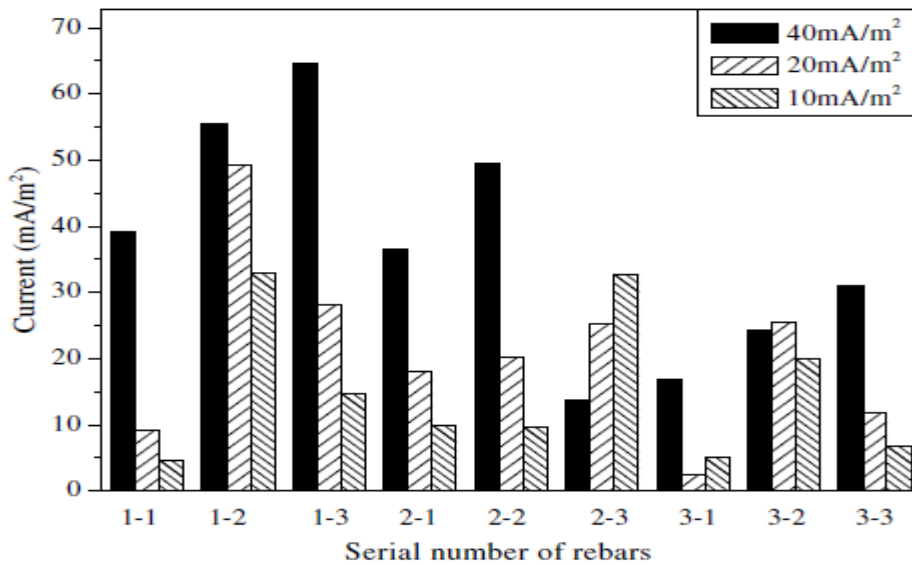


Fig.3.4 Protection current distribution with different impressed current density (Specimen 3) [Source: Xu and Yao 2009]

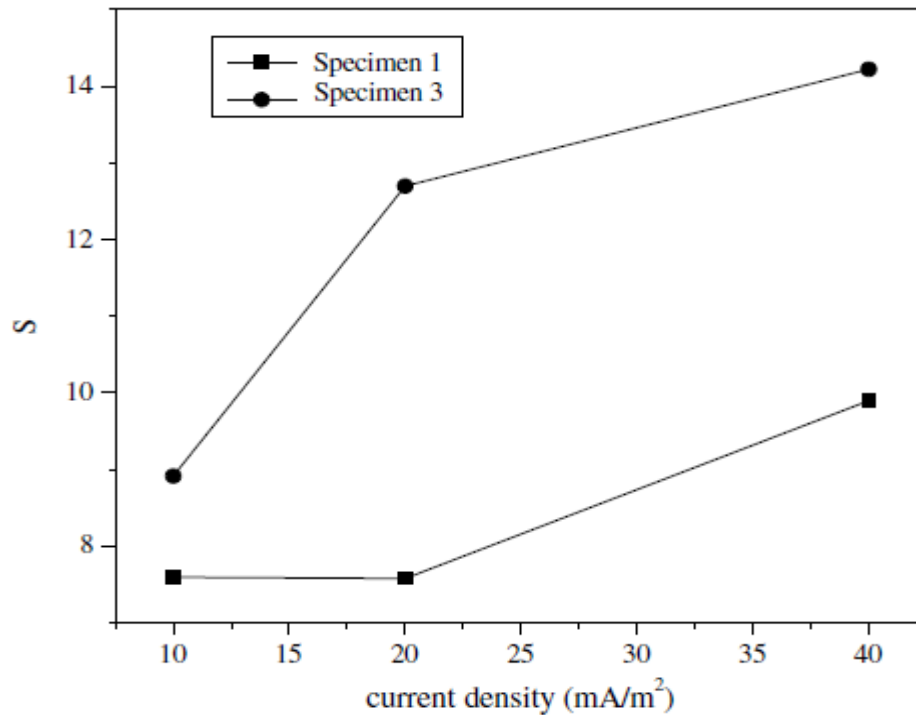


Fig.3.5 The relationship between impressed current density and standard deviation of protection current distribution values [Source: Xu and Yao 2009]

Fig.3.5 shows the change of factor S following different magnitude of impressed current density. The current uniformity was worsened along with increasing impressed current density, especially under the condition of higher corrosion rate, i.e., specimen 3. For specimen 1, change of impressed current density has no distinct influence on the ratio. But for specimen 3, the current received by the layer of rebars farthest from the anode decreases markedly as impressed current density increases. For a given reinforced concrete structure, it is important to determine a suitable magnitude of protection current applied. The impressed current not only influences the protective efficacy of reinforcement, but also has an adverse effect on the anode material.

The initial corrosion state of steel has a great effect on the protection current distribution. The uniformity of current worsens as the corrosion rate increases. There exists a threshold for corrosion rate, beyond which the nonuniformity of current distribution aggravates sharply. Magnitude of impressed current density has little effect on the current distribution when the corrosion rate of steel is relatively low. However, for a structure with high corrosion rate of reinforcement, the current distribution may be worsened along with increasing current density.

Bertolini et al. (1998) deals with the principles of cathodic protection for atmospherically exposed concrete structures, the various protecting effects induced by the cathodic polarization tests and field experience results. The differences between the cathodic protection applied for controlling the corrosion rate of chloride contaminated constructions and that applied to improve the corrosion resistance of the reinforcement of new structures expected to become contaminated are discussed.

Steel reinforcements embedded in 'sound' concrete (that is alkaline, with pH usually higher than 13, and chloride free) are in passive conditions. Passivity breaks down when the chloride content on the steel surface exceeds a critical threshold and pitting attack can initiate. Chloride content also affects the range of potentials in which the reinforcing steel is passive. The upper potential of this range, called the pitting potential (E_{pit}), diminishes typically from +500 to -400 mV passing from sound to very heavily chloride contaminated concrete as shown in fig.3.6. The pitting potential is characterized by a great variability, since, beyond the chloride content, it depends on many other parameters such as pH near the steel surface, temperature, cement and type and content and concrete porosity. The highest chloride content compatible with passive conditions for a given potential is the critical chloride content, which decreases with the potential. In correspondence to the usual corrosion potentials observed on a structure exposed to the atmosphere (around 0 V vs. saturated calomel electrode) the critical content is in the range 0.4-1% of cement weight.

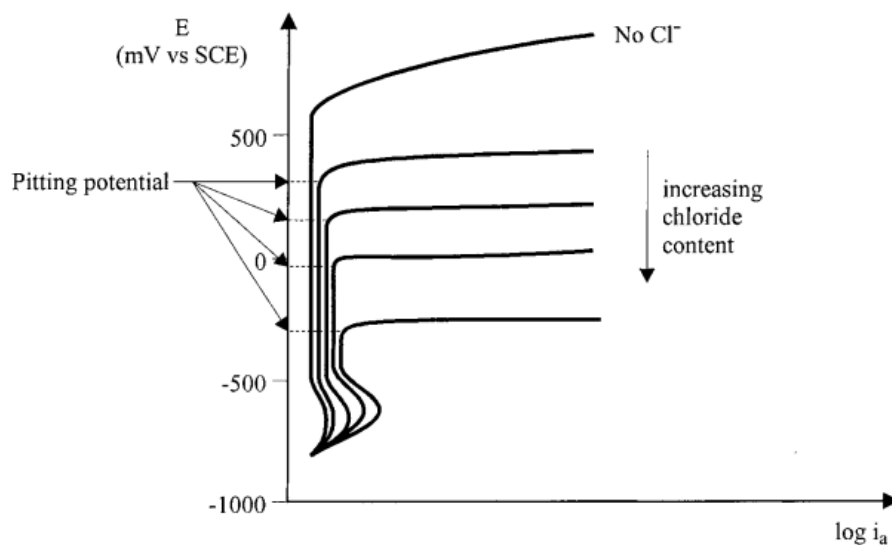


Fig.3.6 Schematic illustration of the anodic behaviour of steel in the presence of chlorides
[Source: Bertolini et al. 1998]

To achieve the Cathodic protection of steel reinforcement embedded in chloride contaminated concrete it is not necessary, to establish 'immunity' conditions, that is lowering the potential below the equilibrium potential E_{eq} . These immunity conditions are normally required on steel in active condition such as on structures in soil or immersed in sea water, where potentials more negative than - 850 mV vs. Cu/CuSO₄ or than - 950 mV in the presence of sulphate reducing bacteria are imposed. Conversely, the target of Cathodic protection in concrete structures is to reduce the corrosion rate by taking the steel into the passivity range or by reducing the macro couple activity on its surface, and this can be done with a small reduction in potential and a smaller current. If the potential is taken into the range from E_{pit} to E_{pro} the initiation of new pits is prevented and the corrosion rate of the existing ones is reduced, the driving voltage of the functioning of active-passive macro cells being decreased. The possibility of achieving protection or negligible corrosion rate at potentials more noble than those for immunity are also connected to a significant increase in the [OH⁻]/[Cl⁻] ratio on the steel surface produced by the cathodic reactions and by the migration of ionic species inside the concrete. This increase favours the development of passivation and/or the onset of passivity conditions. These beneficial effects do not cease if the current is interrupted but can last for months and, under some situations, give rise to the possibility of intermittent application of Cathodic protection, as well as the application of initial pre polarization at high currents in order to achieve passivity or a more persistent protection condition.

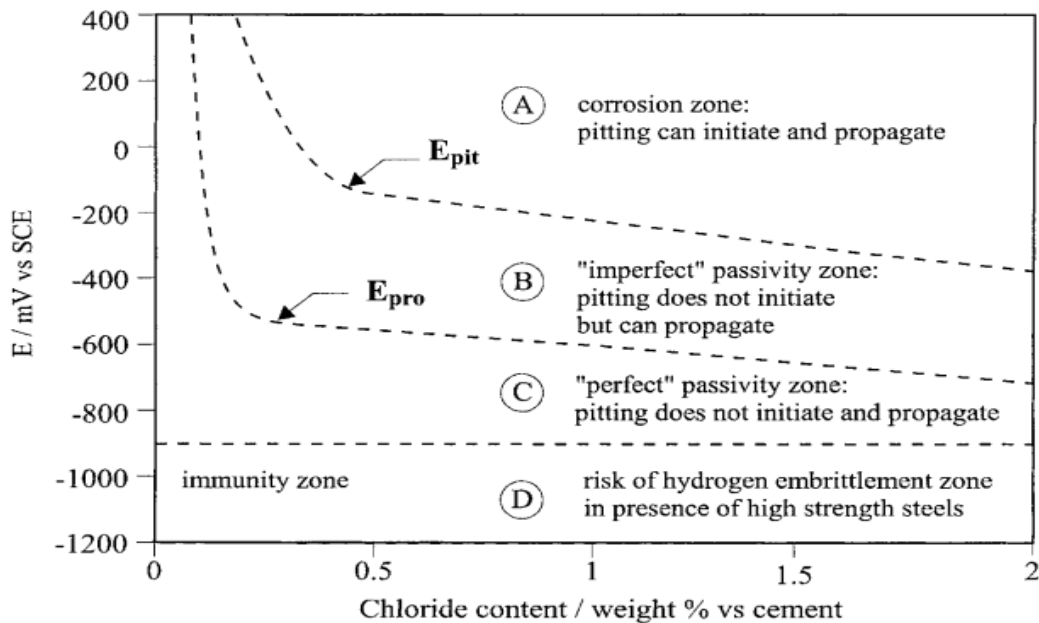


Fig.3.7 Schematic illustration of steel behaviour in concrete as a function of the chloride content

[Source: Bertolini et al. 1998]

To follow the variation in the potential of steel reinforcement of a concrete structure damaged by chlorides and then protected by a CP system are shown in fig.3.8.

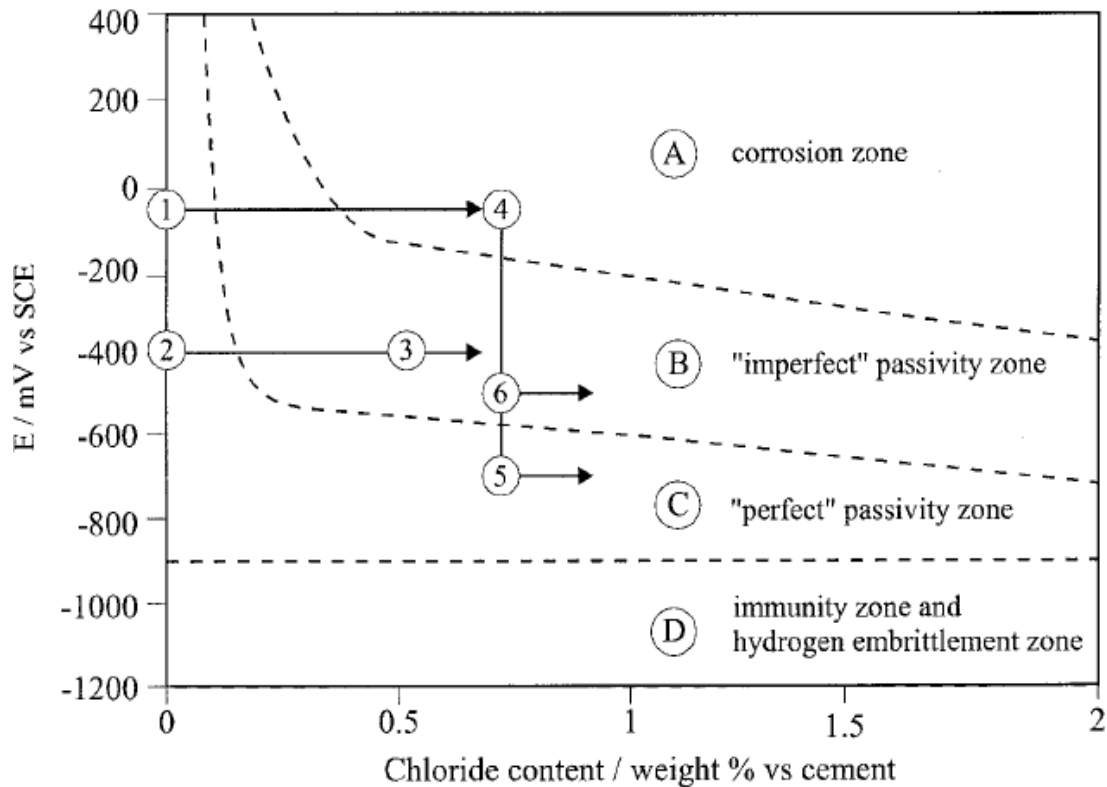


Fig.3.8 Schematic illustration of steel behaviour in concrete for different potentials and chloride contents. Evolution paths of potential and chloride content on the rebar surface of an aerial construction during its service life for: cathodic prevention (①→②→③→); CP restoring passivity (④→⑤→); CP reducing corrosion rate (④→⑥→). Cathodic prevention is applied from the beginning, CP only after corrosion has initiated [Source: Bertolini et al. 1998]

The initial condition is represented by the dot ① where the chloride content is nil and the steel is passive. By increasing the chloride content, the working point shifts to dot ④ within the corrosion region. Corrosion of the steel occurs rapidly by macrocell mechanism. The CP leads to ⑤ so that the passivity is restored or to ⑥ without restoring passivity. In all cases the corrosion rate is reduced. Initial current densities in the range $5-15\text{mA}\cdot\text{m}^{-2}$ are generally needed for protecting constructions exposed to the atmosphere. Much lower current densities are required under conditions which reduce the access of oxygen towards the surface of the steel such as in water saturated concrete. For components operating underwater, the oxygen diffusion limiting current is very low, typically in the range 0.2 to $2\text{mA}\cdot\text{m}^{-2}$ of reinforcing steel surface area. The experience shows that the current required maintaining protection conditions (verified

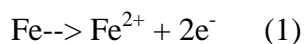
by the so called 4 h 100 mV potential decay empirical criterion) decreases even after months or years from start up. This happens because the cathodic current can bring about repassivation of steel in active zones, by improving the ratio $[\text{OH}^-]/[\text{Cl}^-]$ which increases E_{pro} and/or also because the reduction of the current exchanged by the macrocell leads to the inhibition of the macrocell itself.

In the cases in which the CP path runs according to (④→⑤→); of Fig.3.8, and thus passivity is established on the entire surface of the steel, the current required to maintain passivity is reduced to a few $\text{mA}\cdot\text{m}^{-2}$ (e.g. $2\text{-}5\text{mA}\cdot\text{m}^{-2}$). If the CP path runs according to (④→⑥→), the current density to fulfill the protection criterion remains high and does not decrease with time, since passivity is not obtained.

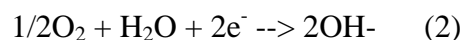
Cathodic protection has proved to be an effective method to control chloride induced corrosion of atmospherically exposed reinforced concrete structures even in the presence of high chloride levels. The risk of hydrogen embrittlement makes its application to prestressed concrete structures possible only in cases of simple geometry and under strict monitoring control. Cathodic prevention has proved to be a viable and safe technique to increase the corrosion resistance of reinforcement in reinforced or pre-stressed structures. Cathodic protection in carbonated concrete can take the pH on the rebar surface from values lower than 9 to values higher than 12 and thus transform the state of the reinforcement from corroding to passive conditions.

Chaussadent et al. (1997) studied the influence of cathodic protection on the properties of concrete cover in concrete slabs. To accelerate deterioration, the slabs were subjected to freezing and thawing cycles and sprayed with sodium chloride solution. Isolated from the atmosphere by the concrete cover, steel is normally passivated in sound concrete by the high pH of the pore solution. The following electrochemical reactions are observed:

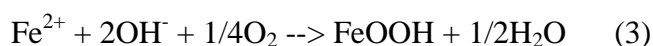
anodic reaction



cathodic reaction



passivation



However, when concrete is carbonated or polluted by chlorides, the passivation layer breaks and the steel can corrode. Cathodic protection is able to mitigate this deterioration. The technique is

based on reducing the rate of the anodic reaction (1) by applying an appropriate potential on the reinforcements.

Cathodic protection was applied for three years. To accelerate ageing, freezing and thawing cycles were applied, and sodium chloride solution was poured on the slab surfaces. After Cathodic protection application, cores were taken from the slabs in order to show both the final condition of the steel and the effects of Cathodic protection on the concrete.

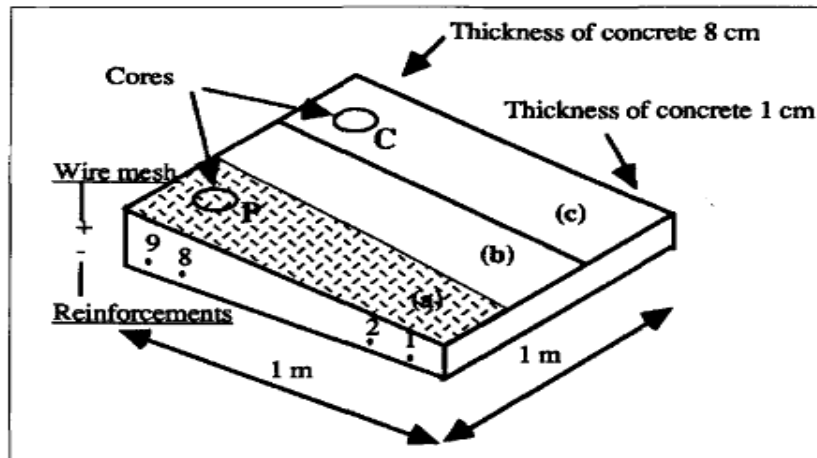


Fig.3.9 Schematic representation of slab and position of the cores
[Source: Chaussadent et al. 1997]

Every slab had three distinct areas:

- zone (a) covered with the anode and shotcrete,
- zone (b) with only shotcrete, and
- control zone (c) where the concrete surface remained uncovered. It should be noted that these last two zones can be influenced by the Cathodic protection.

The anodes consist of a titanium mesh fixed on the concrete surface and covered with shotcrete, approximately 1 cm thick. The Cathodic protection of rebars was obtained with an impressed power supply. The nominal value of the applied potential was equal to $-850 \text{ mV}_{\text{CSE}}$ (Cu/CuSO₄ reference electrode).

In this investigation, cathodic protection was applied to rebars in test pieces under very severe exposure conditions. The main conclusions are:

It was found that the reinforcements were in a very satisfactory condition. Rusting of rebars was observed only in a very porous concrete, or sometimes at weld locations where the access of chloride ions was facilitated. It should also be noted that cathodic protection was effective on

electrically-connected reinforcements even if these were not directly under anode and shotcrete. This influence on the short distance was very significant for real cases where it was technically difficult to cover the entire surface.

The second important point deals with the examination of the steel-concrete interface zones. It showed the formation of alkali-silica reaction gels near the ribs of the reinforcements. This reaction occurred even when the initial alkali content (calculated from the concrete composition) was less than the recommended critical value of $3 \text{ kg}\cdot\text{m}^{-3}$. This means that alkali ions have migrated under polarization, and they have accumulated near the polarized rebars.

Chang (2002) Studied bond degradation of rebar embedded in concrete due to impressed cathodic protection current. Different mix designs of concrete are found to have influence on the degradation percentage of bond strength. More specifically, bond strength degradation percentage with higher water-to-cement (w/c) ratio is found to be larger than that with lower w/c ratio. This is because the concrete of lower w/c ratio has denser microstructure. The results of bond degradation due to the current density and polarization time are shown in figures 3.10-3.12 for concrete of w/c = 0.48, 0.58 and 0.66, respectively. It can be seen that the bond strength decreased as the polarization time increased and/or the cathodic current density increased. It can be seen that the maximum reduction percentage in bond strength was about 55% when the current density was $1200 \mu\text{A}/\text{cm}^2$ and polarization time was 5 months.

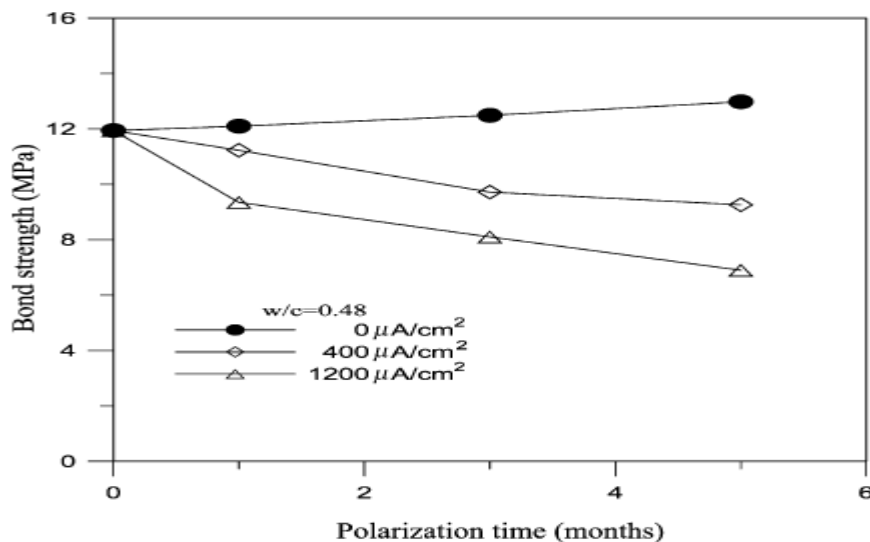


Fig.3.10 Bond strength development for specimens with w/c = 0.48
[Source: Chang 2002]

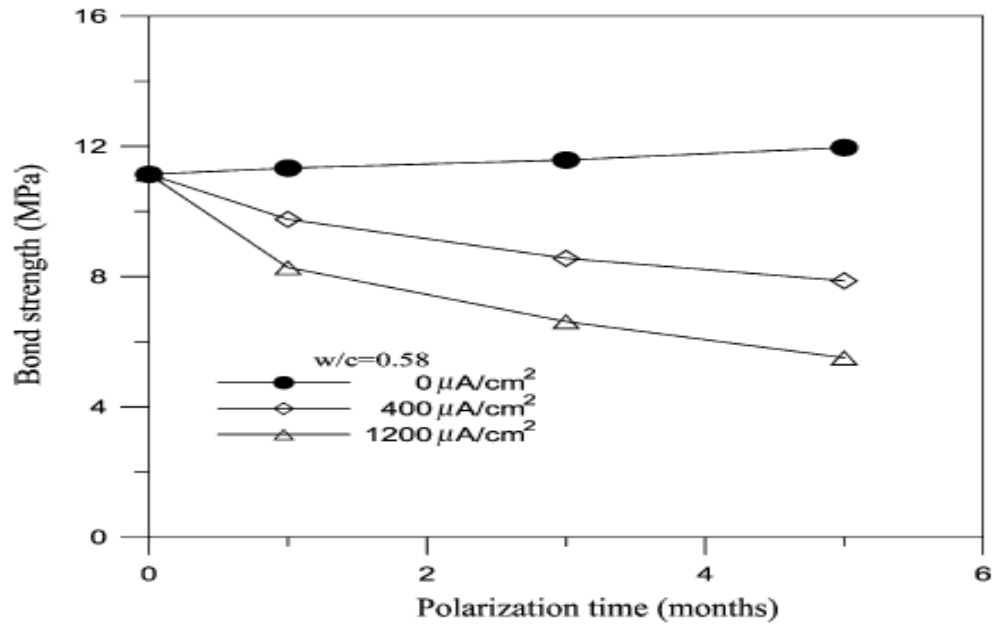


Fig.3.11 Bond strength development for specimens with $w/c = 0.58$
 [Source: Chang 2002]

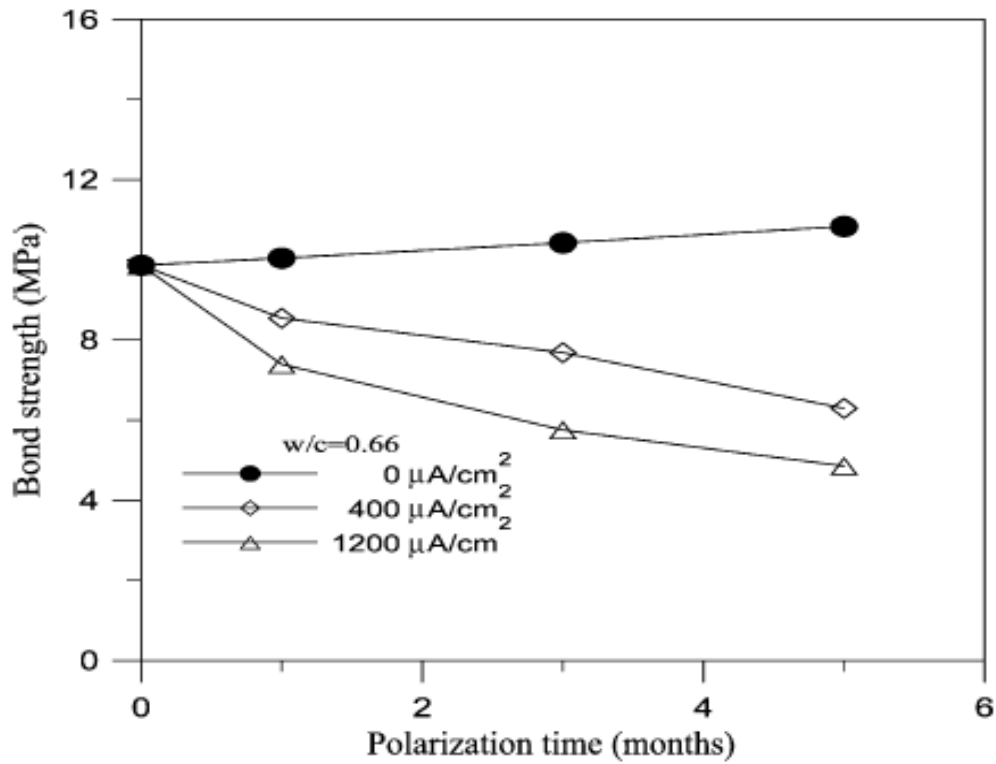


Fig.3.12 Bond strength development for specimens with $w/c = 0.66$
 [Source: Chang 2002]

The microstructure scanning electron microscope (SEM) photos of the concrete near the rebar–concrete interface showed that a loose structure with larger micro voids existed in the interface zone. Further, micro hardness tests on the concrete near the interface and chemical titration to determine contents of potassium and sodium ions were performed to ensure that the main cause of bond degradation is the softening effect of concrete.

In figure 3.13 the average bond strengths of specimens impressed by $1200 \mu\text{A}/\text{cm}^2$ for 1, 3 and 5 months were found to decrease as the total potassium and sodium ion concentrations increased.

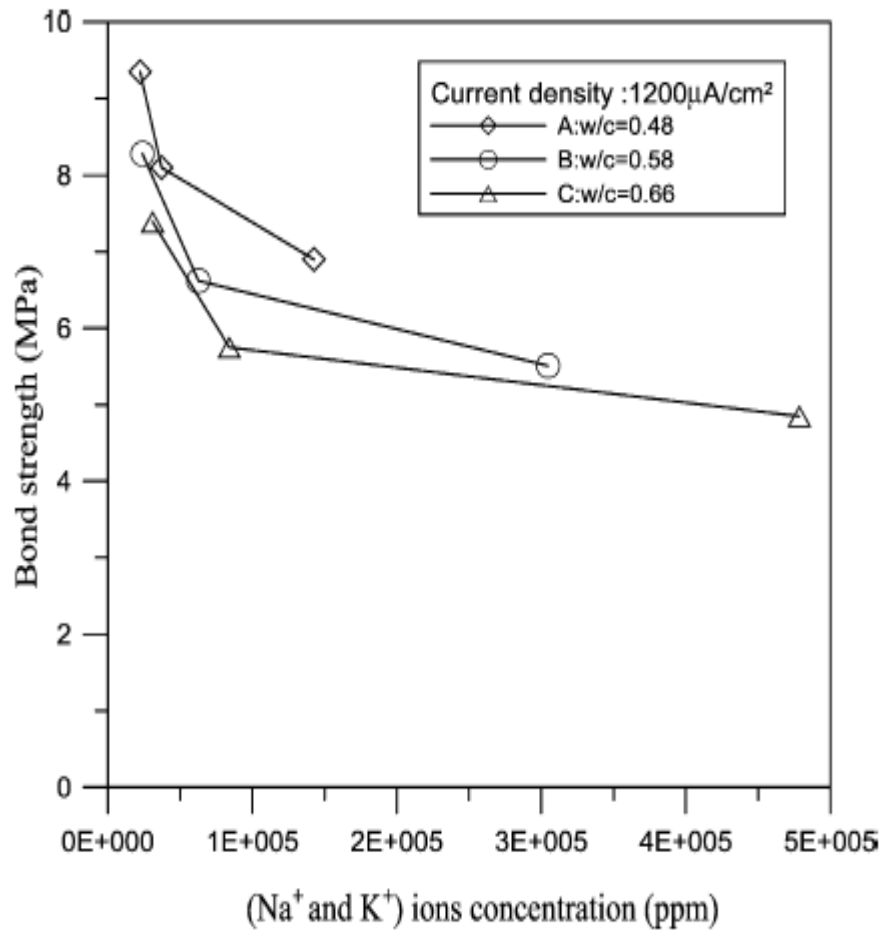


Fig.3.13 Bond strengths versus total concentration of potassium and sodium ions
 [Source: Chang 2002]

Hassanein et al. (2002) studied the current distribution from a surface mounted anode to steel reinforcement in atmospherically exposed concrete as a function of the condition of the steel, the resistivity of the concrete and anode-steel geometry. The boundary conditions at the steel have a significant effect on current distribution with more uniform distribution arising at low steel corrosion rates.

Table 3.2 Typical set of model input parameters
[Source: Hassanein et al. 2002]

| | |
|---------------------------------|-----------------------|
| Layers of steel | 1 |
| Steel bar diameter | 16 mm |
| Bars spacing | 100 mm |
| Slab thickness | 150 mm |
| Concrete cover | 40 mm |
| Steel current density | 10 mA/m ² |
| Anodic tafel slope | 300 mV/decade |
| Cathodic tafel slope | 150 mV/decade |
| Corrosion rate | 2 mA/m ² |
| Oxygen limiting current density | 100 mA/m ² |
| Anode type | Planar |
| Concrete resistivity | 300 Ω m |
| Grid dimensions | 2 mm |

The effect of the corrosion rate between 0.5 and 20 mA/m² (approximately 0.5–20 μm/yr) on the current flowing to the front and back of the bar and on the potential shifts induced by these currents is shown in Fig.3.14. An increase in the corrosion rate has a marked adverse effect on both the current and potential distribution, with almost twice as much current flowing to the front of the bar than to its back at a corrosion rate of 20 mA/m² (cf. a ratio of about 1.4 for marginally passive steel). The potential shifts induced at the front and back of the bar were also reduced significantly with an increase in the corrosion rate. An applied current of 10 mA/m² induced only 15–30 mV of potential shift (back and front of the bar) when the corrosion rate was 20 mA/m². This may be compared with 160–200 mV induced on steel corroding at 1 mA/m².

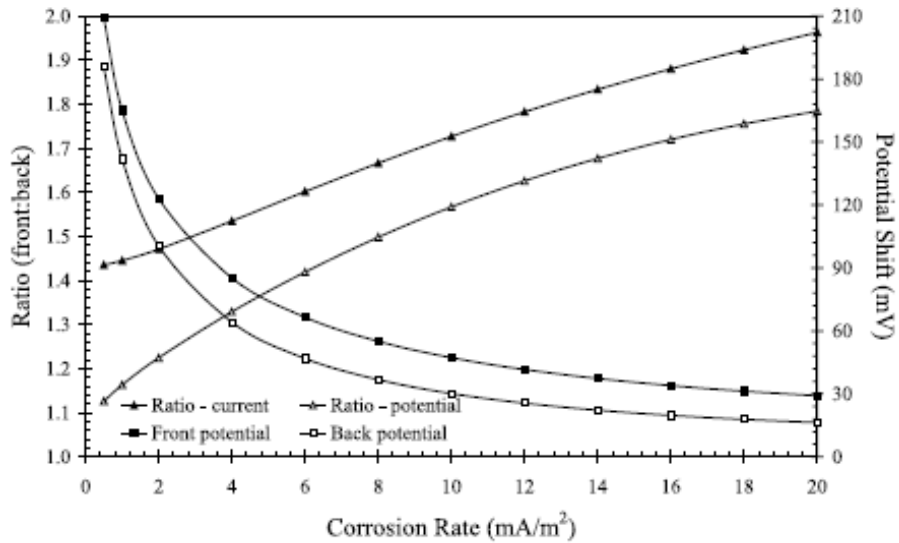


Fig.3.14 Effect of the corrosion rate on current and potential distribution
 [Source: Hassanein et al. 2002]

The effect of concrete resistivity and applied current density on the current flowing to the front and back of the bar and on the potential shifts induced by these currents is plotted in Figs.3.15 and 3.16, respectively. Increasing both the applied current density and concrete resistivity worsened the current distribution between the front and back of the bar with the influence of the concrete resistivity being more dominant. This had an adverse effect on the potential distribution with a lower potential shift being induced at the back of the bar while the potential shift at the front of the bar increased slightly.

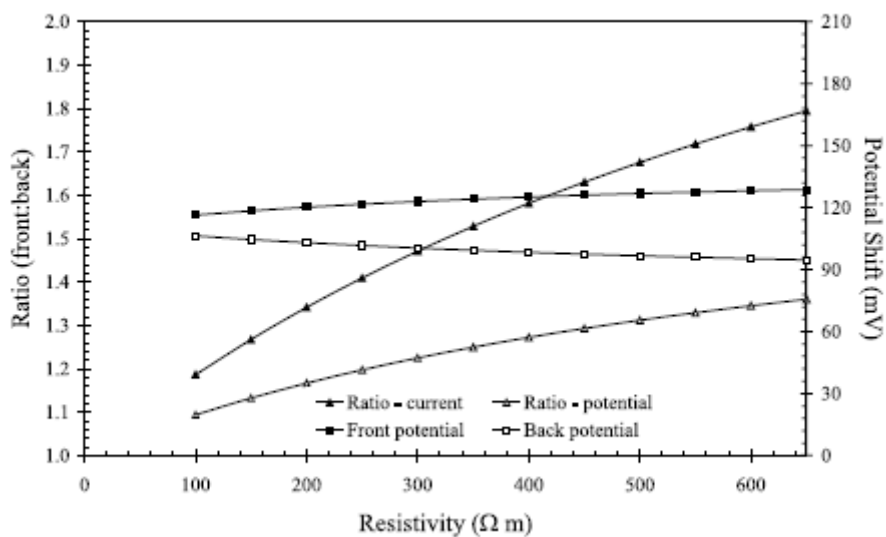


Fig.3.15 Effect of the concrete resistivity on current and potential distribution
 [Source: Hassanein et al. 2002]

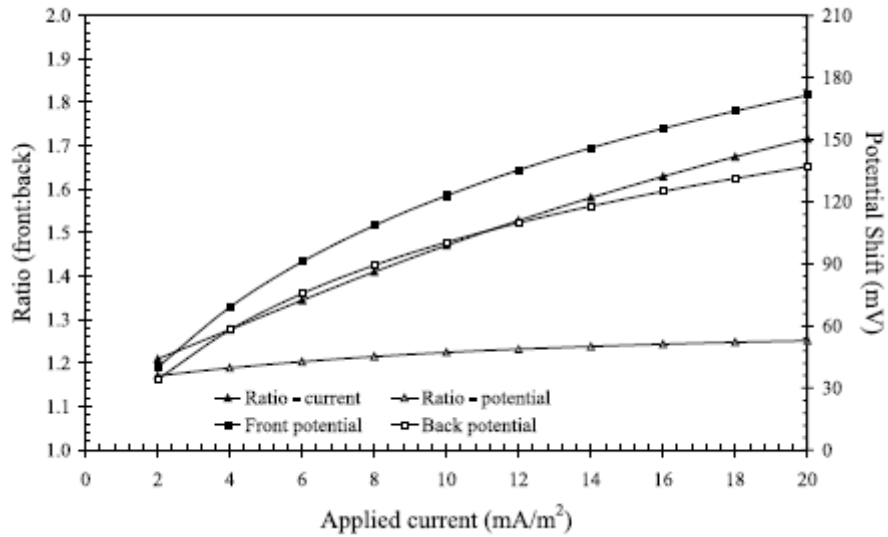


Fig.3.16 Effect of the applied current on current and potential distribution
 [Source: Hassanein et al. 2002]

The effects of concrete resistivity, concrete cover and bar spacing on the current distribution are plotted in Fig.3.17. An increase in the concrete cover at a given resistivity only had a limited effect on the current distribution between the back and front of the bar. By contrast, an increase in the spacing of the bars, with the anode current density kept constant, considerably improved the current distribution.

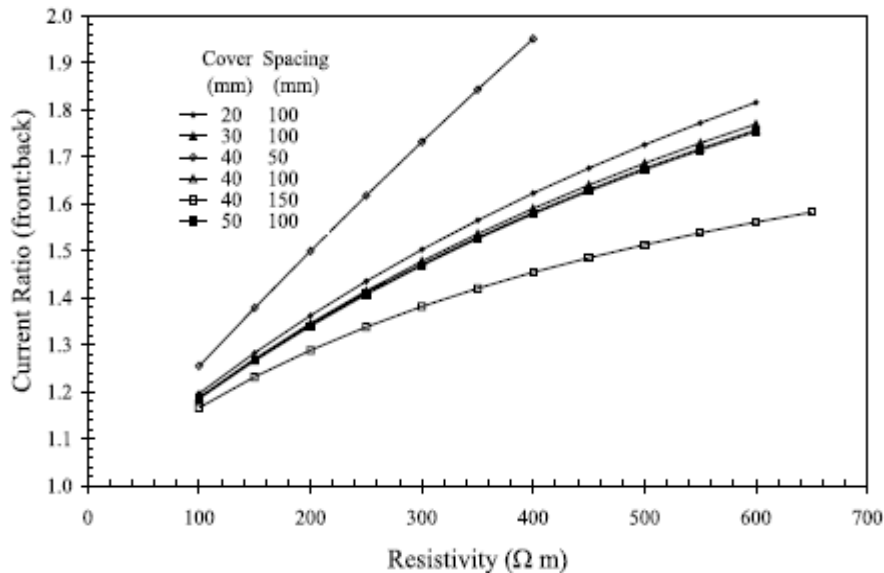


Fig.3.17 Effect of concrete resistivity, bar spacing and cover depth on current distribution
 [Source: Hassanein et al. 2002]

The boundary conditions at the steel have a significant effect on current distribution with factors that increase the potential drop across the steel–concrete interface relative to the potential drop through the concrete improving the uniformity of the current distribution. Thus the current is more uniformly distributed when the corrosion rate is low as the high resistance to polarisation of interface is a controlling factor. For a single layer of reinforcement in typical conditions, the surface of a steel bar facing the anode may receive 1.5 times the current received by the opposite surface. As Cathodic protection is known to work in these cases, a basis for many design decisions that influence current distribution is that their effect is small by comparison. This may be used to define the acceptable voltage drop through the reinforcing steel and anode system which can then be translated into connection spacing and acceptable resistivities of installed components. When more than one layer of reinforcement is present at different cover depths substantially more current may flow to the front bar surface facing the anode than to its back. Furthermore, bars farthest from the anode may receive very little of the total current. In this case the anode should be located close to the layer of steel needing the protection the most and discrete anodes may be necessary to improve current distribution. An increase in the concrete resistivity and concrete cover and a decrease in the cathode to anode area ratio at a constant anode current density will increase the voltage drop in the concrete. These factors are important to consider in the selection of the design current density when the principal protective effect is to generate an improvement in the environment at the steel promoting passivity.

Kim et al. (2003) studied Impressed current cathodic protection of Steel Used for Marine Structures and observed that Cathodic protection in marine structures can result in hydrogen embrittlement, which can cause trouble with high-strength steels, particularly at welds. Therefore, the limiting potential for hydrogen embrittlement should be examined in detail as a function of the cathodic protection potential. This study investigated the effects of post-weld heat treatment (PWHT) on marine structural steels from an electrochemical viewpoint. In addition, the slow strain rate test was used to investigate both the electrochemical and mechanical effects of post-weld heat treatment on impressed current cathodic protection.

High-strength steel was used for slow strain rate test and post-weld heat treatment test specimens. Each test specimen was 358×4×23.6 mm, with a gauge length of 59 mm. The groove angle of the welded part was $35\pm 5^\circ$, and 0.5×4.8 notches (wide×deep) were made on both sides of the base metal to produce fractures in the base metal. Flux-cored arc-welding was used. For post-weld heat treatment, the specimens were heated at 80° C per hour to 550, 600, or 650° C, kept at that temperature for 1.5 hours, and then furnace cooled.

The base metal surface area of the test specimen used to measure the cathodic and anodic polarization trend and corrosion current density was 6.45 cm², including the heat-affected zone and welded metal part. The surface area used to measure the cathodic polarization curves was 1

cm². The curves were measured at a scan rate of 1 mV/sec using a saturated calomel electrode (SCE) as the reference electrode and a Pt counter electrode.

Kim et al. gives the relationship between the maximum tensile strength and constant cathodic potential in as-welded and post-weld heat treatment specimens. The greatest maximum tensile strength in as-welded and post-weld heat treatment specimens was observed in air at 643.4 and 624.2 MPa, respectively. Moreover, the tensile strength was highest at a cathodic potential of -770 mV for both the as-welded and post-weld heat treatment specimens. There were no correlations between yield strength, stress at final failure, and constant cathodic potential, neither for the as-welded nor the post-weld heat treatment conditions.

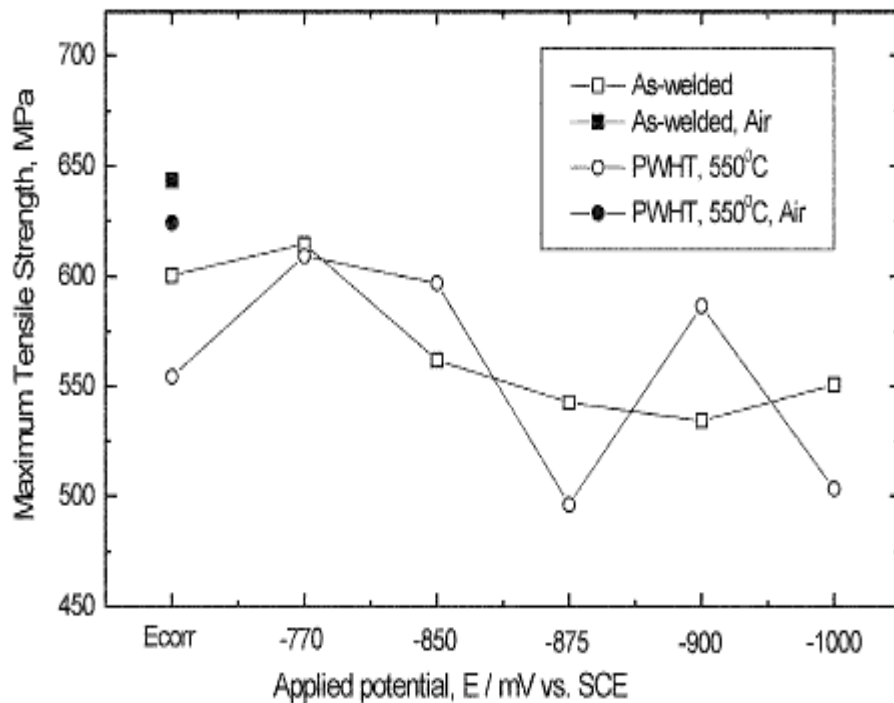


Fig.3.18 Relationship between maximum tensile strength and applied cathodic potential in as-welded and post-weld heat treated specimen [Source: Kim et al. 2003]

The relationship between elongation and constant cathodic potential in the as-welded and post-weld heat treatment conditions is shown in Fig.3.19 Elongation is decreased by shifting to a negative cathodic potential, which readily results in the evolution of hydrogen. However, the elongation values for 550° C post-weld heat treatment specimens are generally greater than for as-welded specimens throughout the range of potentials. This suggests that hydrogen embrittlement readily occurs with gradually increasing negative potential.

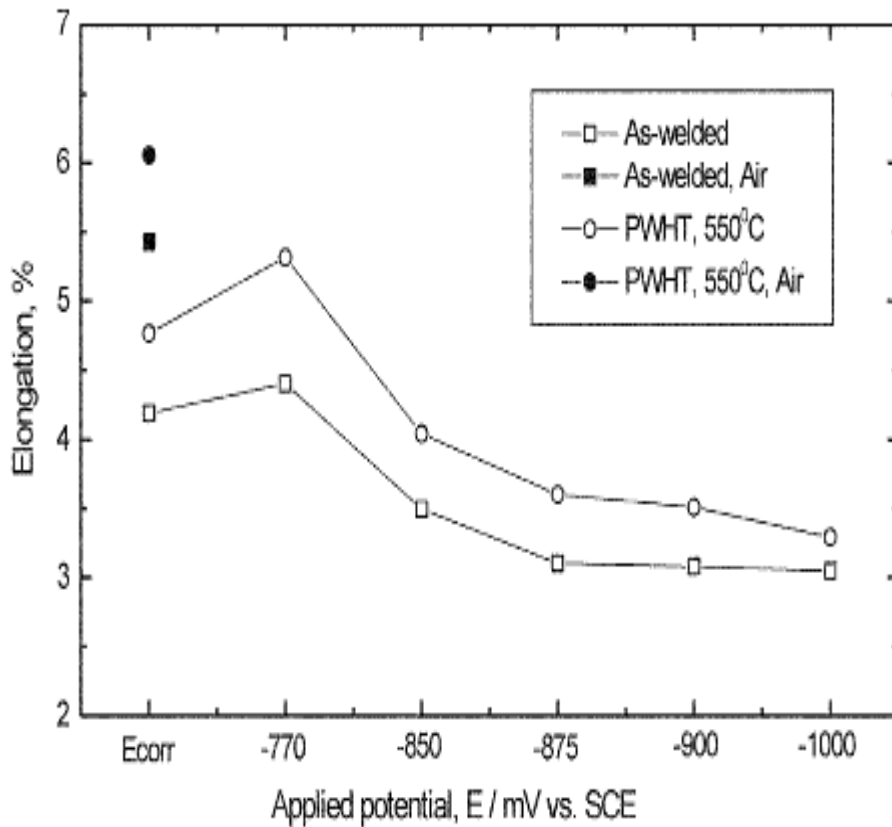


Fig.3.19 Relationship between elongation and applied cathodic potential in as-welded and post-weld heat treated specimen [Source: Kim et al. 2003]

Fig.3.20 shows the relationship between time-to-fracture and constant cathodic potential. The time-to-fracture was greatest when the cathodic potential was -770 mV, regardless of post-weld heat treatment condition. The time-to-fracture decreased as the cathodic potential became more negative, possibly due to the influence of hydrogen embrittlement.

The relationship between the strain-to-failure ratio and the cathodic potential is shown in Fig.3.21 the strain-to-failure ratio is the ratio of the percent elongation in seawater to that in air. This suggests that hydrogen embrittlement decreases with increasing hydrogen embrittlement ratio (strain-to-failure ratio). The hydrogen embrittlement ratios in the as-welded and post-weld heat treatment conditions were greatest at -770mV compared with other potentials. Overall, the hydrogen embrittlement ratio was greater for post-weld heat treatment versus as-welded specimens.

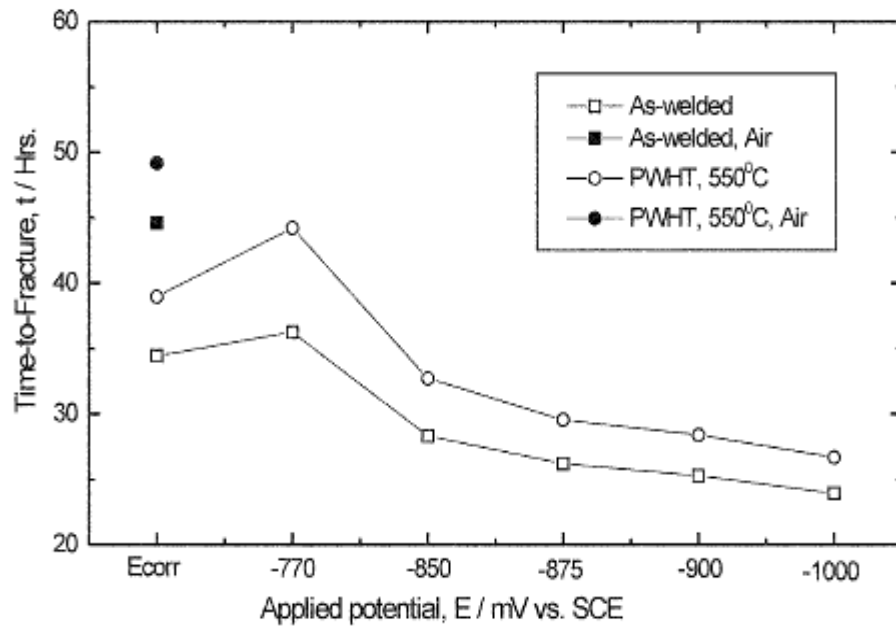


Fig.3.20 Relationship between time-to-fracture and applied cathodic potential in as-welded and post-weld heat treated specimen [Source: Kim et al. 2003]

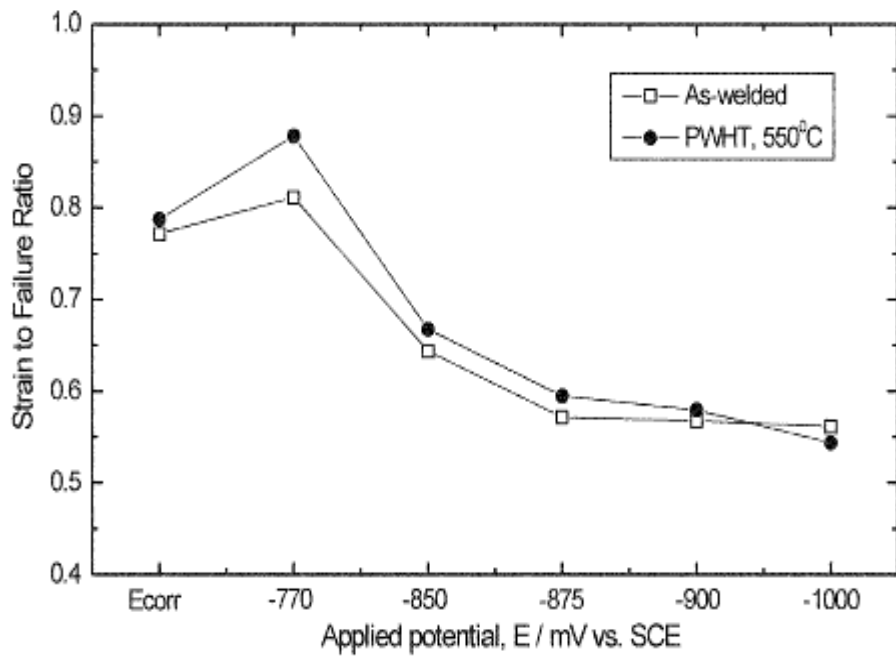


Fig.3.21 Relationship between strain to failure ratio and applied cathodic potential in as-welded and post-weld heat treated specimen [Source: Kim et al. 2003]

Post-weld heat treatment increased corrosion resistance. It also decreased the current generated by the aluminum anode, and anode weight loss when high strength steel was cathodically protected by an Al anode. There did not appear to be any correlation between maximum tensile strength and hydrogen embrittlement. However, the elongation, time-to-fracture, and strain-to-failure ratio decreased as the potential was lowered due to hydrogen evolution. The susceptibility to hydrogen embrittlement increased significantly with decreasing elongation and time to fracture as a result of a shift to lower potential. The susceptibility to hydrogen embrittlement with post-weld heat treatment also decreased with increasing elongation, time-to-fracture, and a large amount of dimpling. In the SEM fractography analysis, the fracture morphology at applied cathodic potentials between -770 and -850 mV showed a dimple pattern with ductile fractures, which changed to a trans-granular pattern at potentials under -875 mV.

Consequently, the optimum cathodic protection potential range, not causing hydrogen embrittlement, is between -770 and -850 mV (saturated calomel electrode) with post-weld heat treatment at 550° C and in the as-welded condition.

Garcia et al. (2012) studied Bond degradation between concrete and steel at protection and overprotection levels. Two types of materials were tested: an ordinary Portland cement (OPC) and a mixture of 85% OPC and 15% fly ash (OPC/FA). Concrete specimens were immersed in a 3.5% sodium chloride (NaCl) solution. Chemical analysis of sodium, potassium and hydrogen ions was performed using atomic absorption Spectrophotometer. Hydrogen ion content was monitored using electrochemical impedance spectroscopy (EIS). Mechanical behaviour was analysed by means of pullout tests.

Table 3.3 Nomenclature of specimens tested for a period of 2–6 months
[Source: Garcia et al. 2012]

| Experimental time/months | Specimen | | | |
|---------------------------------|-----------------|--------|----------|-----------|
| 2 | 2 OPC | 2 OPC+ | 2 OPC/FA | 2 OPC/FA+ |
| 3 | 3 OPC | 3 OPC+ | 3 OPC/FA | 3 OPC/FA+ |
| 5 | 5 OPC | 5 OPC+ | 5 OPC/FA | 5 OPC/FA+ |
| 6 | 6 OPC | 6 OPC+ | 6 OPC/FA | 6 OPC/FA+ |

OPC: ordinary Portland cement at protection level; OPC+: ordinary Portland cement at overprotection level; OPC/FA: 85% ordinary Portland cement and 15% fly ash at protection level; OPC/FA+: 85% ordinary Portland cement and 15% fly ash at overprotection level.

Fig.3.22 (a) shows bond strength measurements versus time for OPC/FA specimens at protection (OPC/FA) and overprotection (OPC/FA+) levels. A significant decrease in bond strength can be observed at protection level 12 MPa after 2 months and 4 MPa after 6 months. The specimens at

overprotection level (OPC/FA+) show variable bond strength values depending on the potassium or sodium ion content at the concrete–steel interface.

Fig.3.22 (b) shows bond strength measurements versus time for OPC specimens at protection (OPC) and overprotection (OPC+) levels. It can be seen that the OPC specimens show higher bond strength, 8.3 MPa for 2 months, than OPC + specimens, 6.3 MPa for 2 months. In general, the OPC specimens at either protection or overprotection level show little variation in bond strength over the tested experimental time. As an hypothesis, it may be suggested that the replacement of 15% OPC with FA does not improve bond properties because FA particles react slowly with Ca(OH)_2 and this reaction has not yet taken place.

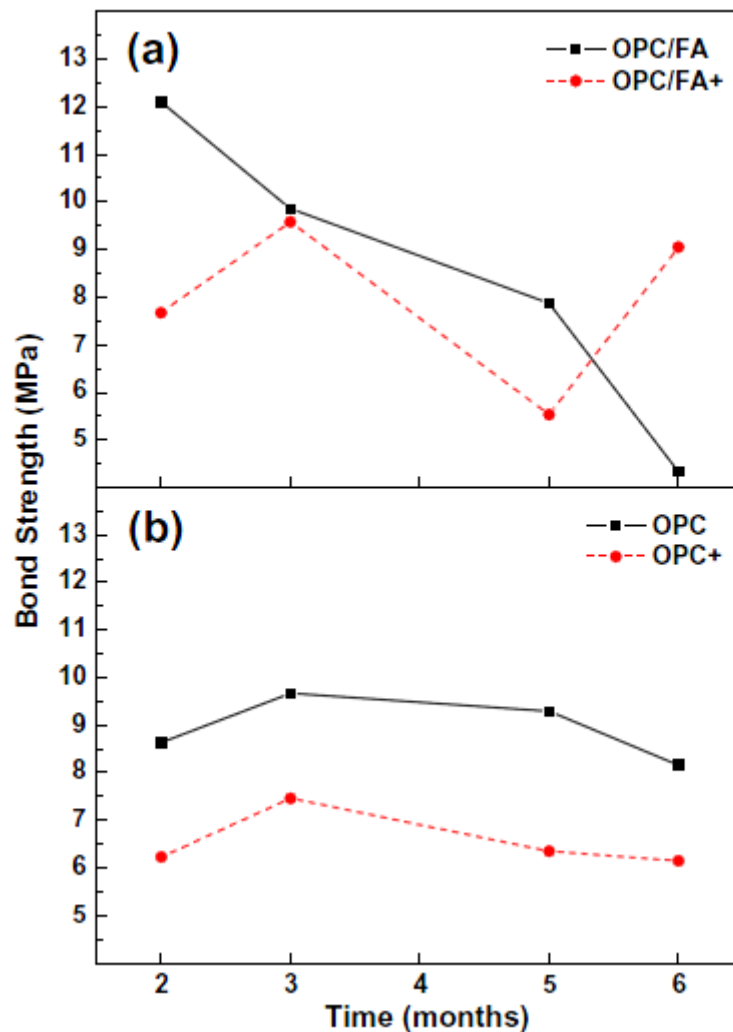


Fig.3.22 Bond strength as a function of time: (a) OPC/FA specimen (85% OPC and 15% FA) at protection level (OPC/FA) and at overprotection level (OPC/FA+) and (b) OPC specimen at protection level (OPC) and at overprotection level (OPC+)

[Source: Garcia et al. 2012]

Fig.3.23 shows hydrogen ion content versus bond strength. Fig.3.23 (a) was obtained using the antilogarithm expression of the pH for the pullout test ($[H^+] = 10^{-pH}$). Fig.3.23 (b) was obtained using the AAS technique for powder extracted from the concrete–steel interface.

Fig.3.23 (a) shows that irrespective of the type of concrete specimen, the hydrogen ion content at the concrete–steel interface decreases as the bond strength increases after 2, 3 and 5 months of exposure. In these specimens a great decrease in the hydrogen ion content is observed for bond strength values in the 8–12 MPa range. In contrast, the specimen after 6 months of exposure shows only a small decrease in the hydrogen content and low bond strength values. Fig.3.23 (b) shows that after 2 months of exposure the specimens present low hydrogen ion content and the highest bond strength value.

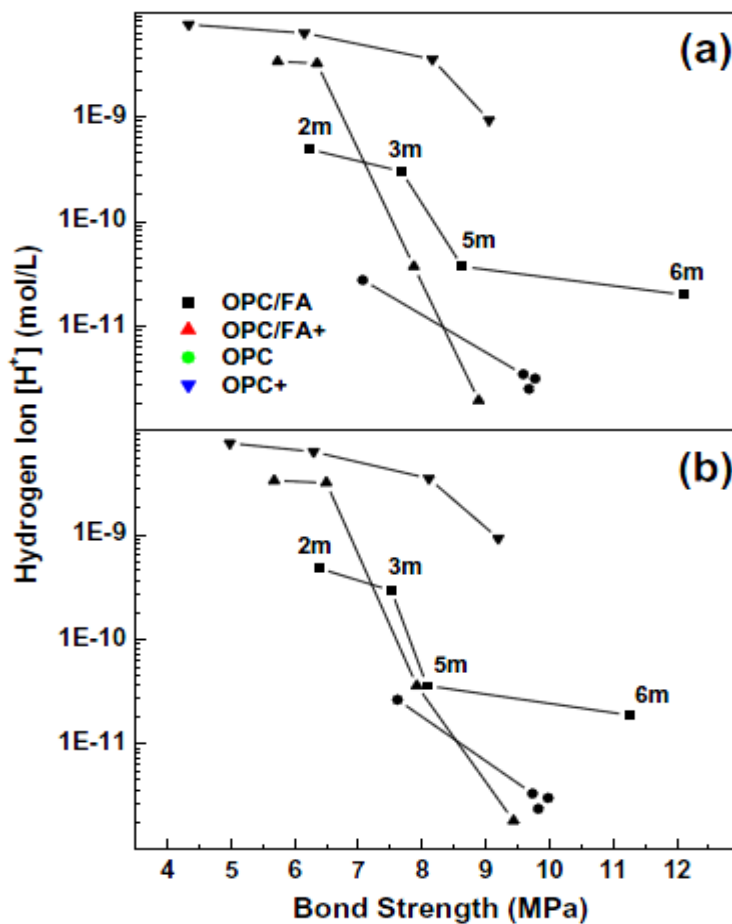


Fig.3.23 Hydrogen ion content at the concrete–steel interface as a function of bond strength for 2, 3, 5 and 6 months (2 m, 3 m, 5 m and 6 m): (a) using the antilogarithm of the pH for the pullout test and (b) using the atomic absorption spectrophotometry (AAS) technique on powder extracted from the concrete–steel interface

[Source: Garcia et al. 2012]

Potassium, sodium and hydrogen ion migration towards the concrete–steel interface plays an important role in bond loss between steel and concrete in structures under cathodic protection by the impressed current method. The potassium ion content is lower in concrete specimens at protection level containing fly ash, due to its reaction with calcium hydroxide, while sodium ion migration is higher in concrete containing fly ash, which is attributed to the small size of the sodium ion. At overprotection level the potassium and sodium ions migrate more easily than at protection level. At overprotection level the hydrogen content is higher than at protection level, which is attributed to the generation of molecular hydrogen at overprotection level.

Tests conducted at different ages indicated that the OPC specimens at either protection or overprotection level show little variation in bond strength with time. The OPC/FA specimens at protection level show 12 MPa for 2 months and 4 MPa for 6 months. At overprotection level (OPC/FA+) the bond strength depends on the potassium or sodium ion content. Hydrogen ion content for OPC/FA specimens decreases as the bond strength increases after 2, 3 and 5 months. In contrast, the specimen after 6 months of exposure shows only a small decrease in the hydrogen content and low bond strength values.

Koleva et al. (2006) studied the morphological and micro structural differences between unprotected and protected (under cathodic protection) reinforced mortars subjected to chloride ingress. Reinforced mortar cylinders (40 mm in diameter and 100 mm long) were cast according to standard experimental procedures using ordinary Portland cement (with cement-to-sand mixing proportion of 1:3 and water cement ratio of 0.6), with a construction steel bar embedded in the centre of the specimen. Three groups of specimens are considered, freely corroding (denoted as N) and cathodic-protected (denoted as P) specimens partially submerged in 7% NaCl solution. Cathodic protection current (mixed metal oxide Ti serving as external anode, the current is in the range of 5–10 mA/m²) was applied to group P from 60 days of cement hydration. At this testing stage, the N group specimens are already actively corroding. The third group is submerged in demineralised water, and act as reference specimens (denoted as R). The electrochemical conditions of all specimens were monitored by electrochemical means (both Linear Polarization Measurements and Electrochemical Impedance Spectroscopy). A cylindrical titanium mesh served as counter electrode and saturated calomel electrode (SCE) as reference electrode.

However, X-ray diffraction analysis and scanning electron microscopy (SEM) observations (combined with energy dispersive X-ray analysis) have revealed that the amount of hematite and magnetite (Hematite and magnetite are categorized in the group of iron oxides) is much higher in the protected specimens (group P), with less akaganeite (Akaganeite is an iron oxide which has been identified as a part of the rust layer formed through the corrosion of steel exposed to chloride environments) and lepidocrocite (lepidocrocite is prominent as corrosion products in rust) at the same time. Another important aspect is the dimension and crystallinity of corrosion

products. The iron oxychlorides in the N specimens display lamellar type and much larger dimensions than in the P mortars. The lamellar morphologies are responsible for volumetric expansion and cracking initiations in the reinforced mortars. Instead of the typical flowery structure of goethite (as observed in N specimens), cotton-ball structures of goethite are revealed to a wide extent in the P specimens. This semi-crystalline goethite is less detrimental to the material structure. The favourable morphology (lower crystallinity) of goethite can be attributed to the relatively high pH value and lower salinity (i.e., lower concentration of chloride ions) in the protected mortar. The morphological and micro structural analysis shed light on the fundamental mechanisms underlying the efficiency of cathodic protection. The protection current could modify the material structure (including the amounts and morphologies of different corrosion products) to a favourable trend in terms of corrosion protection and prevention.

The study demonstrates that cathodic protection current can efficiently prevent further corrosion on the steel surface and successfully decrease the chloride concentration around the steel bar. In local areas with protective layer of $\text{Ca}(\text{OH})_2$, the latter remains intact after 4 months exposure to 7% NaCl solution, maintaining the basicity environment surrounding the steel reinforcement. In the regions where CH layer is absent, the cathodic protection technique can keep the chloride ions 100 μm away from the steel surface, thus efficiently protecting the steel reinforcement.

Chang et al. (1999) studied the degradation of the bond strength between the steel rebar and concrete by the impressed cathodic current.

The pullout specimen was cast in a $\phi 10 \text{ cm} \times 20 \text{ cm}$ ($\phi 4 \text{ in} \times 8 \text{ in}$) steel mold with reinforcing steel positioned at the center. The embedded lengths of rebars were 4, 6 and 8 cm. After demolding, the specimens were cured for 28 days. The compressive strength of concrete at 28 days was 32.8 MPa. Then, the pullout specimens were immersed into 3.5% NaCl solution. The cathodic current densities applied to the pullout specimens were 0, 3, 200 and 600 $\mu\text{A}/\text{cm}^2$. The polarization times were 0, 4, 8 and 12 months. After a given polarization time, pullout tests were performed on three specimens for each group of a specified embedded rebar length and a given cathodic current density. The pullout test was performed in a universal material testing machine at a maximum stroke rate of 1.27 mm/min. The maximum pullout forces were recorded and dividing them by the corresponding embedded area to obtain the bond strengths. The deviation of the bond strengths for specimens of each group was below 9% and the average bond strength was used for analysis.

It was found that the average bond strength for the control specimens increased slightly as the polarization time increased generally as shown in fig.3.24. The continuous Portland cement hydration would increase the bond between rebar and concrete. Also after polarization of 4 months and 8 months, the average bond strength of specimens protected by 3 $\mu\text{A}/\text{cm}^2$ was higher than that of the control specimens (0 $\mu\text{A}/\text{cm}^2$). Other combinations of cathodic current densities

and polarization times did not show the same trend. Nevertheless, for higher cathodic current density and longer polarization time, the degradation of bond strength was more obvious. This may result from the impressed cathodic current effects as follows:

The cathodic current provided energy which would enhance the hydration reaction of cement so that the bond strength increased.

The Na^+ and K^+ ions would be attracted to migrate to the interface, and the C-S-H gel would be attacked by these ions so that the bond strength decreased.

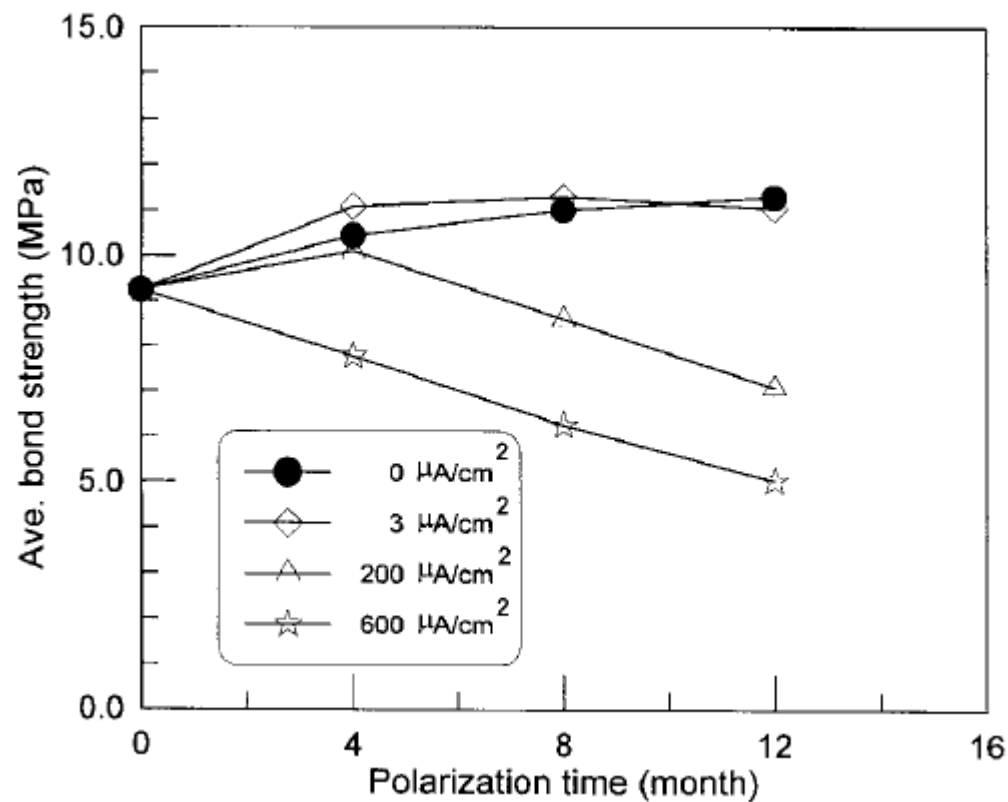


Fig.3.24 The average bond strength versus the polarization time
 [Source: Chang et al. 1999]

For 3 $\mu\text{A}/\text{cm}^2$ protected specimens, the former hydration effect was more apparent than the second effect at polarization times of 4 and 8 months. For other conditions, the ion migration effect was dominant. The percentage of bond strength reduction versus current density was shown in Fig.3.25 the percentage of bond strength reduction was defined as:

$$s \equiv \begin{cases} \frac{\|\sigma_p - \sigma_0\|}{\sigma_0} \times 100\% & \text{when } \sigma_p \leq \sigma_0 \\ 0 & \text{when } \sigma_p > \sigma_0 \end{cases}$$

Where s is the percentage of bond strength reduction σ_p is the bond strength for the specimens at a specific polarization time and σ_0 is the bond strength for the control specimens at the corresponding time. It was found that maximum reduction percentage in bond strength was about 56%.

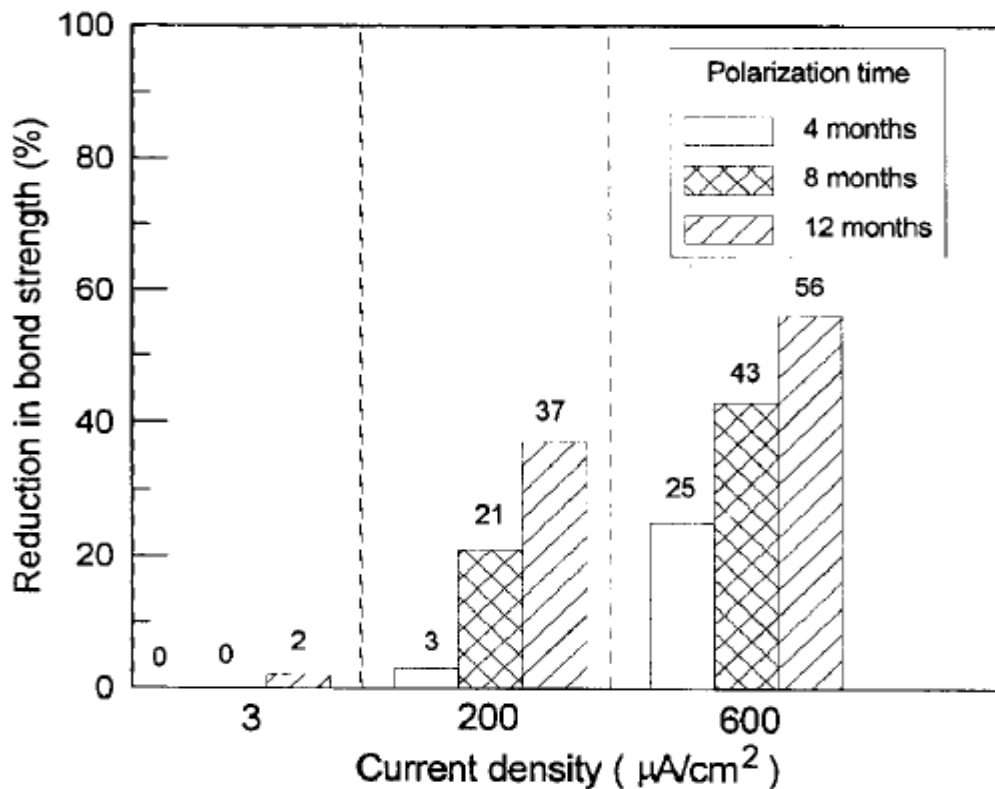


Fig.3.25 Bond strength reduction versus current density
 [Source: Chang et al. 1999]

A new parameter, ψ , was introduced and ψ is equal to the product of the current density and the polarization time. The bond strength versus ψ diagram is shown in Fig.3.26 in which $\psi = i_c \times t_p$ where i_c is the cathodic current density and t_p is the polarization time. The regression curve illustrates that a unified relationship between bond strength and ψ exists. Physically, the bond

degradation is mainly induced by the total amount of Na^+ and K^+ ions nearby the interface. And the accumulated amount of Na^+ and K^+ ions depends on the total transferred electrons during the polarization period. As ψ increased, the amount of Na^+ and K^+ ions per unit protected rebar area increased to attack the C-S-H gel nearby the interface and then resulted in the degradation of bond strength. The curve shows the degradation of bond strength due to the combined effect of the impressed current density and the polarization time.

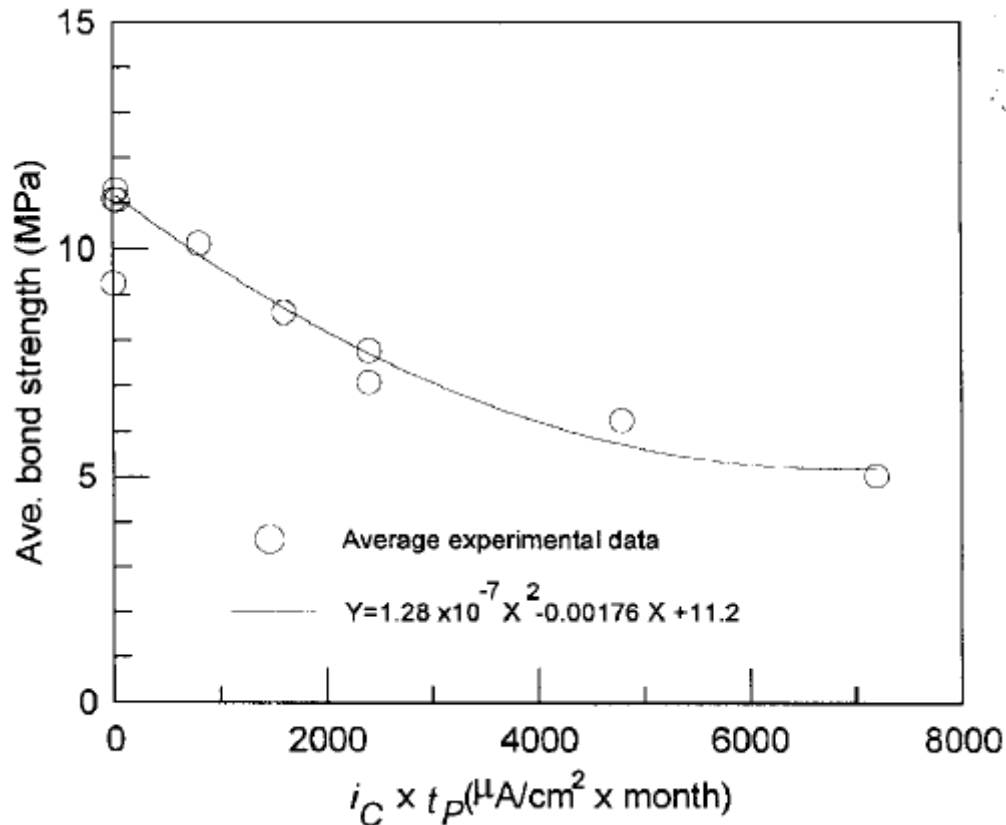


Fig.3.26 The average bond strength versus ψ
[Source: Chang et al. 1999]

Gadve et al. (2009) investigated the progression of corrosion of steel in concrete after it has been treated with surface bonded FRP. Concrete cylinders with embedded steel bars were immersed in NaCl solution and a direct current is passed making the reinforcement bar as an anode and another metal nobler than steel in electrochemical series as cathode. A stainless steel (SS) mesh rolled into a hollow, open cylinder was used as cathode as shown in fig.3.27. The cathode and the specimen were placed in 3.5% NaCl solution for 24 h to ensure full saturation of the test specimen. The level of NaCl solution was 3 cm below the top surface of the specimen to alleviate corrosion at the steel concrete interface. The DC regulated power supplier (DCRPS) used in this study could supply 500 mA DC at 60 V. The reinforcing steel bar was connected to the positive terminal of the external DC source and negative terminal was connected to the SS

mesh. The 100 mA direct electrical constant current ($CD = 1740.67 \mu\text{A}/\text{cm}^2$) was impressed between reinforcing bar and the SS mesh.

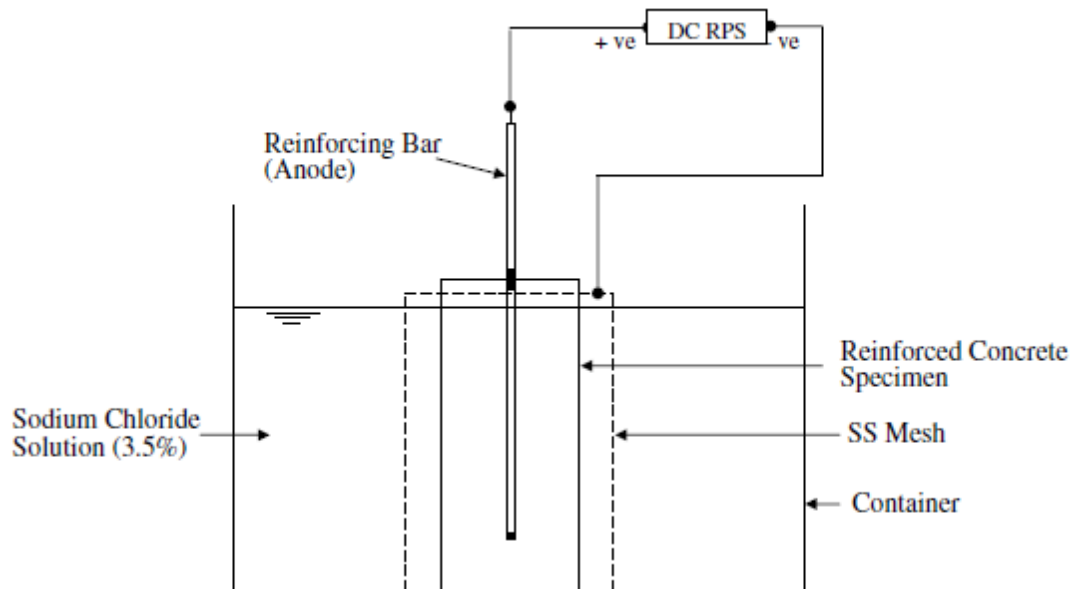


Fig.3.27 Schematic representation of the device for accelerated corrosion
[Source: Gadve et al. 2009]

All specimens were subjected to constant anodic current. The total duration of exposure was 24 days. The control sample was not wrapped and it received the exposure for the entire 24 days continuously. For the wrapped samples the exposure was divided into two stages – before and after the wrap. To simulate corrosion-damaged structures, prior to the application of wrap an initial exposure was applied. In practice, the FRP wraps are applied on structures that are corroded to varying degrees. Therefore, different exposure durations were chosen prior to the application of the wrap. Three exposure durations – 2, 4 and 8 days were applied. In two days the first crack appeared in all the samples. In 4 and 8 days the crack became wider and corrosion products oozed out in larger volumes.

Several performance parameters have been monitored. Half cell potential of reinforcing steel bars in all the specimens was recorded every 24 hours throughout the duration of experiment. Standard silver/silver chloride (Ag/AgCl) electrode was used as a reference electrode. Prior to the measurement of the half cell potential the anodic current was interrupted for an hour. Fig.3.28 shows variation of half cell potential with time. The initial observed potentials indicated that the steel was in passive condition that is virtually no corrosion was occurring. However, the potentials quickly dropped to the zone of active corrosion indicating the initiation of corrosion in all the samples roughly at the same time. The general trend was the movement of the half cell potential was upwards with time. The upward trend was similar in CFRP and GFRP wrapped

cylinders. An aberration was noted in the C8 and G8 samples where there was a sharp drop on potential towards the end of the exposure. Although half cell potential is a good indicator of initiation of corrosion it may not be effective in monitoring its progression. The rate of corrosion is considered proportional to the corrosion current (I_{corr}) for the specimen. It may be noted that the I_{corr} for the fresh specimen is much lower than the exposed specimens. This indicates that all the samples have corroded at varying rates. The bare sample had the highest I_{corr} . In comparison all the wrapped samples had a significantly lower I_{corr} . Lower I_{corr} for all the wrapped samples establishes that wrapping significantly reduces the rate of corrosion. There was no consistent trend between I_{corr} and the number of days of exposure prior to wrapping. However, all samples had a lower I_{corr} in comparison to the control sample. Therefore, it is concluded that impediment to corrosion is effected by FRP wraps at any stage of corrosion although this test was inconclusive of its rate dependence with respect to the length of exposure prior to wrapping. The C-8 sample indicated a lower corrosion potential (E_{corr}) and I_{corr} . This seems to be an aberration of results. It may be recalled that in half cell potential measurements too, C-8 showed inconsistent results. The glass wrapped specimens exhibited lower I_{corr} than the carbon wrapped specimens. This seems to be due to the higher electrical resistance offered by the GFRP than the CFRP.

Table 3.4 Test samples [Source: Gadve et al. 2009]

| Wrap Material | Anodic current duration (days) | | Nomenclature |
|---------------|--------------------------------|----------------|--------------|
| | Before wrapping | After wrapping | |
| Carbon | 24 | | Control |
| | 2 | 22 | C-2 |
| | 4 | 20 | C-4 |
| | 8 | 16 | C-8 |
| Glass | 2 | 22 | G-2 |
| | 4 | 20 | G-4 |
| | 8 | 16 | G-8 |

After 24 days of exposure to anodic current, pullout tests were carried out on all the specimens. This was done by securing the cylinder in a universal testing machine (UTM) and attaching the grip on to the protruding portion of the reinforcing bar. In case of the control specimen the bar pulled out of the specimen causing splitting of the cylinder. The pullout force was much larger in the case of wrapped samples. It may be recalled that there was considerable corrosion and consequent loss of metal at the top interface. As a result, the reinforcing bar of all specimens broke off at the interface. After completing the pullout test the corroded bars were cleaned of corrosion products and weighed to determine mass loss. The mass loss versus pullout strength graph is presented in fig.3.29. The control sample had lost much higher mass and pullout strength than the wrapped specimens. The scatter in data among the wrapped specimen was too high to have a firm inference on the relative performance of 2, 4 and 8 day samples. A linear fit

of the data shows that pullout strength is inversely proportional to the mass loss. As the reinforcement loses mass the bar becomes thinner and the bond is also lost. For each percentage of lost mass of steel the average loss of pullout strength is 1.2 MPa. It was concluded that FRP wrapped samples showed substantially higher resistance to corrosion. Also wrapping dramatically slows down the rate of corrosion.

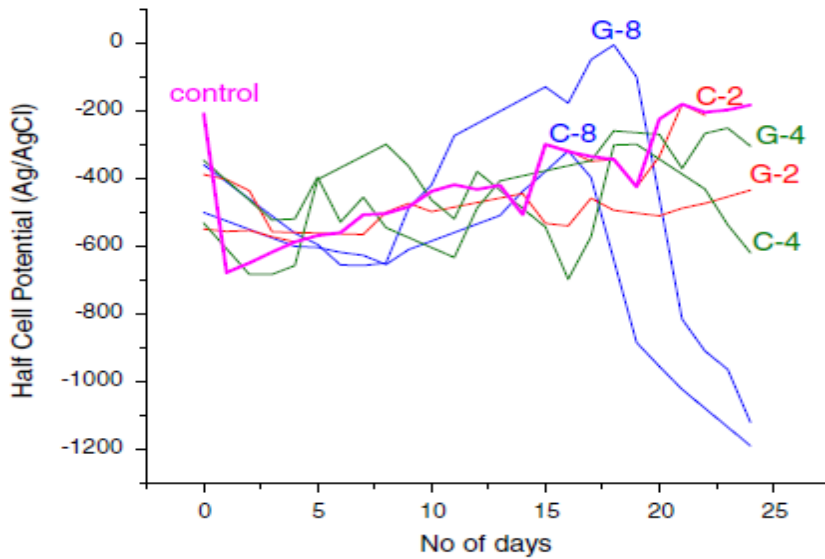


Fig.3.28. Variation of half cell potential with time
 [Source: Gadve et al. 2009]

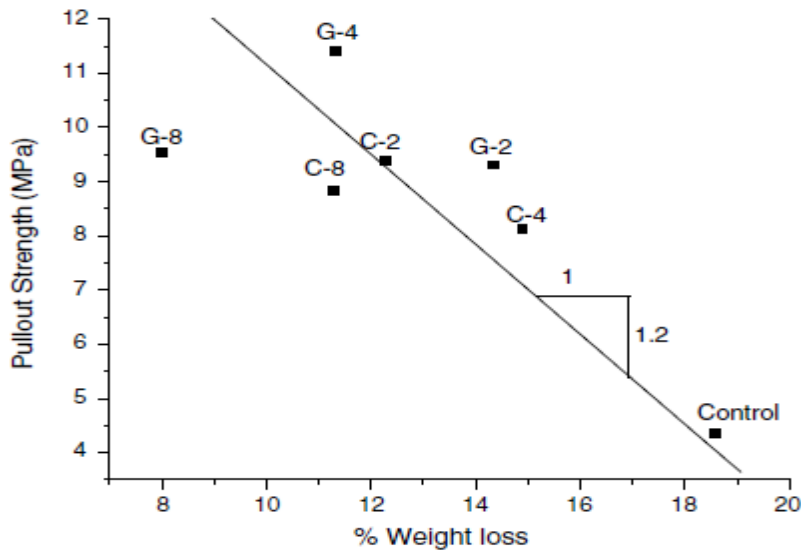


Fig.3.29 Variation of pullout strength with% mass loss
 [Source: Gadve et al. 2009]

Spainhour and Wootton (2008) investigated corrosion performance of steel reinforcement embedded in concrete samples encased by carbon fiber reinforced polymer (CFRP) wraps. Concrete samples were wrapped with 0-3 fabric layers impregnated with one of two different epoxies. To accelerate corrosion, samples were subjected to an impressed current and a high salinity solution. Current flow measurements dynamically monitored corrosion activity during exposure, while reinforcement mass losses were measured following exposure. Test results indicated that CFRP wrapped specimens had prolonged test life, decreased reinforcement mass loss, and lower corrosion rates. The performance of wrapped specimens was superior to that of either control samples or those coated only with epoxy. Results indicated that the level of corrosion abatement provided by the CFRP wraps was influenced both by the type of epoxy used and the number of wrap layers. The cumulative theoretical mass loss was compared to the actual mass loss for each sample. When current is passed through a bare steel bar exposed to water, chlorides, and oxygen, the correlation between actual and predicted mass loss should theoretically be equal to 1. This condition is found when a steel bar is suspended in a saline solution. However, once the steel bars are embedded in concrete this correlation is expected to change somewhat because of the effect of the concrete on current flow. It was found that in general the calculated mass loss under predicts the actual amount of corrosion mass loss; however, the results are actually well correlated.

A comparison of the accumulative predicted corrosion mass loss over time to actual mass loss was performed for control samples and samples treated with one of two different types of epoxies. Within groups, samples were treated with an epoxy coating or with a CFRP wrap having from one to three layers. For samples with or without CFRP wraps, the predicted mass loss based on Faraday's law correlates reasonably well with actual mass loss measured. Although the concrete and other factors may slightly affect the theoretical predictions, the calculated mass loss can be used to examine mass loss over time.

CFRP wrapping is effective at abating reinforcement corrosion by delaying the onset of corrosion, lengthening sample test lives and reducing the rate of corrosion mass loss.

Epoxy type is a significant factor affecting the performance and corrosion resistance of a CFRP wrap. One type of epoxy used for the CFRP wraps in this experiment (SG) is considerably more effective at delaying the onset and reducing the rate of corrosion in samples than another (WS). However, epoxy alone is not effective at abating reinforcement corrosion.

In samples with the WS epoxy, it was found that increasing the number of wrap layers, and thus the ability to develop circumferential confinement, improved a sample's performance. Results indicate that the level of corrosion abatement provided by the CFRP wraps was influenced both by the type of epoxy used and the number of wrap layers. This finding supports a claim that, to a certain extent, the suitability of the epoxy and not the thickness of the wrap is the primary performance factor in regards to the corrosion protection provided by a CFRP composite wrap.

However, even the better performing epoxy alone is not sufficient to significantly improve performance, without at least one carbon fabric layer, while additional CFRP layers improved sample performance with the poorer performing epoxy.

Gadve et al. (2009) investigated active protection of the steel embedded in concrete that is treated with surface-bonded carbon FRP. Cylindrical Specimens are kept immersed in 3.5% sodium chloride (NaCl) solution for 24 h to ensure full saturation. A stainless steel mesh rolled into a hollow, open cylinder is used as the cathode. The cathode and the specimen are placed in 3.5% NaCl solution. The level of NaCl solution is 3 cm below the top surface of the specimen to alleviate corrosion at the steel-concrete interface. The DC-regulated power supplier (DCRPS) used in the present study could supply 500 mA DC at 60 V. The reinforcing steel bar is connected to the positive terminal of the external DC source and the negative terminal is connected to the stainless steel mesh. The 100-mA direct electrical constant current ($I_{DC} = 1,740.67 \mu\text{A}/\text{cm}^2$) is impressed between the reinforcing bar and the stainless steel mesh.

After a specific period of exposure, the cracked RC specimens are treated with surface-bonded FRP. The samples are actively protected while subjecting them to a specified environment for a specific period. Active Protection Since carbon is electrically conductive; Gadve use this property in applying active protection to the reinforced concrete system without using any external anode. In this case, the carbon fiber sheets that were wrapped around the reinforced concrete specimen themselves are used as anodes and the reinforcing steel bar as cathode.

Half-cell potential is noted every day. Cell voltages are observed every day during induction of initial corrosion by impressing the anodic current into the reinforcing bar embedded in concrete. A galvanostat is used to obtain scans. Stainless steel counter electrode and Ag/AgCl reference electrode are used. Scanning is carried out at the rate of 1 mV/s, between the potential range of -1.2 V and 1.2 V , and zero equilibrium time is maintained. The scans are used to determine corrosion current (I_{corr}).

An important parameter for successful active protection is the amount of electrical energy to be supplied. Prior research suggests maintenance of half cell potential to threshold levels. “Instant-off” monitoring potential is used for the specimens exposed to the active protection. A standard Ag/AgCl electrode is used as a reference electrode. Prior to the measurement of the half-cell potential of the specimens subjected to the passive protection, the anodic current is interrupted for an hour.

Takewaka suggests that if some corrosion had been taking place on steel in concrete, subsequent corrosion can be stopped by setting the rebar potential to less than -550 mV (saturated Ag/AgCl). An “instantaneous off” (IR-free) steel potential (measured between 0.1 s and 1 s after switching off the DC source) more negative than -720 mV with respect to a Ag/AgCl/0.5 M potassium chloride (KCl) electrode is recommended for the prevention of steel from corrosion.

The corrosion protection potential maintained at a level less negative than 900 mV with respect to a Ag/AgCl/0.5 M KCl electrode is proposed for prestressing steel in the European Draft Standard (1996). In addition, it is specified that no “instantaneous off” (IR-free) steel potential may be more negative than $-1,100$ mV (for reinforcing steel) or -900 mV (for prestressing steel) with respect to a Ag/AgCl/0.5 M KCl electrode.

In the present study, the corrosion protection potential is obtained from a potentiodynamic scan by extrapolating the cathodic polarization curve. A tangent to the cathodic polarization curve is drawn. Its intercept with the voltage axis was determined. That voltage is maintained for active protection. The maximum value of the voltage is -750 mV. The required voltage is maintained throughout the period of exposure. Every day, the instant-off potential of each cathodically protected specimen is observed and confirmed that it is equal to or more negative than -750 mV with respect to standard Ag/AgCl electrode. The half-cell potentials are measured using a pH meter (input impedance: $1,014 \Omega$) in millivolts measurement mode.

The protected samples, both passive and active, exhibited much lower I_{corr} . This demonstrates that FRP wraps are extremely effective in protecting the corroding reinforcements in concrete. Moreover, the current reduced with time. This indicates passivation of steel. Therefore, the efficacy of the proposed protection systems is established. The initial current is higher in passively protected systems. However, they passivated at a fast rate with time. The active system exhibited a lower I_{corr} throughout the period of exposure. In the active systems the passivation is from the prevention of ionization of iron. It is observed that surface-bonded FRP wrapping protects steel in concrete and reduces the rate of corrosion to a great extent.

CHAPTER 4 EXPERIMENTAL PROGRAMME

4.1 GENERAL

In this chapter the experimental setup is presented to evaluate the performance of FRP wrapped specimens. Laboratory samples of FRP wrapped RC specimens were prepared and exposed to accelerated corrosion by impressing anodic current into the reinforcing bar, which is considered very harsh environment. The procedure for monitoring the progression of corrosion of steel in concrete by using NDT techniques namely electrochemical LPR measurement and half cell measurement is also explained in detail.

4.2 TEST PROGRAMME

The objective of test programme is to find out the corrosion behavior of CFRP retrofitted slabs by applying active protection using current density 10 mA (equivalent to 40 $\mu\text{A}/\text{cm}^2$). The test programme involved:

1. Determinations of basic properties of constituent materials namely cement, fine aggregates, coarse aggregates and steel bars as per relevant Indian standard specifications.
2. Casting of slabs of size 300 x 300 x 100 mm with concentric 25 mm diameter mild steel bar using M 20 grade concrete.
3. Subjecting the slab specimens to accelerated corrosion by providing initial voltage of 10 mV.
4. Retrofitting corroded slab specimens by wrapping with CFRP sheets and further protecting rebars through active protection by applying anodic current of 10 mA. This protection is provided at 3 different stages of corrosion:-
 - Onset of corrosion
 - Onset of crack
 - Two days after onset of crack
5. In order to study the effect of level of anodic current active protection.

Table 4.1: Test Specimens

| S.No. | Dimension (mm) | Level of current | Wrapping levels | Specimen No. |
|-------|----------------|------------------|--------------------|--------------|
| 1 | 300×300×100 | 10mA | Onset of corrosion | C-1 |
| | | | Onset of crack | C-2 |
| | | | 2 days after crack | C-3 |

Test specimens are shown in **Table 4.1**. An accelerated corrosion technique is used so that testing could be completed within a reasonable time. Power supply is used for this purpose. This power supply allowed application of a constant voltage and constant current. The power supply had voltage and current capacities of 150 V and 1000 milliamperes (mA) in increments of 1 V and 1 mA, respectively. An LCD screen displayed the instantaneous voltage and current, which allowed continuous monitoring of the fluctuation in the impressed current with time. **Fig. 4.1** shows a general view of the specimens and the power supply used to accelerate corrosion.



Fig 4.1 Specimens and the Power Supplies Used to Accelerate Corrosion

All specimens are exposed to the same environmental conditions to elucidate the effect of test parameters on corrosion activity and concrete cracking.

4.3 MATERIALS USED

Cement, fine aggregates, coarse aggregates, water and MS bars are used in casting of slabs. The specifications and properties of these materials are as under:

4.3.1 Cement

Ordinary Portland cement of 43 grade is used for the present investigation. The cement is of uniform colour i.e. grey with a light greenish shade and is free from any hard lumps. Summary of the various tests conducted on cement are given in **Table 4.2**. All the tests are carried out in accordance with procedure laid down in IS: 8112-1989.

4.3.2 Fine Aggregates

The fine aggregates used for the experimental work is locally procured and conformed to grading zone III. Sieve Analysis of the fine aggregate is carried out in the laboratory as per IS 383-1870. The sand is first sieved through 4.75 mm sieve to remove any particle greater than 4.75 mm sieve and then washed to remove the dust. The physical properties and sieve analysis of fine aggregates are shown in **Table 4.3 and 4.4**.

Table 4.2: Physical Properties of Cement

| S.No. | Characteristics | Values obtained | Standard values |
|--|----------------------|-----------------|---------------------------------|
| 1 | Normal Consistency | 33% | - |
| 2 | Initial Setting time | 48 min | Not be less than 30 minutes |
| 3 | Final Setting time | 240 min | Not be greater than 600 minutes |
| 4 | Fineness | 4.8% | <10 |
| 5 | Specific gravity | 3.09 | - |
| Compressive strength:- Cement : Sand (1:3) | | | |
| 1 | 3 days | 24.5 MPa | 27 MPa |
| 2 | 7 days | 38 MPa | 41 MPa |
| 3 | 28 days | 45 MPa | 43 MPa |

Table 4.3: Physical Properties of Fine Aggregates

| S.No. | Characteristics | Value |
|-------|---|----------|
| 1 | Specific gravity | 2.46 |
| 2 | Bulk density | 1.4 g/cc |
| 3 | Fineness modulus | 2.56 |
| 4 | Water absorption | 0.85% |
| 5 | Grading Zone (Based on percentage passing 0.60mm) | Zone III |

Table 4.4 Sieve Analysis of Fine Aggregate

| S.No. | Sieve Size | Mass retained (gm) | Percentage Retained | Cumulative Percentage Retained | Percent Passing |
|-------|------------|--------------------|---------------------|--------------------------------|-----------------|
| 1 | 4.75 mm | 4.0 | 0.4 | 0.4 | 99.6 |
| 2 | 2.36 mm | 75.0 | 7.50 | 7.90 | 92.1 |
| 3 | 1.18 mm | 178.0 | 17.8 | 25.70 | 74.3 |
| 4 | 600 µm | 220.0 | 22.0 | 47.70 | 52.3 |
| 5 | 300 µm | 274.0 | 27.4 | 75.10 | 24.9 |
| 6 | 150 µm | 246.5 | 24.65 | 99.75 | .25 |
| 7 | 2.50 | 0.25 | 0.25 | Σ=256.55 | |

Total weight taken = 1000 gm

Fineness Modulus of fine aggregates = 2.56

4.3.3 Coarse Aggregates

Crushed stone aggregate (locally available) of nominal size 10 mm are used throughout the experimental study. The aggregates are washed to remove dust and dirt and are dried to surface dry condition. The aggregates are tested as per IS: 383-1970. The results of various tests conducted on coarse aggregate are given in **Table 4.5** and **Table 4.6** shows the sieve analysis results.

Table 4.5 Physical Properties of Coarse Aggregates

| S.No. | Characteristics | Value |
|-------|------------------------|---------|
| 1 | Type | Crushed |
| 2 | Specific Gravity | 2.66 |
| 3 | Total Water Absorption | 0.56% |
| 4 | Fineness Modulus | 6.83 |

Table 4.6 Sieve Analysis of Coarse Aggregates

| S.No. | Sieve Size | Mass retained (gm) | Percentage Retained | Cumulative Percentage Retained | Percent Passing |
|-------|------------|--------------------|---------------------|--------------------------------|-----------------|
| 1 | 20 mm | 0 | 0 | 0 | 100 |
| 2 | 10 mm | 2516 | 83.89 | 83.87 | 16.13 |
| 3 | 4.75 mm | 474 | 15.8 | 99.67 | 0.33 |
| 4 | PAN | 10 | 0.33 | Σ= 183.54 | |

Total weight taken = 3Kg

FM of 10 mm Coarse aggregate = $(183.54+500) / 100 = 6.83$

4.3.4 Water

Fresh and clean tap water is used for casting the specimens in the present study. The water is relatively free from organic matter, silt, oil, sugar, chloride and acidic material as per Indian standard.

4.3.5 Steel Reinforcement

Mild steel bars of 25 mm diameters and 600 mm length are used as longitudinal reinforcement. The central 300 mm length of rebar is embedded in concrete and 150 mm is exposed on both sides in order to make electrical connections. **Table 4.7** shows the properties of reinforcing bars used for casting of RC beams.

Table 4.7 Properties of Reinforcing Bars Used for Casting of RC Beam

| Type and size of bar | Ultimate Tensile Stress(MPa) | Yield stress(MPa) | Young's Modulus(GPa) | Percentage Elongation |
|----------------------|------------------------------|-------------------|----------------------|-----------------------|
| Mild Steel, 25mm | 410 | 240 | 200 | 23 |

4.3.6 CFRP material

Unidirectional CFRP (electrically conductive) sheets as shown in **Fig. 4.2** having cross section 300 X 0.1176 mm are used for wrapping the corroded samples. The CFRP sheets are obtained from BASF construction chemicals and building systems. **Table 4.8** shows the properties of CFRP Sheets.



Fig 4.2 CFRP sheet used in the experiment

Table 4.8 Properties of CFRP Sheets

| S.No. | Physical properties | Value |
|-------|-----------------------|----------|
| 1 | Tensile Strength | 3800 MPa |
| 2 | Modulus of elasticity | 240 GPa |
| 3 | Density | 1.7 |

4.3.7 Adhesives

The adhesive used for bonding FRP sheets with concrete is a compatible epoxy system provided by the manufacturer. It is blue pigmented epoxy resin for saturation of Embraced fibre sheet to form in-situ FRP Composite. It is made by mixing base saturant and hardener in ratio 100:40. Mixing of saturant and hardener is done thoroughly for five minutes until components are thoroughly dispersed. Graphite powder is added during mixing in order to make the epoxy conductive. Properties of Epoxy are discussed in **Table 4.9**.

Table 4.9 Properties of Saturant

| S.No. | Properties | Values |
|-------|-------------------------------|-------------------------|
| 1 | Aspect | Translucent Blue Liquid |
| 2 | Density | 1.13± 0.03 |
| 3 | Mixing ratio, by weight (B:H) | 100:40 |
| 4 | Pot life | 25 minutes at 25 degree |
| 5 | Tensile strength | > then 17 MPa |
| 6 | Compressive Strength | >40 MPa after 1 day |
| 7 | Flexural strength | >35 MPa |

4.4 DESIGN OF CONCRETE MIX

Concrete mix is prepared using 43 grade Portland pozzolana cement, fine aggregate (medium-sized natural river sand) and crushed stone coarse aggregate with nominal size of 10 mm. The mix is designed as per Indian Standard Guidelines. The ratio of cement: sand: coarse aggregate is 1:1.49:2.48. The water-cement ratio is 0.5 and compressive strength of concrete after 28 days is 29 MPa.

4.5 TEST PROCEDURE

4.5.1 General

Corrosion initiation takes place when the chloride concentration at the rebar level reaches a critical value. The most established of the electrochemical techniques to assess initiation of corrosion activity is half-cell potential mapping. Steel reinforcement potentials relative to a stable reference half-cell, which can be measured from the surface of the concrete, can be related to the probabilities of corrosion using the guidelines in ASTM C876-91. The method of measurement is based on a simple technique and well established equivalence is available for converting the potential obtained from one reference electrode to another. Thus half-cell potential can serve as a determining parameter for indicating initiation of corrosion. In the present study, the half cell potential measurements are carried out with reference to saturated calomel electrode (SCE). Along with half cell potential, linear polarization resistance test is conducted on all slab specimens by monitoring the specimens daily.

4.5.2 Preparation and Preconditioning of Steel Bars

Steel bars are cut to the required length of 600 mm. Each bar is then wire brushed to remove any surface scale. These are then cleaned by soaking in analytical reagent grade hexane and allowed to air dry. This steel specimen preparation is similar as specified in *ASTM G 109*. Before casting of the test specimens, each reinforcing bar is weighed to 0.1 gm accuracy.

4.5.3 Preparation of Slab Specimen

In the present program, a special moulding system is fabricated for casting the specimens. The slabs are cast in mould of size 300 x 300 x 100 mm with steel bars placed concentrically. First of all the interior of slab mould is oiled, so that the slabs can be easily removed from the mould after 24 hours. While embedding these bars in concrete, they are kept in such a way that 150 mm lengths of these bars is protruded outside of the concrete specimen from both sides. Initial weight of all rebars is measured. When the bars have been placed in position, concrete mix is poured and vibrations are given so that the mix gets compacted. The vibration is done until the mould is completely filled and there is no gap left. The slabs are then removed from the mould after 24 hours. After demoulding the slabs are cured for 28 days using jute bags. The concrete surface of the slabs is then cleaned and all dirt and loose materials are removed before initiation of corrosion/work.

4.6 INDUCING CORROSION IN STEEL REBAR

The objective of inducing corrosion to the reinforcing bar is to simulate the corrosion damaged concrete. The commonly used methods of inducing corrosion in RC specimens can be recalled as salt spray (*Debaiky et al. 2002; Gadve et al. 2009*) Chloride diffusion (*Masoud and Soudki 2006*), alternate drying and wetting in salt water (*Debaiky et al. 2002 and Soudki 2006*) and impressing anodic current (*Wootton et al. 2003*). Previous studies have shown that test specimens kept in a salt spray chamber for more than 100 days did not show any visible signs of corrosion. This method was not found suitable considering the time constraint. Method of adding chlorides artificially to the concrete during casting is an effective method of initiating corrosion in steel rebar. This method was not considered because it did not simulate the present condition of interest. Alternate immersion into NaCl (Sodium Chloride) solution and drying of the specimens also induces corrosion. However, the quickest method of inducing corrosion is by impressing anodic current. In this method, NaCl solution is supplied to the specimens and a direct current is passed making the reinforcement bar as an anode and another metal nobler than steel in electro-chemical series as cathode. Incidentally, this method has been used by a number of previous investigators (*Bonacci & Maleej 2000; Masoud et al. 2001; Bhavneet et al. 2010; Gadve et al. 2009*).



Fig. 4.3 View of Stainless Steel Mesh



Fig 4.4 Dripping With 5% NaCl Solution

PRESENT METHOD OF INDUCING ACCELERATED CORROSION

In this investigation, the specimens are kept fully saturated by continuously dripping with 5% NaCl solution as shown in **Fig 4.3**. Mats are placed over the tops to provide even distribution of NaCl solution. The rebar is used as anode. A stainless steel (SS) mesh is rolled around 300 mm length of specimen and tied together with metal ties in order to assure electrical continuity and is used as cathode (**Fig. 4.4**). The reinforcement extended 150 mm on both sides past the concrete to allow easy access for making electrical connections to the steel. The constant voltage of 10 mV is impressed in order to accelerate corrosion. The DC regulated power supplier (DCRPS) used in the present study could supply 1000 mA DC at 30V. The rebar is connected to the positive terminal of the external DC source and negative terminal is connected to the SS mesh. It is more common to maintain a constant voltage between the cathode and the anode (*Soudki 2006; Gadve et al. 2009*). Half-Cell potential and linear polarization measurements are obtained daily for all the specimens throughout the duration of experiment.

4.7 WRAPPING THE PRE-CORRODED SPECIMENS

Two fiber materials are popular in the rehabilitation of structures in India- glass and carbon. Carbon scores higher than glass in terms of strength, stiffness, durability, corrosion and fatigue resistance in structural rehabilitations. Electrically conductive carbon fiber sheets offer a

possibility of cathodic protection of the structure. Therefore, carbon fiber sheets have been used in the present investigation.

Method of applying wraps

The samples are air dried prior to the application of FRP wraps. Manufacturer's specifications are followed in the application of the wraps. A grinder is used for rounding off the sharp corners and removing local unevenness from the surfaces. A mixture of two components of epoxy resin and hardener is mixed in the ratio 100:40 for wrapping the carbon fiber sheets onto concrete. Since the epoxy adhesive used is not electrically conductive, therefore it is made conductive by adding 20-25% of conductive graphite powder.

Unidirectional CFRP sheet is used for wrapping. One layer of CFRP sheet is wrapped throughout 300 mm length of the test specimens and an overlap of 50 mm is provided at the ends of the sheets. This CFRP wrapped test specimen is additionally provided with adhesively bonded 25-30 mm wide carbon ribbon so that uniform distribution of direct current throughout the specimen is possible for effective application of active protection. Sufficient pull is applied to the fiber sheet to ensure uniform direction of fiber and absence of wrinkles. Care is taken to avoid air gaps between the concrete surface and the confining carbon fibers. For this plain rod is rubbed for smoothening on top surface of CFRP sheets so that the sheet makes uniform bond with epoxy. All the wrapped specimens required one day to cure.

4.8 ACTIVE PROTECTION

Active protection is a technique which aims at stopping rebar corrosion in chloride contaminated concrete. The alkalinity of the concrete around the rebars is restored, and an environment favorable to the passivation of steel is re-created. The technique is based on the application of a DC current in which the rebar acts as cathode and CFRP sheets wrapped on the external surface of the concrete, are used as anode. It is an electrochemical process, exactly opposite to that of corrosion process, which also involves anode, cathode and electrolyte.

4.9 CORRODING THE WRAPPED SPECIMENS

One of the objectives of study is to investigate the effect of impressed current for active protection. To simulate corrosion damaged structures, prior to the application of wrap an initial exposure is applied. In practice, the FRP wraps are applied on structures that are corroded to

varying degrees. Therefore, different exposure durations are chosen prior to the application of the wrap. Three exposure durations - onset of corrosion, onset of visible crack, and 2 days after onset of visible crack are applied. The total duration of exposure is 80 days for all specimens. For this all specimens are subjected to constant anodic current. 10 mA current is applied for all specimens. Ponding with 5 % NaCl is done. The positive terminal is connected to the carbon fibre ribbon and the negative terminal is connected to the rebar. Corrosion monitoring is done as explained earlier using half cell and LPR.

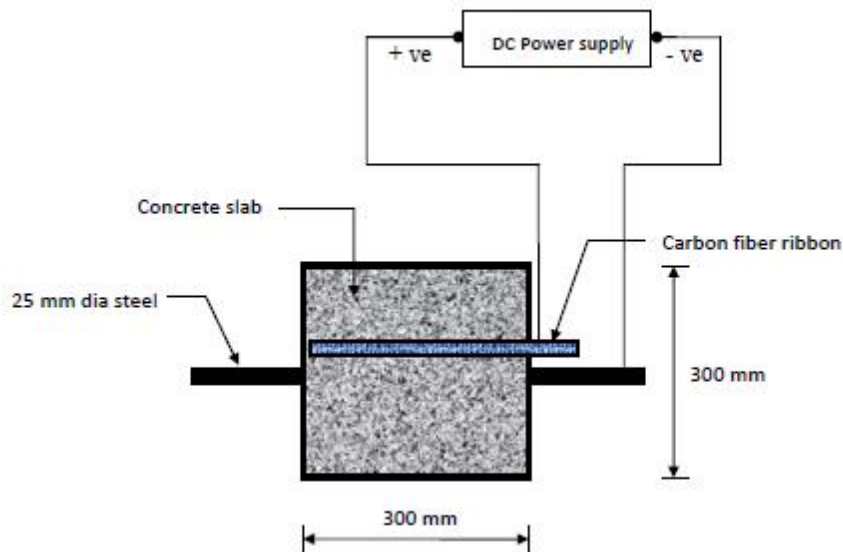


Fig. 4.5 Top View of Beam Showing Terminals for Active Protection

4.10 CORROSION MONITORING TECHNIQUES

Corrosion of steel embedded in concrete is not visually evident until the damage reaches to the external signs of deterioration as rust spots, cracks or spalling. In order to predict the corrosion service life of reinforced concrete structures and to determine the need of repair or rehabilitation, it is necessary to use non-destructive techniques for assessing the corrosion activity and measuring the corrosion rate of the reinforcements. In the present study, the corrosion rate of rebar is monitored by electrochemical methods.

4.6.1 Electrochemical Techniques

The electrochemical measurements are carried out using a versatile instrument that is capable of performing various electrochemical tests such as potential measurement, AC impedance technique, potentiostatic cyclic sweep test, LPR measurements etc. **Fig 4.6** shows ACM setup

used for electrochemical monitoring. The instrument is capable of processing the data and plotting the outputs automatically.

The half cell potential measurement gives only an indication of the corrosion risk of the steel and is linked by empirical comparisons to the probability of corrosion. Therefore along with half cell, linear polarisation (corrosion rate) measurements are taken which provides a valuable insight into the instantaneous corrosion rate of the steel reinforcement, giving more detailed information than a simple potential survey. The LPR data enables a more detailed assessment of the structural condition and is a major tool in deciding upon the optimum remedial strategy to be adopted. Hence the two important electrochemical techniques that are used for the studying the corrosion activity are corrosion potential (E_{corr}) and corrosion current /current density (I_{corr}). These determining parameters indicate the corrosion initiation which account for steel surface condition and the chloride ion concentration in concrete (*Pradhan and Bhattacharjee 2009; Bhavneet 2010*).

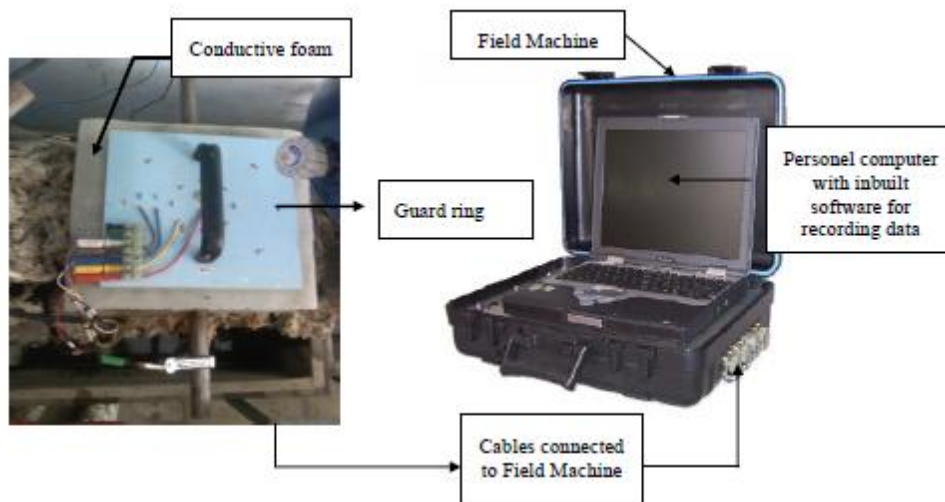


Fig. 4.6 ACM Setup Used for Electrochemical Monitoring

4.10.1.1 Half cell potential measurements

In the present study, all the specimens are monitored daily by half-cell potential using a saturated calomel reference electrode by placing the electrode on top surface of the concrete. The procedure followed is ASTM Standard C 876. The power supply is switched off one hour before taking the half cell readings in order to completely depolarize it. To maintain a consistent testing environment of 80-day experimental test period, the dripping salt water is replaced daily, electrodes are cleaned daily. If the corrosion potential reading is more positive than -200 mV, probability is that no reinforcing steel corrosion is occurring in the area at the time of

measurement and if the potential reading is more negative than -426 mV , probability is that the reinforcing steel corrosion is occurring. The ASTM interpretation of half-cell potential (SCE) is summarized in **Table 4.10**. The experimental arrangement for half cell measurement is shown in **Fig. 4.7**.

Table 4.10 The ASTM Interpretation of Half-Cell Potential Readings

| Open circuit potential (OCP) values | Corrosion condition |
|-------------------------------------|--|
| $< -426\text{ mV}$ | Severe corrosion, corrosion induced cracking may occur |
| $< -276\text{ mV}$ | High risk, 90% probability of corrosion |
| $-126\text{ to }-275\text{ mV}$ | Intermediate risk, corrosion activity in uncertain |
| $0\text{ to }-125\text{ mV}$ | Low risk, 10% probability of corrosion |



Fig 4.7 Half Cell Arrangement

4.10.1.2 Linear polarization resistance (LPR) measurements

Electrochemical LPR technique is especially good at measuring the localized corrosion. LPR measurements on concrete surfaces are performed using guard ring that is supplied with the field machine for precise location of rebar areas. The Guard Ring simply connects to the front panel via the supplied cables. Incorporated into the Guard Ring is a Cu/CuSO_4 reference electrode. Before performing the test, conducting sponge is wetted with NaCl solution and placed on the surface of the slab specimen to have proper electrical contact with the guard ring. Guard ring assembly is then placed above the wetted sponge. The electrical connections are made to the steel rebar.

For linear polarization resistance measurement, the working electrode i.e. the steel rebar is polarized to ± 20 mV from the equilibrium potential at a scan rate of 0.1 mV per second. The experimental arrangement for LPR measurement with guard ring arrangement is shown in **Fig. 4.8**. The polarized surface area of the steel rebar is taken to be that lying under a circle intersecting the midpoint between the two sensor electrodes and only the top half surface area of the steel reinforcement is assumed to be polarized.



Fig. 4.8 Guard Ring Arrangement

For calculation of the corrosion current density I_{corr} , Stern-Geary equation is used; (*Song and Saraswathy 2007*)

$$I_{\text{corr}} = B/R_p$$

Where B is the Stern-Geary constant and is given by $B = (\beta_a \times \beta_c) / 2.3(\beta_a + \beta_c)$. β_a and β_c are anodic and cathodic Tafel constants respectively. The value of B is taken as 26 mV considering steel in active condition. R_p is the polarization resistance.

CHAPTER 5

RESULTS AND DISCUSSIONS

In this chapter, the findings of an experimental investigation are presented, wherein various corrosion tests have been conducted to evaluate the performance of FRP wrapped specimens actively protected against corrosion.

5.1 GENERAL

A number of techniques are available that can be used to carry out assessment of a structure facing problem of corrosion to the reinforcement. In order to determine the rate of deterioration of the structure, it is preferable to monitor the condition change with time. The objective of our present study is to investigate the efficacy of active protection with CFRP composites used for the repair of corroded reinforced concrete slabs. First, the slabs are subjected to acceleration corrosion process to initiate corrosion. They are then repaired and actively protected so that further corrosion of steel can be prevented. Monitoring is done using two test methods namely half cell and LPR measurements.

5.2 ELECTROCHEMICAL MEASUREMENTS

5.2.1 Half cell measurements

Half-cell potential of reinforcing steel bars in all the specimens is recorded everyday throughout the duration of experiment. Saturated calomel electrode is used as a reference electrode. Prior to the measurement of the half-cell potential, the anodic current is interrupted for an hour. The major objective of our study is to investigate the effect of applied current during active corrosion protection on behavior of slabs. 10 mA ($40 \mu\text{A}/\text{cm}^2$) applied current is used for this purpose. **Fig.5.1** and **fig.5.2** and **fig.5.3** show the variation of half cell potential during the test period for the all three slabs protected at different level of corrosion.

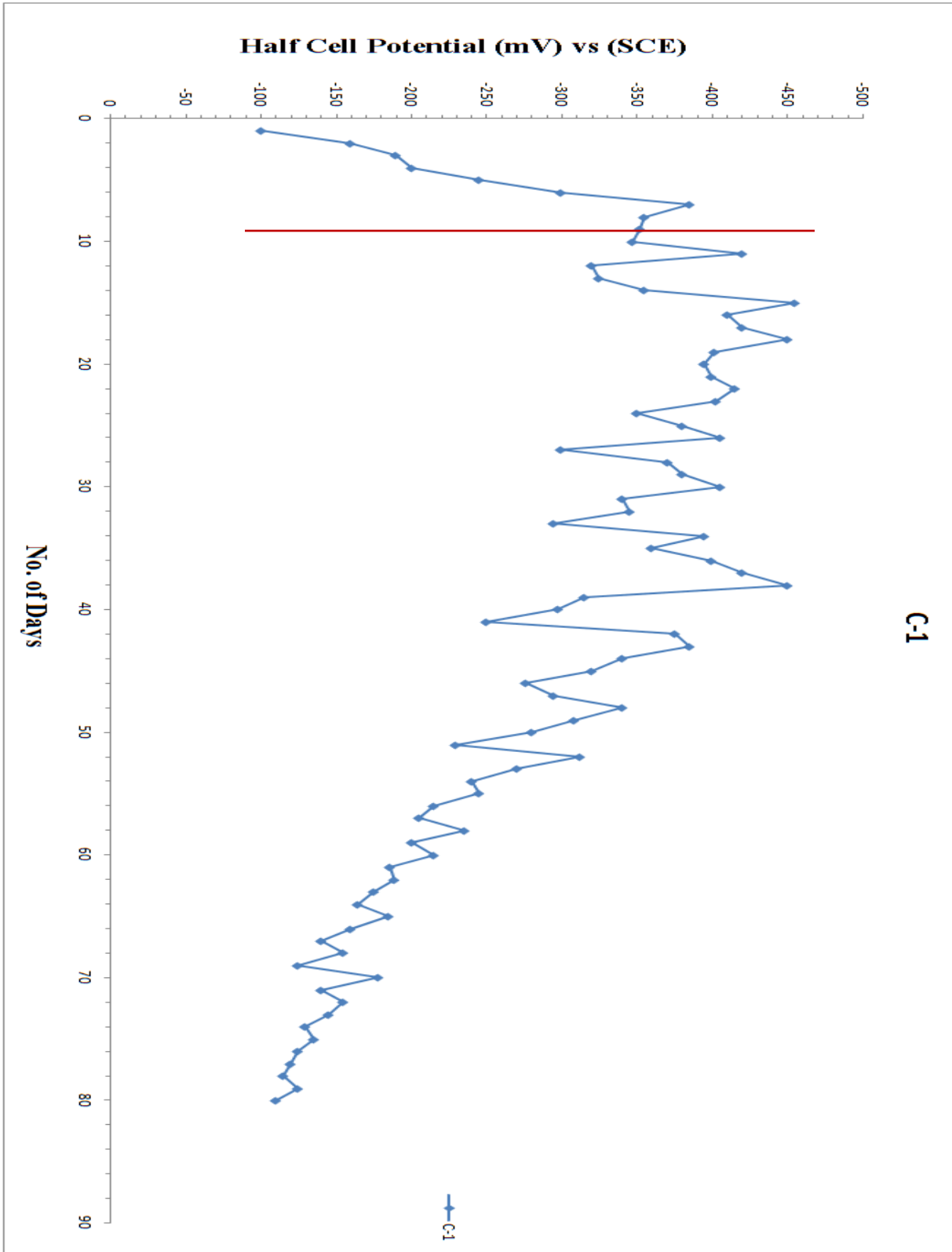


Fig. 5.1 Variation of half-cell potential with time for slab C-1 protected after onset of corrosion

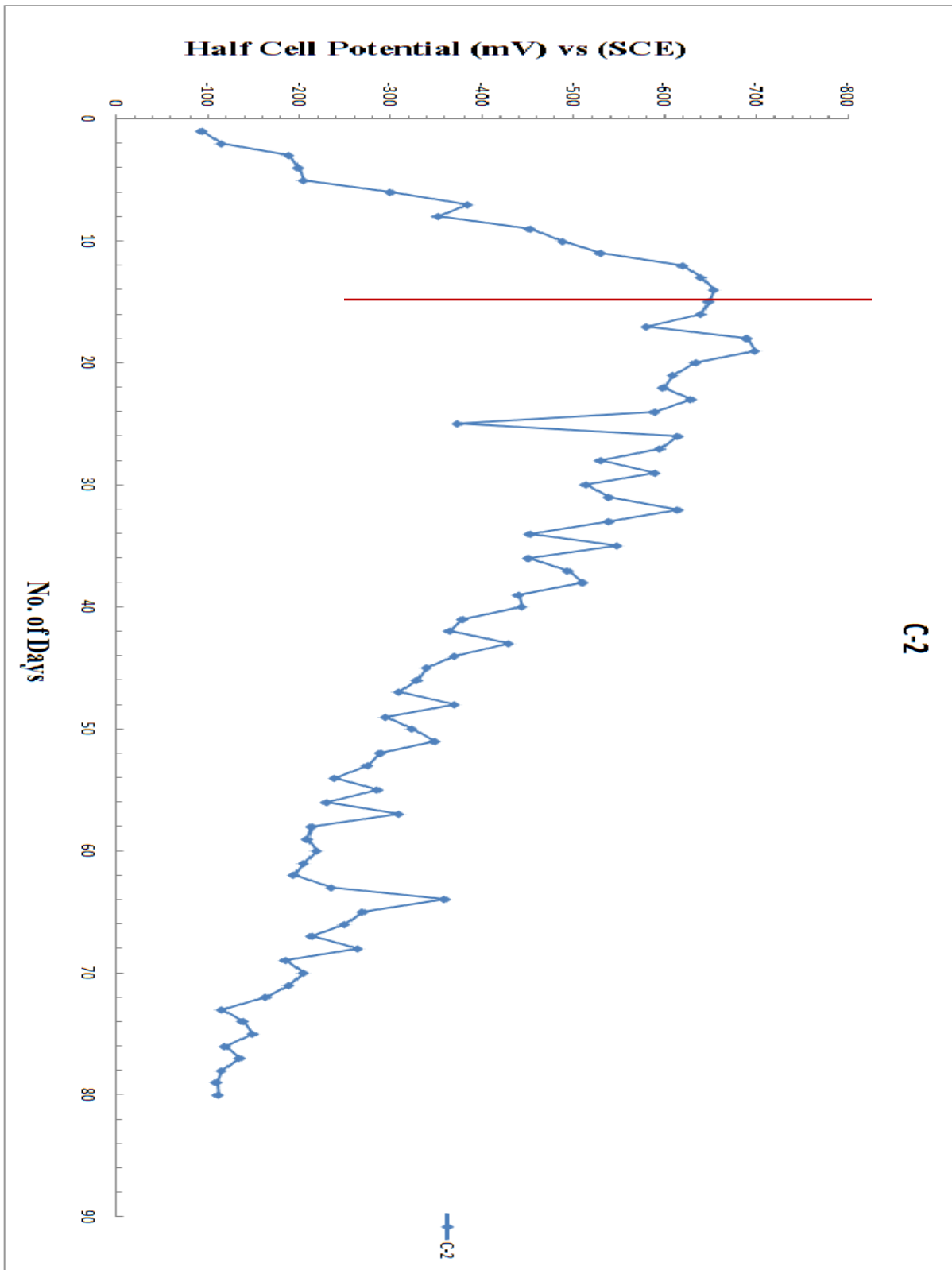


Fig. 5.2 Variation of half-cell potential with time for slab C-2 protected after onset of visible crack

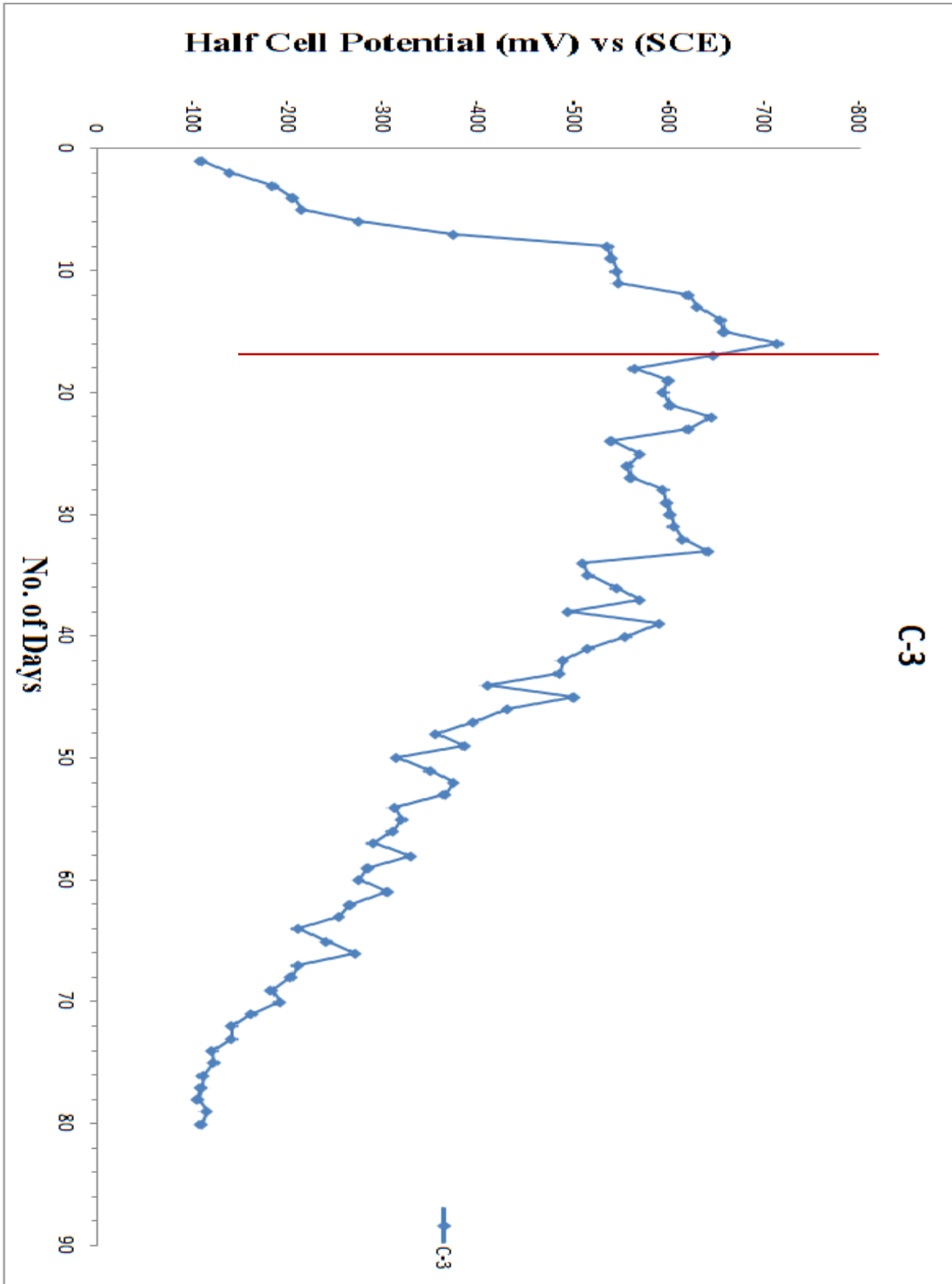


Fig. 5.3 Variation of half-cell potential with time for slab C-3 protected at two days after visible crack

5.2.1.1 Observations

Establishing structures potential map, according to ASTM C876-91, is the most commonly applied electrochemical technique for diagnosing the corrosion risk of reinforced concrete structures (*Pradhan and Bhattacharjee (2009); Saily et al.(2010)*). ASTM C876-91 suggests that the corrosion possibility of rebar embedded in concrete is higher than 90% when the open circuit potential is lower than -426 mV (SCE).

From the experimental results, it is observed that the half cell measurements keep on varying with time but within a certain defined range. In the initial stages of corrosion acceleration, the half cell potential values are less than the corrosion threshold values ie -426 mV, which indicates that corrosion, has not started yet. Then the values kept on decreasing towards the more negative side indicating depassivation of rebar, until it reached a stage of severe corrosion. This rate of drop is nearly uniform for all specimens. With the passage of time longitudinal cracks appeared along the length of the rebar as shown in **Fig.5.4**. The reason behind this is due to the formation of corrosion products around the rebar that occupies volume larger than the original volume of the rebar, causing bursting stresses in the concrete. This indicates that corrosion has caused enough steel cross section loss and the structural capacity of the element is significantly impaired. The occurrence of longitudinal cracking if not repaired May often be precursors to more critical and dangerous situation. That is why retrofitting of slabs is required at this stage.

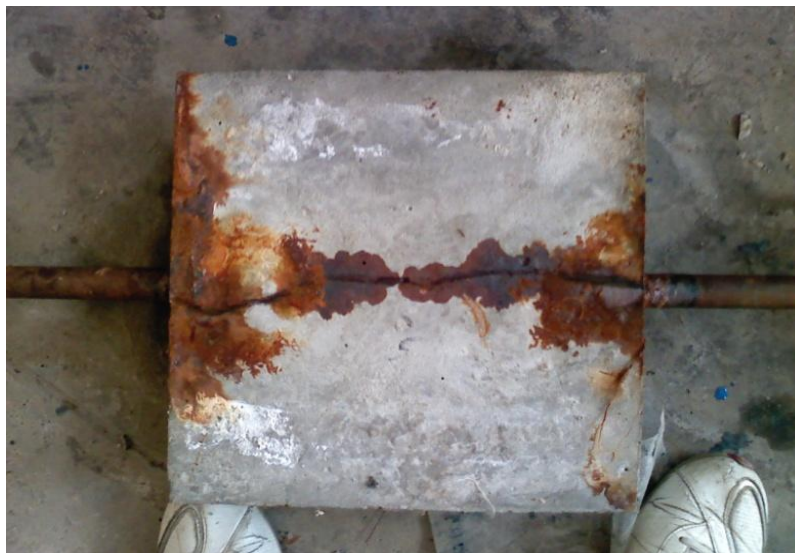


Fig.5.4 Longitudinal crack along the length of rebar

From the results, it is observed that, there is sudden drop in half-cell potential of the rebar specimens after a certain interval of time. This indicated that a certain amount of chloride has reached the steel bar as expected and is responsible for the corrosion initiation as it has become anodic.

However, after active protection i.e. after wrapping and providing impressed current of 10 mA, the half cell value rises slowly, in all the specimens irrespective of time of wrapping and applied current. It indicates that FRP did serve as an effective barrier for chlorides and prevented corrosion activity from taking place to some extent. Similar observations were made by *Gadve et al. (2010)* for FRP wrapped samples. From the results, it is observed that, E_{corr} values of specimens are reached at passive stage. It shows that the active protections of FRP wrapped specimens are very effective in prevention of corrosion.

5.2.2 Corrosion Rate by LPR Technique

Half cell potential (E_{corr}) is effective only in monitoring the corrosion initiation. *Feliu et al. (2009)* found that E_{corr} depends on the degree of wetness of the concrete to a great extent. *Xu and Yao (2009)* concluded that the corrosion state of steel in chloride containing and chloride-free structures tends to be confused if the decision is based exclusively upon the E_{corr} values. Therefore LPR measurements are necessary as the values obtained from corrosion current density (I_{corr}) indicate the progression of corrosion in the propagation phase.

5.2.2.1 Observations

From the determined corrosion current density values by LPR method it is observed that the corrosion current density (I_{corr}) increased with days of exposure to applied voltage due to increase in chloride concentration around the rebar in all the specimens. As the corrosion progresses in the slabs the value of corrosion current (I_{corr}) rises. This is because of the depassivation of layer formed around the rebar due to the concentration of chlorides. From the graphs, it is concluded that during the acceleration process, the I_{corr} values are between 6 – 15 $\mu\text{A}/\text{cm}^2$ which indicates low corrosion. As we are increasing the exposure value the I_{corr} rises upto 20 $\mu\text{A}/\text{cm}^2$ which indicates moderate corrosion. Further as the exposure value increases, I_{corr} reaches 26 $\mu\text{A}/\text{cm}^2$ which indicates severe corrosion and crack is observed. Similar observations were made by *Martínez and Andrade (2009)*. **Fig.5.5** and **fig.5.6** and **fig 5.7** show the Variation of LPR with time for the 80-day test period for the all three slabs protected at different level of corrosion.

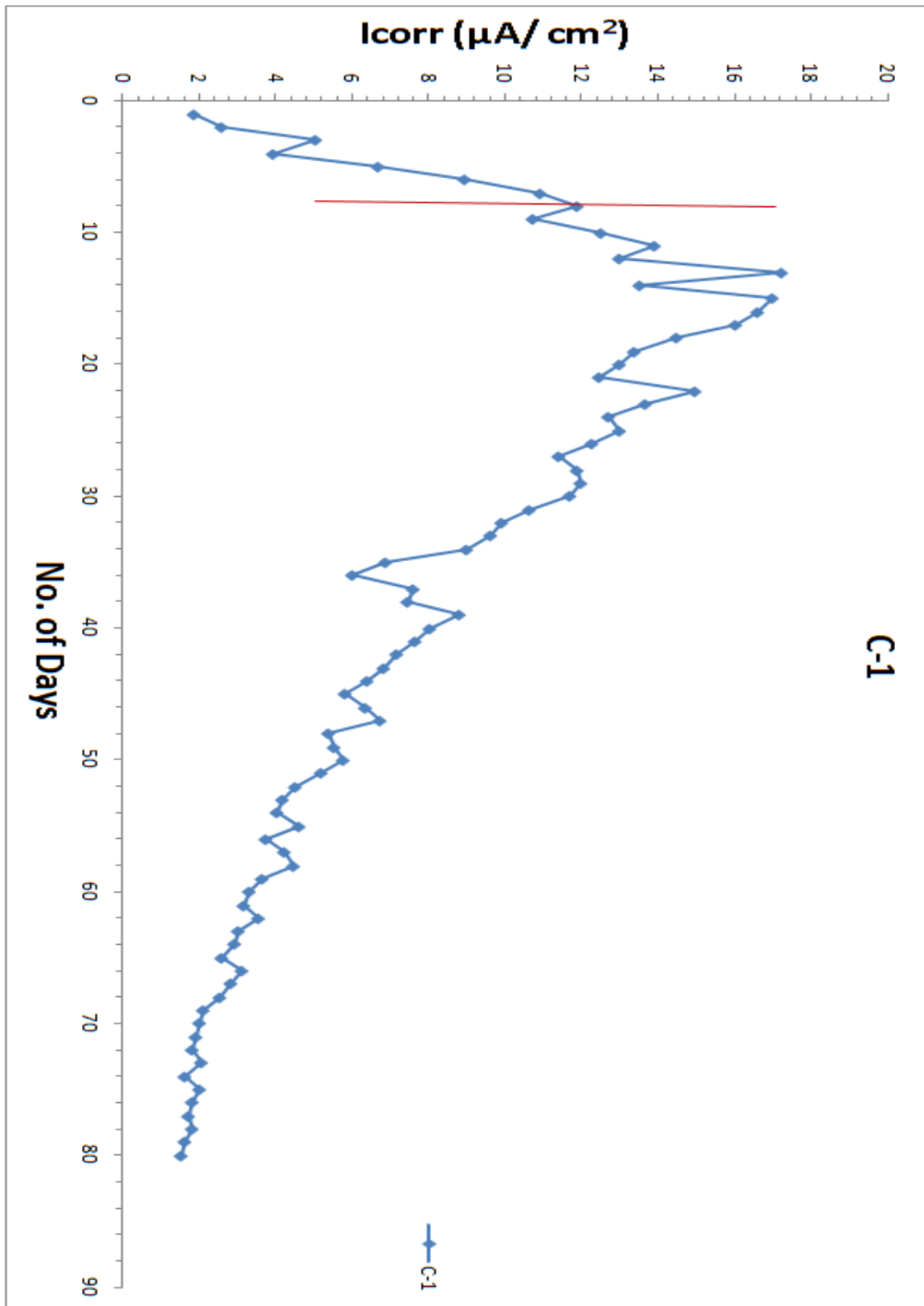


Fig.5.5 Variation of LPR with time for slab C-1 protected after onset of corrosion

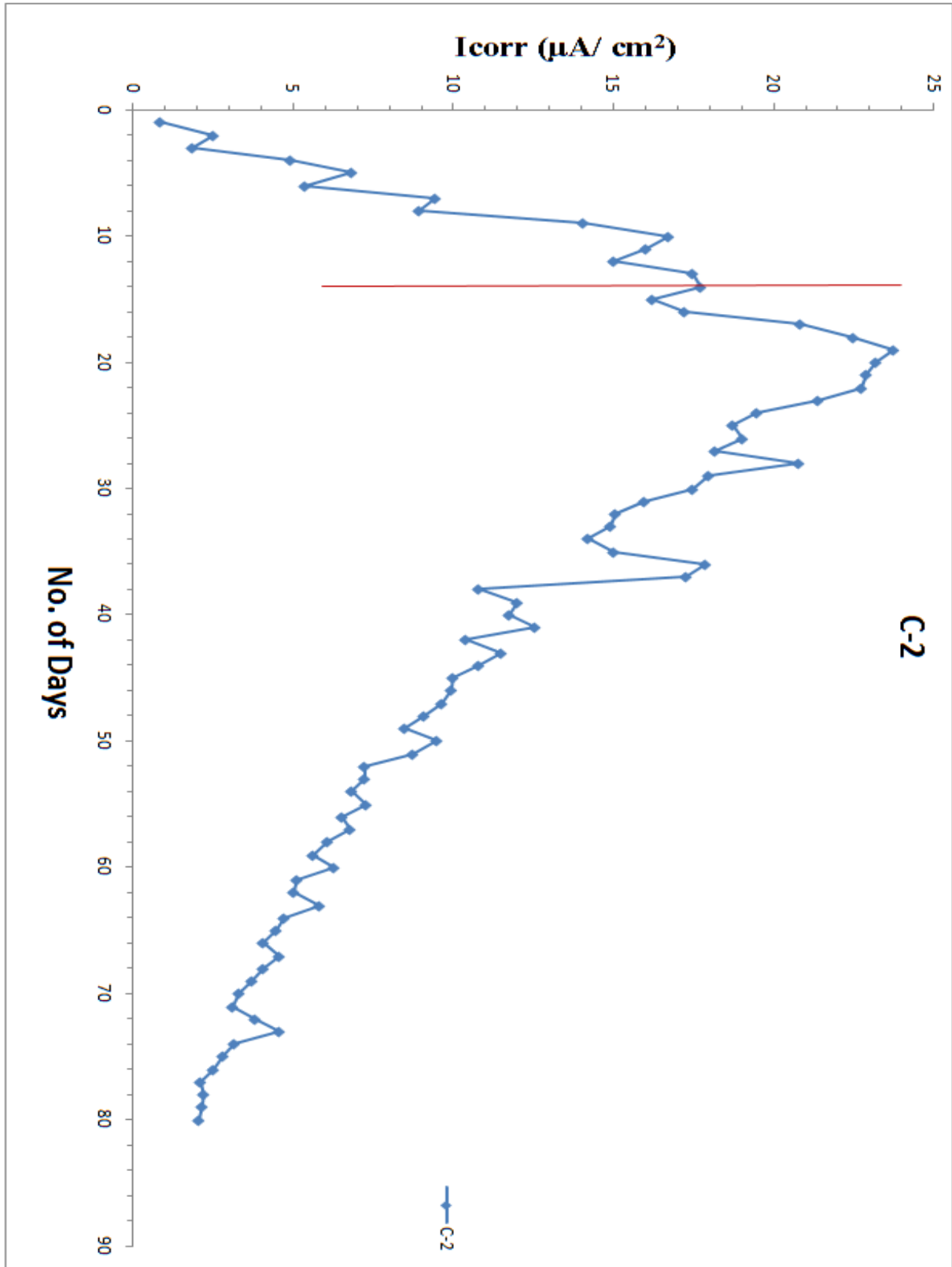


Fig.5.6 Variation of LPR with time for slab C-2 protected after onset of visible crack

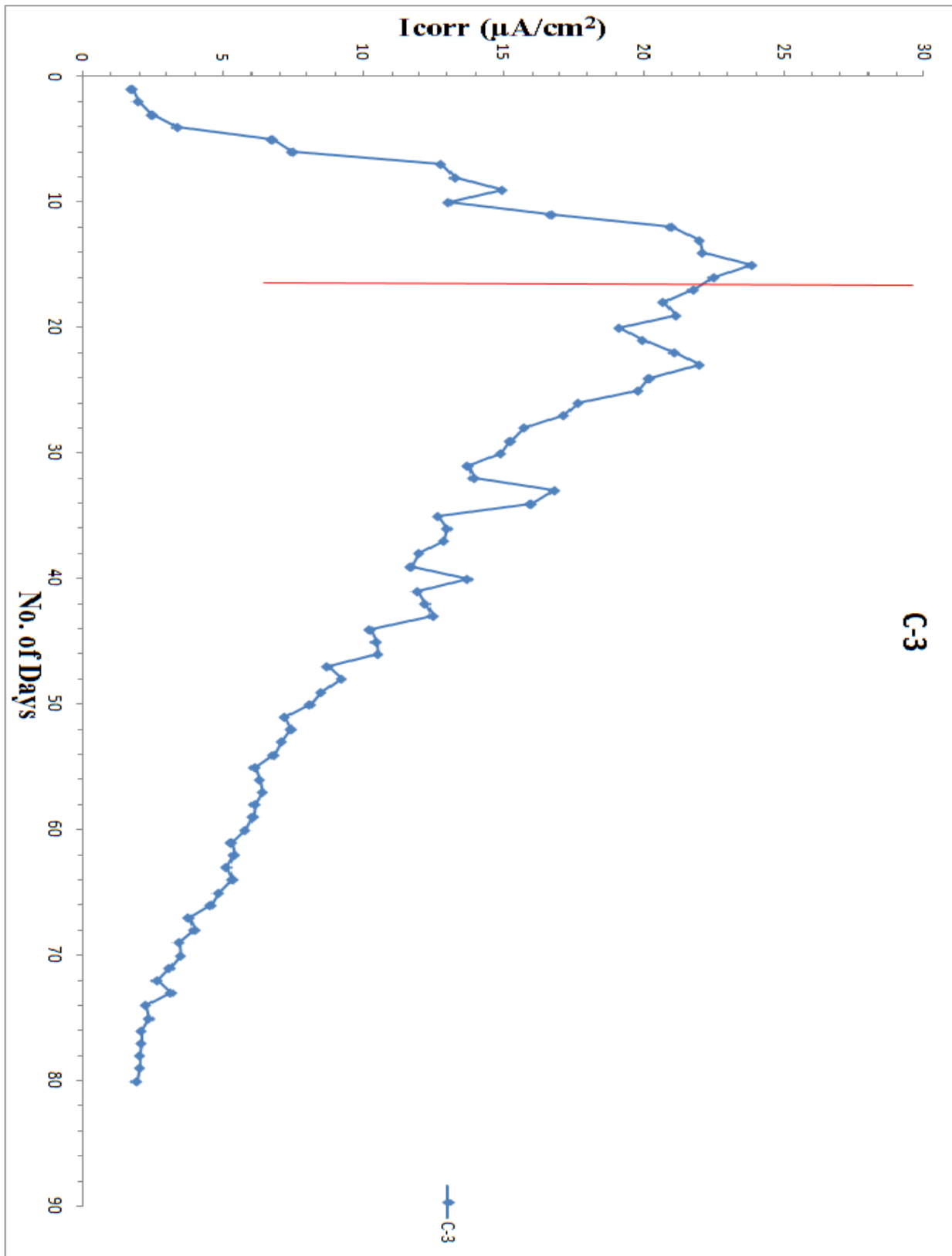


Fig.5.7 Variation of LPR with time for slab C-3 protected at two days after visible crack

However, after active protection i.e. wrapping with CFRP sheet, the value of I_{corr} starts decreasing and corrosion risk is coming down from high to moderate. This trend is common irrespective of level of retrofitting and of applied current. *Koleva et al. (2006)* applied active protection by passing direct current to steel reinforcement and observed that corrosion current density decreases as the period of exposure increases. Lower I_{corr} for the wrapped samples establishes that wrapping significantly reduces the rate of corrosion. Similar observations were made by *Gadve et al. (2010)* in which the FRP wrapped samples had lower I_{corr} than the control sample. In the active systems the passivation is from the prevention of ionization of iron.

This demonstrates that FRP wraps are extremely effective in protecting the corroding reinforcements in concrete. Moreover, the value of I_{corr} reduced with time. In the active systems the passivation is from the prevention of ionization of iron. Therefore, the efficacy of the proposed protection systems is established. The active system exhibited a lower I_{corr} throughout the period of exposure. It is observed that the active protection with FRP sheets are very effective with applied current of 10 mA. This indicates passivation of steel.

CHAPTER 6

CONCLUSIONS

The objective of this experimentation has been to evaluate possibility of successful application of active protection to CFRP wrapped RC specimens. The conclusions drawn during the experimentation are as follows.

Active protection can be effectively applied to the carbon FRP wrapped reinforced concrete structural components using carbon wrap itself as anode and modifying the adhesive epoxy to conduct electric current. This active protection by FRP is able to bring the corrosion current in the passive stage in the duration of around 80 days from even severely corroded specimens, when the impressed current is kept at 10 mA.

The active protection system is found to be stable for all the systems, irrespective of the level of corrosion already present in the specimen.

The half-cell potential is the most stable and reliable determining parameter for indication of rebar corrosion initiation in chloride contaminated concrete. Although half cell potential is a good indicator of initiation of corrosion it is not effective in monitoring its progression. LPR provides a valuable insight into the instantaneous corrosion rate of the steel reinforcement and is a reliable method than half cell potential method.

REFERENCES

ASTM C 876 - 91, (reapproved 1999). "Standard test method for half-cell potentials of uncoated reinforcing steel in concrete." West Conshohocken, PA.

ASTM C 876-95. "Standard test method for half-cell potentials of uncoated reinforcing steel in concrete." 1999.

Ball J. C., Whitmore D. W. (2005). "Innovative corrosion mitigation solutions for existing concrete structures." *Int. J. Materials and Product Technology*, Vol. 23, Nos. 3/4, pp. 219-239.

Bennett, J. E., Bushman, J. B., Clear, K. C., Kamp, R. N., Swiat, W. J. (1993). "Cathodic protection of concrete bridges: A Manual of Practice," Strategic Highway Research Program (SHRP), SHRP-S-372.

Bertolini L., Bolzoni F., Tommaso P., Pedferri P. (2004). "Effectiveness of a conductive cementitious mortar anode for cathodic protection of steel in concrete." *Cement and Concrete Research*, Vol. 34, pp. 681–694.

Bertolini L., Bolzoni F., Pedferri P., Lazzari L., Pastore T. (1998). "Cathodic protection and cathodic prevention in concrete: principles and applications." *Journal of applied electrochemistry*, Vol. 28, pp. 1321-1331.

Callon R., Daily S. F., Funahashi M. "Selection guidelines for using cathodic protection system on reinforced and prestressed concrete structures." www.corrpro.com.

Chang J. J. (2002). "A study of bond degradation of rebar due to cathodic protection current." *Cement and Concrete Research*, Vol. 32, pp. 657–663.

Chang J. J., Yeih W., Huang R. (1999). "Degradation of the bond strength between rebar and concrete due to the impressed cathodic current." *Journal of Marine Science and Technology*, Vol. 7, No. 2, pp. 89-93.

Chaussadent T., Raharinaivo A., Grimaldi G., Arliguie G., Escadeillas G. (1997). "Study of reinforced concrete slabs after three years of cathodic protection under severe conditions." *Materials and Structures*, Vol. 30, pp 399-403.

Cramer S. D., Covino B. S., Jr., Holcomb G. R., Bullard S. J., Collins W. K., Govier R. D., Wilson R. D., Laylor H. M. (1999). "Thermal Sprayed Titanium Anode for Cathodic Protection

of Reinforced Concrete Bridges.” Journal of Thermal Spray Technology, Vol. 8, No. 1, pp. 133-145.

Daily S. F. “Understanding Corrosion and Cathodic Protection of Reinforced Concrete Structures.” www.corrpro.com

Garcia J., Almeraya F., Barrios C., Gaona C., Nunez R., Lopez I., Rodriguez M., Villafane A. M., Bastidas J. M. (2012). “Effect of cathodic protection on steel–concrete bond strength using ion migration measurements.” Cement & Concrete Composites, Vol. 34, pp. 242–247.

Gadve S., Mukherjee A., Malhotra S.N. (2009). “Corrosion of steel reinforcements embedded in FRP wrapped concrete.” Construction and Building Materials 23 (2009) 153–161.

Gadve S., Mukherjee A., Malhotra S.N. (2010). “Active Protection of Fiber-Reinforced Polymer-Wrapped Reinforced Concrete Structures Against Corrosion” Corrosion Science Section Vol. 67, No. 2.

Hassanein A. M., Glass G. K., Buenfeld N. R. (2002). “Protection current distribution in reinforced concrete cathodic protection systems.” Cement & Concrete Composites, Vol. 24, pp. 159–167.

[http:// www.corrpro.com](http://www.corrpro.com).

IS 8112 – 1989 (Reaffirmed 2005). “Specification for 43 grade ordinary Portland cement.” Bureau of Indian Standards, New Delhi.

Jing X., Wu Y. (2010). “Conductive Mortar as Anode Material for Cathodic Protection of Steel in Concrete.” Journal of Wuhan University of Technology-Mater. Sci. Ed., Vol.25, No.5, pp. 883-888.

Kathodischer G. H. “Cathodic protection of reinforced concrete structures.” www.vc-austria.com.

Kim S. J., Okido M., Moon K. M. (2003). “An Electrochemical Study of Cathodic Protection of Steel Used for Marine Structures.” Korean J. Chem. Eng., Vol. 20, No. 3, pp. 560-565.

Koleva D. A., Hu J., Fraaij A. L. A., Stroeven P., Boshkov N., Breugel K. V. (2006). “Cathodic protection revisited: Impact on structural morphology sheds new light on its efficiency.” Cement & Concrete Composites, Vol. 28, pp. 696–706.

Martínez, I., and Andrade, C., (2009). “Examples of reinforcement corrosion monitoring by embedded sensors in concrete structures” *Cement & Concrete Composites*, 31, 545–554.

National Association of Corrosion Engineers, (2000). “Standard recommended practice for impressed current cathodic protection of reinforcing steel in atmospherically exposed concrete structures.” *NACE RP 0290-2000*, Houston.

Pradhan, B., and Bhattacharjee, B., (2009). “Performance evaluation of rebar in chloride contaminated concrete by corrosion rate” *Construction and Building Materials*, 23, 2346–2356.

Sethy M. S., “Text Book of Concrete technology” (2005): S. Chand and Company Ltd, New Delhi.

Spainhour L.K., Wootton I.A. (2008).” Corrosion process and abatement in reinforced concrete wrapped by fiber reinforced polymer.” *Cement & Concrete Composites* 30, 535–543.

Xu J., Yao W. (2009). “Current distribution in reinforced concrete cathodic protection system with conductive mortar overlay anode.” *Construction and Building Materials*, Vol. 23, pp. 2220-2226.